In silico analysis of the mechanism and regulation of germinal centre shutdown

Von der Fakultät für Lebenswissenschaften

der Technischen Universität Carolo-Wilhelmina zu Braunschweig

zur Erlangung des Grades einer

Doktorin der Naturwissenschaften

(Dr. rer. nat.)

genehmigte

D i s s e r t a t i o n

von Theinmozhi Arulraj

aus Nagercoil, Tamil Nadu / Indien

1. Referent: Professor Dr. Michael Meyer-Hermann
2. Referent: Professor Dr. Stefan Dübel
3. Referent: Professor Dr. Stefan Bornholdt

eingereicht am: 27.05.2021
mündliche Prüfung (Disputation) am: 30.08.2021

Druckjahr 2021

Vorveröffentlichungen der Dissertation

Teilergebnisse aus dieser Arbeit wurden mit Genehmigung der Fakultät für Lebenswissenschaften, vertreten durch den Mentor der Arbeit, in folgenden Beiträgen vorab veröffentlicht:

Publikationen

Arulraj T, Binder SC and Meyer-Hermann M (2021). Rate of Immune Complex Cycling in Follicular Dendritic Cells Determines the Extent of Protecting Antigen Integrity and Availability to Germinal Center B Cells. *The Journal of Immunology*, 206(7), 1436-1442.

Arulraj T, Binder SC, Robert PA and Meyer-Hermann M (2019) Synchronous Germinal Center Onset Impacts the Efficiency of Antibody Responses. *Front. Immunol*. 10:2116.

Arulraj T, Binder SC and Meyer-Hermann M. *In-silico* analysis of the longevity and timeline of individual germinal centre reactions in a primary immune response. *Submitted*.

Arulraj T, Binder SC, Robert PA and Meyer-Hermann M. Germinal centre shutdown (review), *Submitted*.

Tagungsbeiträge

Arulraj T, Binder SC and Meyer-Hermann M (2021) Antibody mediated intercommunication of germinal centres. *12th Virtual Annual Retreat, HZI graduate school*.

Arulraj T, Binder SC and Meyer-Hermann M (2020) Mathematical modelling of the shutdown of germinal centre reactions. *11th Virtual Annual Retreat, HZI graduate school.*

Arulraj T, Binder SC and Meyer-Hermann M (2019). Modeling the cycling of antigen in follicular dendritic cells. *12th PhD symposium, HZI graduate school, HZI Braunschweig.*

Arulraj T, Binder SC, Robert PA and Meyer-Hermann M (2019) Mathematical modelling of the shutdown of germinal centre reactions. *10th Annual Retreat, HZI graduate school, Haus der wissenschaft, Braunschweig.*

Posterbeiträge

Arulraj T, Binder SC and Meyer-Hermann M (2021). *In silico* analysis of germinal center shutdown. *CSHL virtual conference on Systems Immunology.*

Arulraj T, Binder SC and Meyer-Hermann M (2021). Modeling the immune complex cycling in follicular dendritic cells. *11th Lorne virtual conference on Infection and Immunity.*

Arulraj T, Binder SC, Robert PA and Meyer-Hermann M (2018). Mathematical modelling of the shutdown of germinal centre reactions. *11th PhD symposium, HZI graduate school, HZI Braunschweig.*

Summary

Induction of humoral immunity following a natural infection or vaccination relies on Germinal centres (GCs), transient structures in the secondary lymphoid organs. B cells, while in the GCs undergo affinity maturation resulting in the production of high affinity plasma and memory cells. GCs undergo shutdown after a defined period of time and dysregulations in GC shutdown are associated with various pathological conditions. As the mechanism and factors regulating GC shutdown are not well understood, the main focus of this study is to contribute to an improved understanding of GC shutdown with mathematical models.

Antigen accessibility is a potential factor that regulates GC shutdown, and can be modulated by antibody feedback, a process where soluble antibodies mask the antigen on Follicular dendritic cells (FDCs). Simulations suggested a strong influence of soluble antibodies on GC shutdown and predicted that antibody feedback could also impair the affinity maturation of GC B cells by terminating GCs earlier. Similarly, changes in immune complex (IC) cycling kinetics impacted GC dynamics and shutdown by regulating antigen protection from degradation. Blocking IC cycling terminated GCs *in silico* suggesting a therapeutic opportunity to disrupt ectopic GCs.

In a system of asynchronous GCs, shutdown of individual GCs was analyzed using published experimental data on GC kinetics. Analysis suggested that lifetime of GCs in the same lymphoid organ might be highly variable potentially due to differences in antigen availability or founder cell composition among individual GCs. Simulations of GC-GC interactions by soluble antibodies predicted changes in GC kinetics and affinity maturation. Finally, several mechanisms were proposed and tested for their ability to terminate GCs independently. Simulations predict that GCs could be terminated by antigen limitation, changes in Tfh signals, decreased B cell division capacity and faster terminal differentiation. In all mechanisms, GC shutdown was ultimately due to decrease in GC B cell proliferation. GC simulations with B cells harboring lymphoma associated mutation in *BTG1* gene, predicted that a small increase in number of cell divisions can confer dramatic competitive advantage. This suggested that a deeper understanding of the regulation of GC B cell divisions is important for understanding lymphomagenesis in addition to the natural GC shutdown.

These findings predict strategies for improving GC responses to vaccination, namely altering IC cycling dynamics by engineering IC particles and overcoming antibody mediated inhibition by persistent antigen delivery. These results also improve our understanding of the potential role of different processes in GC shutdown and suggest ways to design future experiments to gain a more complete understanding of GC shutdown.

Zusammenfassung

Die Induktion der humoralen Immunität nach einer natürlichen Infektion oder Impfung beruht auf Keimzentren (GCs), vorübergehenden Strukturen in den sekundären lymphoiden Organen. B-Zellen durchlaufen in den GCs eine Affinitätsreifung, was zur Produktion von Plasma- und Gedächtniszellen mit hoher Affinität führt. GCs werden nach einer definierten Zeitspanne abgeschaltet, und Fehlregulationen beim Herunterfahren der GC sind mit verschiedenen pathologischen Zuständen verbunden. Da der Mechanismus und die Faktoren, die das Herunterfahren des GC regulieren, nicht genau bekannt sind, liegt der Schwerpunkt dieser Studie darauf, mit mathematischen Modellen zu einem besseren Verständnis des Herunterfahrens des GC beizutragen. Die Zugänglichkeit von Antigenen ist ein potenzieller Faktor, der das Herunterfahren der GC reguliert und durch Antikörper-Feedback moduliert werden kann. Dabei werden lösliche Antikörper das Antigen auf follikulären dendritischen Zellen (FDCs) maskieren. Simulationen deuteten auf einen starken Einfluss löslicher Antikörper auf das Herunterfahren der GC hin und sagten voraus, dass die Rückkopplung von Antikörpern auch die Affinitätsreifung von GC B-Zellen beeinträchtigen könnte, indem GCs früher beendet werden. In ähnlicher Weise beeinflussten Änderungen der Zykluskinetik des Immunkomplexes (IC) die GC-Dynamik und das Herunterfahren, indem sie den Antigenschutz vor Abbau regulierten. Das Blockieren von IC-Zyklen beendete GCs *in silico*, was auf eine therapeutische Möglichkeit hinweist, ektopische GCs zu stören. In einem System asynchroner GCs wurde das Herunterfahren einzelner GCs unter Verwendung veröffentlichter experimenteller Daten zur GC-Kinetik analysiert. Die Analyse legte nahe, dass die Lebensdauer von GCs im selben lymphoiden Organ möglicherweise aufgrund unterschiedlicher Antigenverfügbarkeit oder Zusammensetzung der Gründerzellen zwischen einzelnen GCs sehr unterschiedlich sein könnte. Simulationen von GC-GC-Wechselwirkungen durch lösliche Antikörper sagten Änderungen der GC-Kinetik und der Affinitätsreifung voraus. Schließlich wurden mehrere Mechanismen vorgeschlagen und auf ihre Fähigkeit getestet, GCs unabhängig zu beenden. Simulationen sagen voraus, dass GCs durch Antigenbegrenzung, Änderungen der Tfh-Signale, verringerte B-Zellteilungskapazität und schnellere terminale Differenzierung beendet werden könnten. Bei allen Mechanismen war das Herunterfahren des GC letztendlich auf eine Abnahme der Proliferation der GC B-Zellen zurückzuführen. GC-Simulationen mit B-Zellen, die eine Lymphom-assoziierte Mutation im *BTG1* Gen aufweisen, sagten voraus, dass eine geringe Zunahme der Anzahl von Zellteilungen einen dramatischen Wettbewerbsvorteil bringen kann. Dies legt nahe, dass ein tieferes Verständnis der Regulation der GC B-Zellteilung wichtig ist, um die Lymphomagenese zusätzlich zum natürlichen GC-Shutdown zu verstehen. Diese Ergebnisse sagen Strategien zur Verbesserung der GC-Reaktionen auf Impfungen voraus, nämlich die Veränderung der IC-Zyklusdynamik durch Engineering von IC-Partikeln und die Überwindung der durch Antikörper vermittelten Hemmung durch anhaltende Antigenabgabe. Diese Ergebnisse verbessern auch unser Verständnis der möglichen Rolle verschiedener Prozesse beim Herunterfahren von GC und schlagen Wege vor, um zukünftige Experimente zu entwerfen, um ein vollständigeres Verständnis des Herunterfahrens von GC zu erhalten.

Acknowledgements

Firstly, I wish to express my sincere gratitude to my supervisors, Prof. Michael Meyer-Hermann and Dr. Sebastian Binder for the continuous support and motivation throughout my Ph.D. In addition, I would like to thank my thesis committee members, Prof. Carlos Guzman and Prof. Thomas Pietschmann for their insightful comments and constructive suggestions that helped me stay right on track in research. I also wish to acknowledge my collaborators, Dr. Coraline Mlynarczyk and Prof. Ari Melnick for all the interesting and fruitful discussions.

I am grateful to the funding from European Union's Horizon 2020 research and innovation programme COSMIC under the Marie Sklodowska-Curie Grant [grant agreement no. 765158] for generously supporting my Ph.D. research at Helmholtz Center for Infection Research.

I owe a great debt of gratitude to the present and past members of Systems Immunology Group for enriching my student life in countless ways. A special thanks to Ozge Gizlenci and Dr. Philippe Robert, for all the discussions that were very helpful in preparing this thesis. I also wish to thank ESRs and PIs of the COSMIC consortium for their constant support, encouragement and feedback.

Finally, I would like to thank my friends and family. Their support and care helped me overcome setbacks and stay focused on my research. Especially, I thank my father and mother for their constant support, encouragement and sacrifice; my family members, Malar, Sreenivasan, Thangaraj and Thamayanthi and my friend, Srilekha for believing in me and helping me to achieve this feat.

Contents

Chapter 1

Background

Immune system has a wide range of functions that collectively promote effective surveillance and protection against invading pathogens. From an evolutionary perspective, immune system has evolved from a rather primitive form with cellular receptors and some phagocyte-like cells in invertebrates to a more sophisticated system with specialized capabilities in the higher vertebrates [17]. Despite this diversity, a fully functional immune system is critical for the survival of all organisms.

Dysregulation of the immune system can result in impaired protection from invading pathogens and lack of ability to prevent tumor development, highlighting the importance of its role. However, excess immune activation can lead to autoimmune diseases as the immune system turns against the body's own tissues [28]. Hence, in addition to the exceptional defense strategies, immune system is also equipped with several regulatory mechanisms to achieve immune homeostasis [145].

1.1 Innate and adaptive immune system

Immune system can be divided into two intricately connected branches - innate and adaptive immune system. The innate immune system is evolutionarily conserved [17] and comprises the physical barriers, chemical substances, phagocytes and other cell types. It mounts an early immune response against foreign agents and is not very specific to the invading pathogen. Nevertheless, it is necessary to restrict the pathogen spread and is also effective in clearing certain kind of infections. When a pathogen invades across the surface barriers of the body, tissue resident macrophages engulf the pathogen, secrete cytokines and chemokines that collectively influence the permeability of blood vessels and attract cells such as neutrophils. This results in accumulation of immune cells and an inflammatory response at the site of infection [113].

While the innate immune system mainly recognizes conserved pathogen associated molecules, many pathogens have evolved ways to overcome this. In vertebrates, this limitation is circumvented by the adaptive immune system [25] that acts in concert with the innate immunity in order to provide most efficient protection against pathogens. Adaptive immune system comprises of B and T lymphocytes that have different effector functions. Lymphocytes have greatly diversified receptors such that each lymphocyte bears a unique cell surface receptor generated by the recombination at developmental stages and hence, target the pathogens more specifically when compared to the innate immune system. Effector functions of the activated T lymphocytes include killing the pathogen infected cells or assisting the activation of other immune cells such as the B cells. On the other hand,

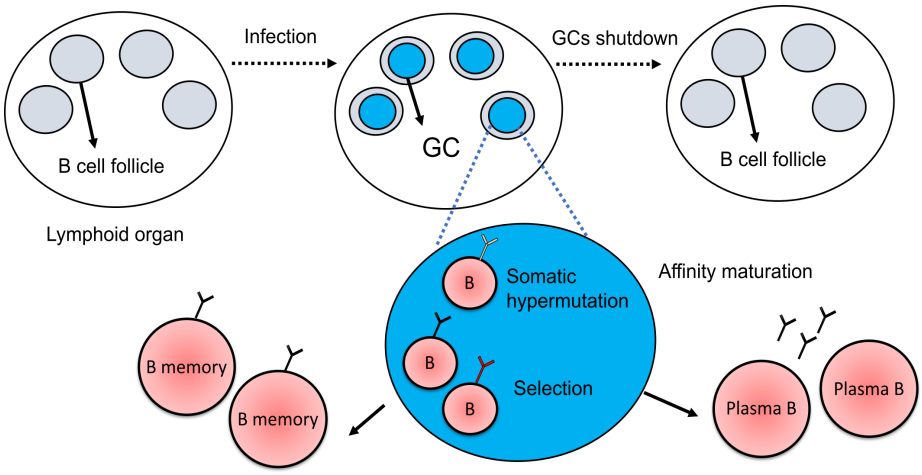

Figure 1.1: Schematic representation of germinal centre (GC) formation and shutdown in a lymphoid organ. GCs are formed inside the B cell follicles of secondary lymphoid organs after an infection, and support the affinity maturation of B cells through antibody diversification and selection. GCs produce high-affinity memory and plasma cells that contribute to the humoral immune response. GCs have a definite lifetime and undergo shutdown. GC: Germinal centre, B memory: Memory B cell, Plasma B: Plasma cell.

the central role of B lymphocytes is to mount an antibody response to clear the infection and is referred to as the humoral immune response [73].

1.2 Soluble antibodies and affinity maturation

Main mediators of the humoral immune response are the soluble antibodies secreted by the B lymphocytes. These antibodies, also called immunoglobulins have a typical Y shaped structure, with two antigen binding variable regions and a conserved constant region [139]. Secreted antibodies have several important roles ranging from specifically binding to pathogen molecules and restricting their functions to the activation of Fc receptors which are a family of inhibitory and activating receptors present on the surface of several immune effector cells, by binding via the antibody constant region [114, 168]. Antibodies exist as different isotypes (IgG, IgA, IgM, IgE and IgD) that differ in their properties and effector functions [139]. Furthermore, Fc portion of the antibodies can be modified by glycosylation which influences the nature of the response initiated [168]. Eisen discovered that affinity of serum antibodies increase over time after an immune response [37] and this phenomenon is referred to as antibody affinity maturation. Although the exact mechanisms and their contributions to this process are still under investigation, it is well established that affinity maturation of B cells in structures called germinal centres play a role in increasing the affinity of serum antibodies.

1.3 Germinal centres (GCs)

Germinal centres (GCs) were first discovered by Flemming in 1885 and were initially characterized as sites with large proliferating lymphocytes in the secondary lymphoid organs [44]. Subsequent experimental studies found that these are the sites where the affinity maturation of B cells (schematically shown in Figure 1.1) take place resulting in emergence of high-affinity memory and plasma cells [9, 72].

Early experimental investigations were restricted to histological studies which revealed the

presence of GCs within the B cell follicles of lymphoid organs. GCs are formed 2-3 days after immunization with a T-dependent antigen. Examination of GCs at different time points revealed the dynamic nature of GCs as they initially expand and then few weeks later start to shrink gradually and undergo shutdown [87]. Shutdown of GCs is one of the regulatory mechanisms that prevents excess production of memory and plasma cells and is critical for the homeostasis of humoral immune response after an infection. Subsequent studies with different model antigen showed that the kinetics and lifetime of GCs vary depending on immunization conditions [10].

Inside each GC, cell types other than B cells are also present. This includes the stromal cells called Follicular Dendritic Cells (FDCs) [79] and a small number of T follicular helper (Tfh) cells that assist in the affinity maturation of GC B cells. In addition, macrophages called tingible body macrophages (TBMs), stromal cells producing CXCL12 and Tfr (T follicular regulatory) cells are also found in the GCs. Within the short lifetime, GCs give rise to highly specific B lymphocytes from a pool of relatively low affinity lymphocytes that initially recognize the foreign antigen [91]. Affinity maturation happens in a step wise manner and involves mutating the BCR genes followed by a process of selection by interactions with FDCs and Tfh [84].

Evolution of B cells in the GCs resembles the evolution of living organisms happening at a larger time scale. Although GCs formed in different organs and under different settings have distinct characteristics such as the kinetics, certain common models for development of GCs and B cell selection have been put forward with some assumptions that are still unverified [95]. As studies continue to explore the GCs, these models are being revised. Given the complexity and dynamic nature of GCs, mathematical models are a highly useful tool to study their behavior [106]. These models are differential-equation based or agent-based and have been developed to explain the mechanisms behind the underlying processes of GC reactions [16]. As mathematical models have been an integral part in the evolution of our knowledge on GCs, they are discussed here along with the information acquired through experimental investigations.

1.3.1 GC formation and extrafollicular reaction

Due to the low frequencies of antigen specific lymphocytes, they are concentrated in structures such as lymphoid organs in order to achieve timely coordination and initiating an adaptive immune response [53]. A secondary lymphoid organ such as a spleen or lymph node consists of T cell zone and many B cell follicles. T cells and dendritic cells are present in the T cell zone and the B cell follicles host naive B cells [135]. GC formation is preceded by the activation of helper T cells by the dendritic cells in the T cell zone and activation of B cells by the binding of antigen to BCR. This is followed by the interaction of helper T and B cells at the border region [115] between the T cell zone and the primary B cell follicles. When, the activated T cells come in contact with BCR-primed B cells, some B cells differentiate into GC precursor cells. Alternatively, other B cells differentiate into short-lived plasmablasts and produce antibodies with relatively low affinity [20]. Low affinity antibodies produced are critical for the initial control of infection until the new waves of plasma cells with high affinities are produced from the GCs. Activated GC precursor cells enter the follicular areas, clonally expand to form GCs within the follicles [87]. Interaction with B cells also triggers the helper T cells to differentiate into Tfh cells that migrate to the B cell follicles to assist the GC B cells [29].

1.3.2 Cellular events and B cell evolution inside GCs

Overview of the GC reaction

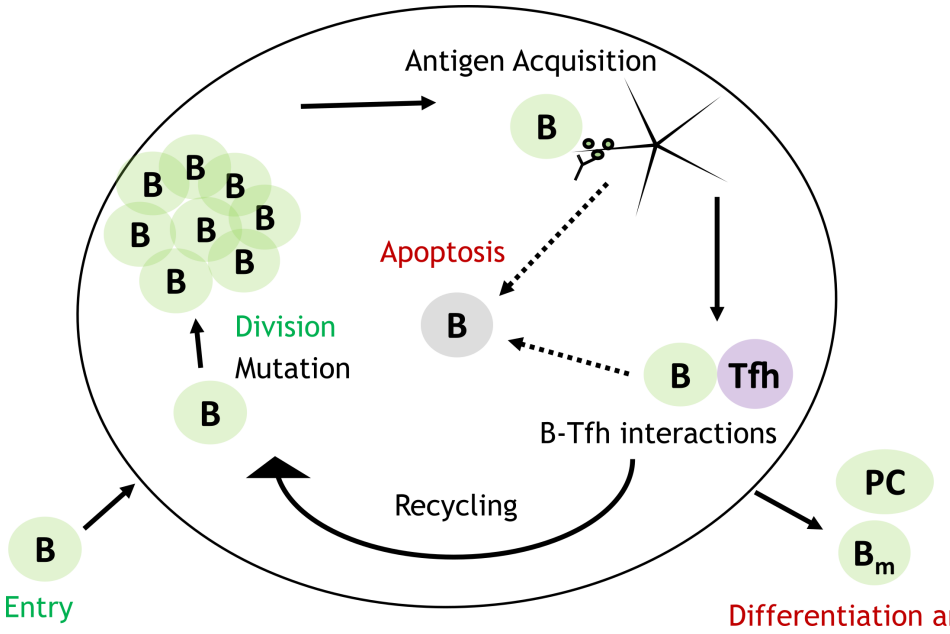

Figure 1.2: Overview of GC reaction. Proliferation of GC B cells is accompanied by Somatic hypermutation that introduces random point mutations in BCR gene. B cell with different BCR variants undergo selection which is a two-step process, absence of which leads to apoptosis. It involves collecting antigen from FDCs and subsequently presenting the antigen to Tfh cells. Ultimately, selection of GC B cells by Tfh leads to further divisions or differentiation into memory or plasma cell precursors. B: B cell, Tfh: Tfh cell, PC: Plasma cell, B_m: Memory cell.

The cellular events happening inside the GCs are outlined in this section (schematically shown in Figure 1.2) followed by a detailed explanation. About 10-100 B cell clones seed each GC [154]. These founder cells expand the GC as they undergo clonal expansion. Eventually GC B cells go through distinct stages that leads to antibody diversification and selection [91]. These steps include generation of B cells with antibody variants by a process called somatic hypermutation (SHM) that induces BCR affinity changes. This is followed by interactions with FDCs that result in acquisition of immune complexes displayed on FDCs and survival signals. Interactions with Tfh induces CD40 signals in B cells that leads to molecular changes in the GC B cells that allow them to proliferate further or differentiate into plasma and memory cells that exit the GC. Iterative rounds of mutation and selection results in the optimization of GC B cell affinities.

Camacho et al. performed a detailed investigation of anatomical changes in the GC after immunization and showed the development of two zones in mouse GCs [18]. Hence, fully formed GCs have two distinct compartments: Dark zone (DZ) and light zone (LZ), named after their histological appearance. Analysis of GC B cells suggested that GC B cells with distinct stages are in distinct regions of the GC. DZ is primarily associated with proliferating cells called centroblasts. LZ hosts FDCs and Tfh cells that could interact and provide signals to the GC B cells. Although classically it was thought that DZ is the compartment where the cells proliferate and LZ is the region where no dividing cells are present, there is no such strict separation and cells also proliferate while in the LZ [18].

GC B cell proliferation and SHM

Most GC B cells are constantly in a state of proliferation. At initial stages of the GC, founder cells clonally expand and increase the GC volume. Cells selected by Tfh also

proliferate and contribute to the maintenance of the GC reaction. GC B cells have a uniquely controlled proliferation program that enables efficient divisions. Beguelin et al., discovered that EZH2 histone methyl transferase is a master regulator of GC B cell proliferation and identified a positive feedback loop regulating the cell cycle checkpoint [8].

As GC B cells express an enzyme AID (Activation-induced cytidine deaminase), during cell divisions, random point mutations are introduced into the V region of BCR genes resulting in changes in affinities [9]. This process is referred to as the somatic hypermutation (SHM). As such random mutations are capable of resulting in increased affinity BCRs, these B cells are subsequently selected in the GCs. However, SHM might also introduce deleterious mutations that will result in the apoptosis of GC B cells [148]. Dysregulation of AID activity can lead to malignant transformations by inducing off-target mutations and translocation events [123, 180].

GC B cell apoptosis

Enormous number of B cells undergo apoptosis in both the LZ and DZ compartment of GCs [97]. Apoptotic GC B cells are engulfed and disposed by TBMs [146]. In addition to apoptosis of GC B cells due to the deleterious mutations introduced by SHM, GC B cells in the LZ primarily undergo apoptosis due to lack of selection signals from FDCs and Tfh [97]. This is because GC B cells are constantly in a state where they are prone to undergo apoptosis as supported by the highly active apoptotic program [161]. Timely interactions of the GC B cell with FDCs, acquisition of antigen and interactions with Tfh cells provide necessary survival signals and prevent the apoptosis of GC B cells [161].

Interactions with FDCs

Interaction of GC B cells with FDCs is considered as the first step of GC B cell selection. FDCs are very well known for their ability to trap and retain native antigen in the form of immune complexes [93, 155]. Heesters et al., discovered that antigen in FDCs is internalized and recycled back to the surface of FDCs after entering non degradative vesicles [62]. The trapped immune complexes are maintained for several months in a stable form and are thought to act as a depot that constantly supplies GC B cells with antigen. Immune complex acquisition is believed to drive the affinity maturation of GC B cells [91] as subsequent pMHC presentation to Tfh cells enables GC B cells to receive survival and differentiation signals. This view was challenged by Hannum et al., as GCs progressed normally in the absence of any detectable immune complexes on FDCs, in a mouse model that lacks soluble antibodies [56]. However, immune complexes are still considered important for efficient GC and memory responses [79].

In addition, several accessory activities of FDCs have also been recognized. FDCs are a source of BAFF (B cell activating factor) [57, 124] that can promote the survival of GC B cells. FDCs also produce cytokines such as IL-6. Wu et al, found that IL-6 is produced by FDCs upon stimulation by immune complexes and absence of IL-6 resulted in reduced number and size of GCs [175]. FDCs also influence the clonal diversity of GCs through the receptor FcγRIIB through an unknown mechanism as lack of these receptors on FDCs increased the GC B cell diversity and was able to allow the persistence of clones with low fitness [160].

Interactions with Tfh

Second step of selection after interactions with FDCs involves interactions with Tfh cells present in the outer LZ of the GCs. Interactions with B and Tfh cells is highly complex and involves an array of receptor ligand interactions [143] that triggers intracellular signaling

and several feedback events. Tfh cells highly express CD40L that stimulates the CD40 of GC B cells. Despite short B-Tfh interactions, ICOS-ICOSL interactions promotes enhanced signaling and extensive surface engagement [86]. Furthermore, human Tfh cells were found to release dopamine while interacting with B cells and triggers the translocation of ICOSL to the surface of B cells which increases the CD40L expression, resulting in a positive feed forward loop that enhances synaptic area and accelerates GC output [117].

In addition, there are inhibitory receptors that are being activated such as PD-1 [51] when Tfh and B cells interact and likely play a role in preventing excessive stimulatory signals. Tfh cells also supply the GC B cells with cytokines such as IL-21 and IL-4 [170]. Interactions with Tfh cells has been shown to induce several transcription factors that in turn determine the fate of GC B cells [40, 42, 70, 90]. Tfh cells are clearly necessary for the maintenance of GC B cells [31].

Interactions with Tfr

Subsets of CD4+ T cells called regulatory T cells (Tregs), have suppressive functions and are involved in preventing excessive immune responses [27]. Tregs present in the follicular regions are referred as Tfr (T follicular regulatory) cells. They were initially characterized as cells with some characters resembling Tfh and at the same time having distinct characteristics and suppressive phenotype as opposed to the Tfh cells [173]. Tfr cells follow a dynamics that reaches peak when the GC B cell numbers start to decline [166, 174]. In addition to this observation, the inhibitory nature of Tfr cells has resulted in the idea that these cells might play a role in down regulating the GC response. Both direct inhibition of B cells by Tfr and indirect action by Tfh inhibition are proposed as mechanisms of Tfr mediated inhibition of GC [130, 136, 173]. However, studies exploring the impact of Tfr deletion on GC reactions have resulted in conflicting observations [173]. Furthermore, it has also been found that IL-10 produced by Tfr cells support the GC development following acute LCMV infection [83]. Hence, the precise role of Tfr cells in GCs remains to be understood.

GC B cell positive selection and recycling

GC B cell selection by the Tfh cells leads to return of B cells to the DZ to undergo divisions [163]. Kepler and Perelson predicted that GC B cells might undergo multiple rounds of mutation and selection by theoretical analysis [76]. Further, mathematical models also predicted the LZ to DZ transition of GC B cells [105]. Later on, experimental studies confirmed that GC B cells indeed migrate from LZ to DZ after selection [5] to undergo further rounds of division. Mathematical model predicted that the number of divisions of GC B cells is dependent on the intensity of pMHC presentation [107] and was experimentally confirmed by Gitlin et al [47].

GC B cell selection by Tfh signals involve several transcriptional factors at the molecular level. Transcription factors mTOR, cMyc and FoxO are essential for GC B cell maintenance as they are necessary to sustain cell divisions [40, 42, 70]. Positively selected GC B cells have been shown to transiently express cMyc transcription factor [36]. This transient induction promotes the activation of gene expression program that sustains GC B cell proliferation. cMyc has also been shown to control the number of cell divisions in the DZ [42]. Luo et al., showed that although either BCR and CD40 signals can efficiently induce cMyc in naïve B cells, both BCR and CD40 signals are synergistically needed to induce cMyc in GC B cells [90]. Further, they showed that BCR signaling alone weakly activates the PI3K pathway, which is sufficient to efficiently inactivate FoxO and translocate it from the nucleus to the cytoplasm [90]. Ersching et al., showed that induction of mTOR expression by interaction with Tfh cells is necessary for the anabolic growth of GC B cells

and for upregulating glycolytic program prior to undergoing clonal expansion [40]. By integrating experimental data from these studies, three *in silico* models have to proposed to explain how the transcription factors contribute to B cell selection [103]. These models suggested a separation of signals that control B cell divisions and selection and were able to explain previously unexplained experimental findings such as the LZ enrichment of DEC205+ cells upon injection of anti-DEC205ova and the phenotype observed due to mTOR overexpression [103].

In addition to the transcriptional control of various genes, post-transcriptional modifications and alternative splicing of genes are also involved in the GC B cell selection and maintenance. Monzon-Casanova et al., showed that the RNA binding protein, PTBP1 is involved in regulating mRNA expression changes and alternative splicing of genes such as M-type pyruvate kinase (*Pkm*) and thymidylate synthase (*Tyms*) in GC B cells, that control glycolysis and nucleotide synthesis, respectively [110]. These post transcriptional changes are necessary for cell cycle progression and proper affinity maturation of B cells [110].

Differentiation and exit of GC B cells

Memory cells and plasma cells constitute the output cells of the GC. Weisel et al., found that GC output temporally evolves such that large proportion of long-lived memory cells are produced at early phases of the GC reaction, while most long-lived plasma cells are produced at later stages of GC reaction [172]. This led to a model where there is a time dependent switch in differentiation of GC B cells to plasma or memory cell precursors. Mechanistic basis of decision making in differentiation between memory or plasma cells remains poorly understood. However, it has been shown that high affinity GC B cells have the tendency to differentiate into plasma cells and relatively low affinity GC B cells become memory cells [162]. Mathematical model integrating [107] and [96], suggested a combined role of affinity dependent CD40 signaling and asymmetric division of B cells in mediating the temporal switch in GC output [98].

GC B cell migration

Chemokines secreted by the stromal cells and FDCs such as CXCL12 and CXCL13 respectively, guide the chemotaxis of GC B cells. Real time imaging showed that GC B cells migrate between the two zones [5, 58, 141]. An agent-based model was used to reanalyze the two-photon imaging experimental data and predicted that chemotaxis is necessary to maintain the distinct compartments [41]. This study further suggested that chemokine sensitivity of the B cells is downregulated [41]. It was shown experimentally that CXCR5 expression is relatively similar among LZ and DZ B cells [3]. However, the CXCR4 expression was higher in the DZ GC B cells [3]. This suggested a model where the CXCR4 down regulation is associated with the transition of the GC B cells to the LZ and re-return of cells from LZ to DZ might be regulated by the upregulation of CXCR4 [4].

There are also other receptors in GC B cells that are necessary to retain the GC B cells within the center of B cell follicles. This involves receptor P2RY8 that binds to the ligand GGG (geranylgeranyl glutathione) [89]. FDCs degrade the GGG ligand and provide GC B cells with an environment with a low concentration of GGG to retain the GC B cells in the center of follicular region [89]. As extensive cytoskeletal rearrangements are involved in B cell migration, molecular control of these elements is also being studied. Reimer et al., discovered that EfhD2 (Swiprosin-1), an F-actin bundling protein inhibits actin dynamics in GC B cells and decreases the B cell speed [128] revealing a molecular mechanism controlling GC B cell speed and persistence. Furthermore, absence of EfhD2 decreased GC B cell contacts with FDCs and mathematical modeling predicted that such

changes could impact GC B cell output and affinity maturation [128].

Clonal evolution

Analysis of clonal evolution of GCs is revolutionized by the development of techniques such as multi-color brainbow labelling [88]. *In silico* analysis of brainbow technique suggested guidelines that needs to be taken into account in the data interpretation of multi color brainbow labeling results [104]. Degn et al., studied the clonal evolution in autoreactive GCs and found that a single autoreactive clone in the GC can trigger the emergence of other autoreactive B cell clones via TLR-7 activation [32]. Pelissier et al. extended a previously developed model of GC B cell development, with an intracellular network and stochastic interaction between GC cell types [158] to include a sequence based BCR representation [120]. Their analysis of clonal evolution dynamics suggested a time lag of 7 days between the initial advantageous affinity acquisition to the clonal bursts [120]. Reshetova et al., developed an ODE based model of the affinity maturation of GC B cells and predicted that subclones with highest abundance do not necessarily have the highest affinity [129] suggesting the importance of further studies along this direction.

Class-switch recombination

Antibody class-switching is a critical process for the antibody response. Previously, GCs were considered as predominant sites where the class-switching happens. Recently, Roco et al showed that class-switching mostly occurs outside the GCs [134]. Levels of GLT transcripts, markers of class switch recombination were higher before the GC is formed and is associated with the initial interaction of T-B cells outside the GCs, subsequently, GTL transcript expression declined when the GC began to form. Furthermore, when the diversity of GCs with different isotypes was examined, GCs with predominantly IgM cells were also observed. Mathematical modeling predicted that in a scenario with constant switching probability as thought classically, GCs with IgM isotypes is reduced. In contrast, a decaying switching probably was consistent with the experimental data and showed diverse GCs in terms of antibody isotypes [134].

1.3.3 Interactions between GCs

After an infection, hundreds of GCs are formed in a lymphoid organ such as spleen and 10-16 GCs are seen in a single lymph node [66, 149]. Evidence of exchange of molecules and cells between GCs led to the idea that GCs are not isolated entities but might be able to intercommunicate and influence each other. For instance, Tfh cells [144] dynamically migrate between GCs, although the implications of such cell exchange is unknown. GCs might also be able to exchange soluble antibodies. Passively administered soluble antibodies are able to influence the affinity maturation and kinetics of GCs [178]. Further, mathematical modeling predicted that GC derived soluble antibodies could induce timely shutdown of the GC reaction [178]. Hence, it can be speculated that GCs regulate each other by such intercommunication. Impact of GC-GC interactions on kinetics and affinity maturation of GCs is discussed in Chapter 6.

1.3.4 GC shutdown

GCs are typically transient and are terminated by an unknown mechanism after a defined period of time. Lifetime of GCs and timing of shutdown are found to vary depending on the experimental settings [10]. Moreover, chronic viral infections can induce long-lasting GCs [82] and GCs in the Peyer's patches of the gut are constitutive [147] as opposed to the GCs induced by model protein antigens. GC shutdown is known to be regulated by various factors such as the Tfh help, antigen availability, presence of soluble antibodies

and possibly the presence of Tfr cells. However, the exact cause and how these factors interact with each other to influence GC shutdown are not understood. A large number of mechanisms have been proposed in the literature to explain the GC shutdown [77, 111]. This includes the changes in morphology of FDCs, antigen access and nature of Tfh help over the course of GC reaction that in turn leads to changes in GC B cell fate decisions. There is no direct experimental evidence to any of these mechanisms as a signal for GC shutdown.

Although, GC shutdown gained the attention of several groups, experimental analysis of GC shutdown is challenging. Due to technical challenges, mathematical modeling analysis [77, 111] is more prevalent in exploring the problem of GC shutdown. Aberrations in the GC shutdown is capable of inducing chronic pathologic GCs and premature termination following infection leads to poor B cell affinity maturation. Hence, it is important to understand the mechanism and regulation of GC shutdown. Investigating these mechanisms is the main objective of the work presented in this thesis. Mechanisms capable of terminating GCs *in silico* are discussed in Chapter 7.

1.3.5 GCs in vaccination

As GCs are the primary sites of B cell affinity maturation, functioning of GCs is critical for the vaccination response. Modulating the GC lifetime for efficient response to vaccination is a promising application of GC research and is a focus of several studies. Strategies to enhance the GC responses or longevity of GCs such as different dosing schemes [23, 22, 153] have been discovered. Slow delivery/immunization strategy was found to be more efficient than the conventional single bolus dose for enhancing GC responses [22].

In the case of GC response towards multiple antigens or antigens with multiple epitopes, not all epitopes are equally targeted by the GC B cells. GC B cells might affinity mature predominantly to some of the epitopes which are referred to as immunodominant. Epitopes towards which efficient GC response is not initiated are referred to as the subdominant epitopes. Slow delivery immunization has also been shown to change the immunodominance of GC responses [22]. Further, injection of antibodies against an immunodominant epitope has been predicted to redirect the GC responses towards subdominant B cells [102].

Another application of GCs is in the development of broadly neutralizing antibodies against pathogens such as influenza, HIV etc. Broadly neutralizing antibodies either bind to the conserved region of multiple virus strains or is capable of binding to multiple variable regions. As viruses such as influenza and HIV mutate at a higher rate, development of such broadly neutralizing antibodies is necessary for efficient anti-viral humoral responses. The factors that hinder their development and ways to overcome this are of great interest and are widely being explored [60]. *In silico* models with different affinity representations have also suggested ways to develop broadly neutralizing antibodies [131].

1.4 GCs in pathological conditions

Auto-reactive B cells are produced as by-products of SHM in the GCs. Inappropriate B cell selection due to defects in GC components such as qualitative/quantitative changes in antigen availability and T cell help can give rise to pathologic GCs producing autoantibodies [127, 164]. GC-derived autoantibodies characteristically have high-affinity towards antigen and large number of mutations, thus result in long-term complications [164]. In addition, GCs are also seen in non-conventional sites in patients with various autoimmune diseases including Rheumatoid arthritis, Multiple sclerosis etc.[6, 125, 142, 152] and ap-

pear to be associated with the pathogenesis and production of autoantibodies [68]. Ectopic GCs have also been observed to support the selection of B cells and affinity maturation as in the case of a normal GC [26]. Beyer and Meyer-Hermann, mathematically analyzed the impact of chemokine receptor dynamics on cell aggregate formation due to chemotaxis [13]. Their analysis suggested that when cells migrate faster than the diffusion of chemokines, unstable cell aggregates are formed and this might explain the organization of ectopic lymphoid structures [13].

GCs are also involved in the development of B cell lymphomas. Specialized characteristics of GC B cells, that are critical to promote efficient affinity maturation are hijacked in the case of lymphomas [109]. For instance, aberrations in GC B cell proliferation, differentiation or apoptosis can lead to uncontrolled GC responses and eventually lead to lymphomagenesis as additional mutations accumulate [138, 140, 176]. Such dysregulated GCs are also associated with a defect in GC shutdown.

Further, certain pathogens hijack GC machinery to remain protected. HIV virions in the FDCs remain protected for long-periods of time employing GCs as a reservoir and constantly infect the Tfh cells [61]. EBV has been shown to alter the GC B cell machinery and enhance the survival of virus infected cells by altering their apoptotic program [92]. Hence, better understanding of GCs have numerous implications ranging from targeting lymphomas, ectopic GCs, pathogens such as HIV and EBV that utilize the GC machinery.

Chapter 2

Agent-based model of GC reaction

Mathematical models are powerful tools used in the analysis of complex biological systems. A mathematical model is an abstract representation of the system of interest that is designed in order to address specific questions and predict unanticipated behavior of dynamical systems.

2.1 Agent-based models

Mathematical models can be differential equation or agent based. Agent-based models (ABMs) consider the individual entities of a system to study the consequence of their behavior and interaction dynamics. In this way, emergence of complex behavior from simple interaction rules are often observed, which is hard to predict by intuition and is the main feature that is making ABMs highly useful. The work presented in this thesis extended a previously developed ABM of GC reaction. The basic structure of the model is explained in this Chapter which forms the base for the extensions adapted in the upcoming Chapters.

2.2 GC model *Hyphasma*

2.2.1 Overview of the model

Hyphasma is an ABM of the GC reaction, which incorporates a detailed mechanism of GC B cell dynamics and selection. The basic versions of the model are introduced in [101, 107, 15]. This model has been parameterized to recapture several experimental results [154, 163]. Further, it has shown great predictive power and potential in explaining the mechanism behind experimental observations and testing the consistency of different hypotheses [133].

2.2.2 Spatial representation

ABMs are useful in investigating how the interactions between entities of a system result in an emergent spatial pattern. Considering the typical spatial organization of GCs with two distinct compartments - Dark zone (DZ) and Light zone (LZ) [18], role of cellular interactions in generating the spatial organization can be analyzed with the agent-based GC model. The model includes a 3D discrete lattice with central spherical portion representing the GC space where the B cells proliferate, mutate and undergo selection by interactions with FDCs and Tfh cells (Schematically shown in Figure 2.1). GC B cells in the model transition through different stages, as they interact with FDCs and Tfh cells.

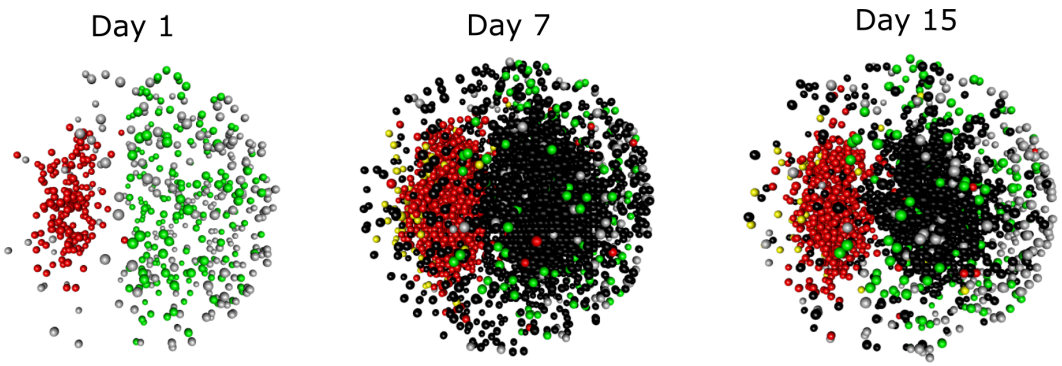

Figure 2.1: Visualization of different cell types in the lattice at 3 different time points (Days 1, 7 and 15) of the simulation. Sphere with each color represents a different cell type [red: centroblasts, green: FDCs, grey: Tfh cells, black: centrocytes and yellow: output cells].

Subsequently, differentiation of GC B cells into output cells lead to the exit of these cells from the GC. Radius of GC space is fixed to 160 µm and dimensions of each voxel is 5 x 5 x 5 µm. Volume of GC space is assumed to be constant while the number of GC B cells vary during the GC reaction. GC space is further subdivided equally into LZ and DZ.

2.2.3 Signal molecules in the lattice

Reaction diffusion models are used for describing the spatial distribution of molecules due to diffusion and are based on partial differential equations. Gradient of CXCL13 and CXCL12 signal molecules are calculated using a reaction diffusion system of equations resulting in the CXCL13 and CXCL12 concentration in each voxel of the above-described lattice. CXCL12 is produced by the stromal cells that are present in the DZ and FDCs are assumed to be the major producers of CXCL13. Due to this, the concentration of CXCL12 and CXCL13 are higher in the DZ and LZ, respectively. Different cell types/stages of the same cell have different sensitivities to these chemokines which govern the motility of these cell types. For instance, Tfh cells are sensitive to CXCL13 and hence, they tend to accumulate in the LZ where CXCL13 concentration is higher.

2.2.4 Properties of different cell types

Each individual cell is considered as an agent and is simulated following the rules determined based on experimental observations. While cell types such as the B cells and Tfh cells are considered motile, FDCs and stromal cells are considered immotile pertaining to their sessile nature. Motile cells respond to the chemokine gradient established on the lattice. B and Tfh cells occupy a single lattice voxel, however, FDCs occupy multiple lattice sites and form a network in the LZ of the GC space.

Follicular dendritic cells (FDCs)

FDCs are randomly distributed in the LZ region. As FDCs have dendrite like structures, FDCs are assumed to occupy multiple sites in the lattice. In the simulations, 200 FDCs are considered. For each FDC, the central soma is assumed to give rise to six dendrites. Soma occupies a single voxel. Each dendrite is assumed to be 40 µm long and is extended into 8 lattice sites from the soma along different directions. Each voxel occupied by a FDC would be referred here as a fragment of the FDC. A predefined total amount of antigen (usually 3000 antigen portions) is distributed equally between the different fragments of

the FDC at the start of the simulation. Each antigen portion corresponds to antigen concentration of 10^{-6} M. Uptake of antigen by an interacting B cell is assumed to take place with a probability dependent on the BCR affinity. Interaction with B cell and subsequent consumption of antigen, reduces the amount of antigen in a given fragment of FDC by one antigen portion. This results in a gradual decrease in the amount of antigen in the FDC during the course of the simulation. However, if the antigen amount at a given FDC site reduces below 20 antigen portions then the antigen acquisition probability is linearly reduced. In the basic version of the model, entire fraction of antigen in a given FDC is assumed to be presented on the surface in a static manner and is available for uptake by B cells. A dynamic antigen presentation due to cycling between the surface and interior of FDCs has also been implemented and is described in Chapter 4.

Tfh cells

In the model, 250 Tfh cells are considered. Number of Tfh cells is assumed to be constant throughout the GC reaction. Tfh interacts with neighboring GC B cells in the appropriate state. Tfh cells are assumed to be capable of being bound to multiple B cells at the same time. An interacting GC B cell receives signals from the bound Tfh, if the Tfh polarizes towards this GC B cell. Tfh is assumed to polarize only towards the B cell that has collected highest amount of antigen among all the bound B cells. Polarization state of Tfh is updated at every time step and GC B cell towards which Tfh polarizes receives 1 unit of Tfh signal. Hence, depending on the number of GC B cells, the competition for Tfh signals vary during the different stages of the GC reaction. Each GC B cell has an interaction period of 0.6 h. GC B cells failing to receive minimum Tfh signals of 0.5 at the end of the interaction time, become apoptotic. This is a simplified version of the model which considers only a single interaction of B cell with the Tfh cell. Other versions of the model used in Chapter 7 include interaction of B cells with multiple Tfh cells for a short duration and involves integration of signals collected from the individual interactions. pMHC dependent intensity of Tfh signaling is another assumption that is considered in Chapter 7. Tfh cells are assumed to be motile unless they are bound to GC B cells. Further, Tfh cells respond to CXCL13 signal gradient and have a tendency to accumulate in the LZ of the GC.

GC B cells

GC B cells exist in various states that have distinct properties. The different states considered include *Unselected*, *FDCcontact*, *FDCselected*, *TFHcontact*, *Selected* and *Apoptotic*, that distinguish the different stages of GC B cells during a GC reaction. As changes in GC B cell affinities due to SHM, is central to affinity maturation, affinity of each GC B cell is monitored and is updated when SHM takes place.

A 4D lattice is used for affinity representation [121] and for computing antigen binding probabilities (explained in Figure 2.2). Every B cell is assigned a position in the 4D space that represents its affinity. A central position is chosen for the antigen, which also corresponds to the position with highest possible affinity to the antigen. Mutations are accounted by random shift in the shape space position to one of the neighboring lattice sites. This affinity representation is referred to as the shape space representation.

To calculate the antigen binding probability, 1-Norm with respect to the optimal position $\|\phi - \phi^*\|_1$, which corresponds to the minimum number of mutations needed to reach the optimal clone is used. Antigen binding probability (a) of a given B cell as follows

$$a = e^{-\|\phi-\phi^*\|_1^2/\gamma^2} \tag{2.1}$$

where ϕ represents the shape space position of GC B cell and ϕ^* represents the optimal

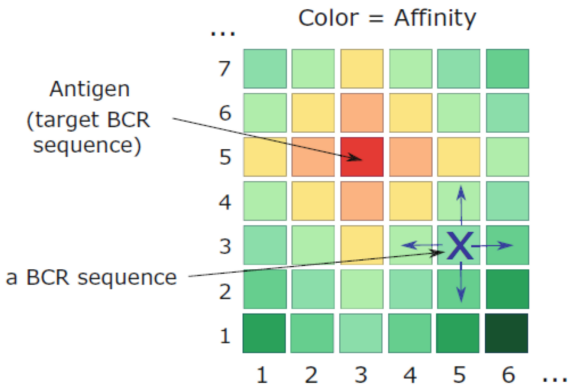

Figure 2.2: Simplified two-dimensional representation of the four-dimensional shape space used for affinity calculation. Position shown in red is the optimal position that represents the highest affinity towards the antigen considered. X represents the position corresponding to affinity of a B cell and the arrows denote the random directions the B cell is allowed to mutate its BCR. Figure reproduced from [133]. BCR: B cell receptor.

.

position. Value of γ is chosen as 2.8. Optimal position is taken as 3333 in single epitope simulations unless specified. To consider multiple epitopes in the simulations, many such optimal positions are chosen as in Chapter 6. As an alternative for the shape space, a sequence-based representation of GC B cell affinity was introduced in [132]. This representation considers a more realistic sequence and lattice-based model to calculate the binding energy of BCR sequences to a given antigen structure [132]. However, this sequence-based representation is not used in the work discussed in this thesis.

2.2.5 GC B cell state transitions

GC B cells transition through different states by following certain rules that are described below.

Influx and divisions

GC B cells enter the GC at a rate of 2 cells/h for a period of 96 h at the beginning of the simulations. These newly arrived GC B cells are in the DZ B cell state and undergo six divisions. During each cell division, BCR mutation is assumed to happen with a probability of 0.5. At the end of six divisions, DZ B cells transition to *Unselected* state.

Antigen collection and selection by FDCs

Unselected cells correspond to GC B cells entering the LZ and are in search for FDCs to collect antigen. An *Unselected* cell simply migrates, and if it comes in contact with FDC, it transitions to the state *FDCcontact*. *FDCcontact* state lasts for a fixed time period of 3 minutes after which the B cell detaches from the FDC. While in the state *FDCcontact*, B cell tries to capture antigen from the interacting FDC fragment with a probability calculated based on the BCR affinity. If the attempt is successful, the number of antigen units consumed by B cells is increased and the antigen in the interacting fragment of FDC is reduced by 1. At the end of the interaction period, the B cell switches from the state *FDCcontact* back to the *Unselected* state, to enable further antigen collection. However, there is an inactive time period of 1.2 minutes after every interaction, during which the B cell cannot establish further contacts with the FDC.

Such transitions between *Unselected* to *FDCcontact* and back to *Unselected* occurs multi-

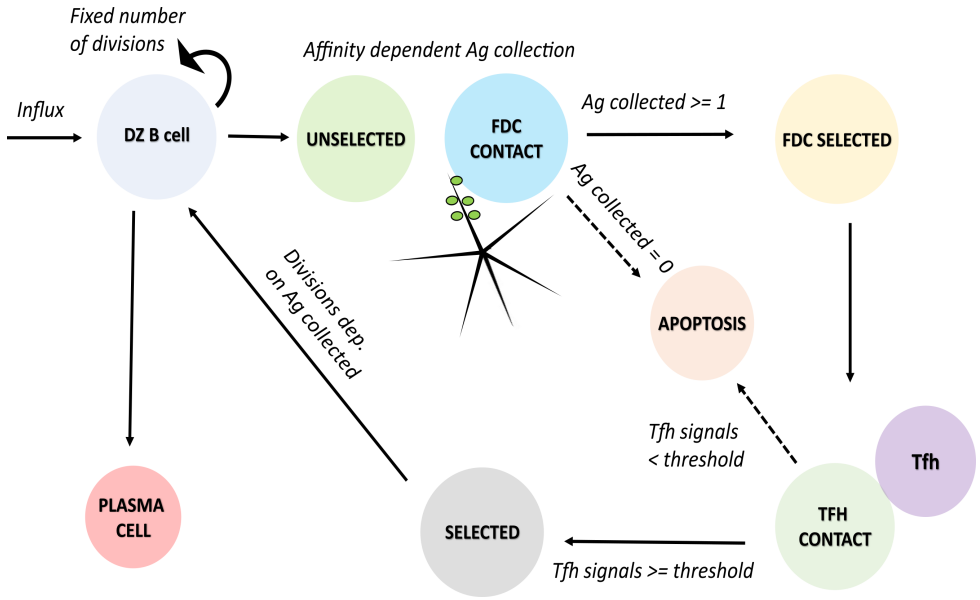

Figure 2.3: Schematic representation of different states of GC B cell and rules for transition between different states. DZ: Dark zone; Ag: Antigen; Tfh: T follicular helper cell.

ple times during a time period of 0.7 h referred to as the antigen collection period. At the end of the antigen collection period which is considered independently for each GC B cell, a decision is made and it takes the cell either to the apoptotic state or to the *FDCselected* state. If the cell has collected at least a single unit of antigen, it reaches the *FDCselected* state, otherwise the cell undergoes apoptosis. Apoptotic cells are left in the lattice for a duration of 6 hours, after which they are removed. This corresponds to the phagocytic activity of TBMs that clear apoptotic debris.

Alternatively, in a recent version of the model [103] used in Chapter 8, collection of antigen is not limited to *Unselected* state but continues in *FDCselected* state during search for Tfh help.

Selection by Tfh cells

FDCselected cells, migrate to interact with Tfh. When a *FDCselected* cell comes in contact with a Tfh, it remains bound for a period of 0.6 h and hence, switches to the state *TFHcontact*. B cell in *TFHcontact* might/might not receive signals from Tfh at every timepoint, which depends on competition with other B cells. At the time of detachment, if the B cell has received Tfh signals above a selection threshold which is set to 0.5, then the B cell transitions to the state selected. If the signals received are less than the selection threshold, the B cell goes to apoptotic state. Another recent improvement of the model (used in Chapter 8) is the incorporation of signaling molecules involved in GC B cell selection [103]. In the new version, dynamics of induction of signaling molecules such as cMyc, FoxO inactivation and mTOR activation are explicitly modeled by ODEs described in [103]. This includes three selection theories namely, DisseD, MiXed and BCinTime. In these three theories, a selection criteria is considered for the transition of B cells from *FDCselected* state to *Selected* state, and is checked when the decision time is reached. Decision time and selection criteria differ in the three theories. In the BCinTime theory, a hypothetical signal called differentiation signal is considered that increases over time for each *FDCselected* B cell. Acquisition of antigen slows down the increase in differentiation signal. When the differentiation signal reaches 1, the decision time is reached. *FDCselected* cells acquiring Tfh signals above a rescue threshold are selected. In the DisseD and MiXed

theories, while antigen acquisition leads to activation of mTOR and downregulation of FOXO, Tfh signaling activates mTOR and upregulates cMyc. Decision time is reached either when mTOR reaches 1 or when the time exceeds a fixed value of 18 h in DisseD theory. Alternatively, in the MiXed theory, this time period is not fixed and every antigen acquisition event extends the time by 0.5 h. Cells with cMyc and mTOR levels above threshold values are selected.

Return of selected cells to DZ

Selected cells return back to the DZ state and undergo further rounds of division with the number of divisions n_{divs} determined by the amount of antigen collected (p) during the selection process by interaction with the FDCs as follows.

$$n_{\text{divs}} = n_{\text{min}} + (n_{\text{max}} - n_{\text{min}})p^{\text{n}}/(p^{\text{n}} + K^{\text{n}}) \tag{2.2}$$

n_{min}=1 is the minimum number of divisions, n_{max}=6 is the maximum number of divisions, n=2 is the Hill coefficient and K=9 is the amount of antigen when n_{divs}=$n_{\text{max}}/2$. Alternatively, in Chapter 7, it is also assumed that Tfh signals received determine the number of divisions and in the DisseD and MiXed theories used in Chapter 8, cMyc levels determine the number of cell divisions. Before undergoing divisions, the selected cell remains in the state selected for a period of 6 hours after which it differentiates to the DZ state. During this period of delay in differentiation, B cells are assumed to go through the different stages of the cell cycle.

Cell divisions of selected cells and differentiation to output

GC B cell divisions are assumed to happen either symmetrically or asymmetrically. It is assumed that asymmetric division leads to unequal distribution of antigen collected to the daughter cells leading to different fates of the daughter cells. The daughter cell retaining the antigen differentiates to the output cells and the other daughter cell goes to the state *Unselected* for further rounds of selection and division. Seventy two percent of the divisions are assumed to happen in an asymmetric manner [107, 157]. In subsequent divisions of selected GC B cells, mutation probability p_{mut} is reduced from $p_{\text{max}} = 0.5$ based on the affinity of the B cell (a) using the following equation. Value of p_{min} is set to 0.

$$p_{\text{mut}} = p_{\text{min}} + (p_{\text{max}} - p_{\text{min}})a \tag{2.3}$$

2.2.6 Motility of cells

Motility of cells in the model is calibrated based on the data from imaging experiments and the position of the cells are updated at every time step. Each motile cell type is assigned a speed, which determines the movement probability at every time step of the simulation. Speed of the GC B cells, output cells and Tfh cells are 7.5 µm/min, 3 µm/min and 10 µm/min, respectively [108].

Each cell has a polarity that determines the direction of movement of the cell and this is updated depending on the persistence time of the cell. During the persistence time, the cells tend to maintain the same polarity and move in a relatively straight path. Persistence times are 1.5 min for B cells, 0.75 min for output cells and 1.7 min for Tfh cells [108]. Polarity of B cells is determined based on the chemokine distribution and the turning angle distribution measured from the experiments. The polarity vector obtained is thus a combination of randomly chosen polarity and polarity due to chemotaxis.

GC B cells are assumed to de- and re-sensitize towards the chemokines depending on the chemokine concentration at the position of the B cell. Threshold concentrations for de-sensitization are 6 nM and 0.08 nM for CXCL12 and 13, respectively. This is done to avoid the formation of cell clusters at the center of the LZ and DZ.

2.2.7 Antibody feedback

Output cells leaving the GC space, are allowed to differentiate into plasma cells with a rate corresponding to half-life of 24 hours. Plasma cells secrete antibodies with a fixed rate. Antibodies produced have a half-life ($t_{1/2}$) of 30 days (in Chapter 3) or 14 days (in Chapters 6 and 7) and hence, undergo degradation. As the antibodies produced might have a range of affinities depending on the affinity of the plasma cell that secretes them, in order to make the computation feasible, the antibodies produced are classified into 11 bins. Time evolution of antibody concentration $A(i)$ in each bin follows

$$dA(i)/dt = k_1 n_{\mathrm{p}}(i) - k_2 A(i) \tag{2.4}$$

n_{p} is the number of plasma cells with affinities corresponding to bin i, antibody production rate $k_1 = 10^{-17}$ mol/h per plasma cell and degradation rate $k_2 = \ln 2/t_{1/2}$. Binding of antibodies to the antigen held on FDCs is modelled by chemical kinetics equation as described below. Each bin is associated with a different k_{off} but has same k_{on}. k_{off} varies such that the dissociation constants are between $10^{-5.5}$ and $10^{-9.5}$ M. Immune complex formed with antibodies from bin i, C_{FDC} (i) is calculated as follows

$$dC_{\mathrm{FDC}}(i)/dt = k_{\mathrm{on}} G_{\mathrm{FDC}} A(i) - k_{\mathrm{off}}(i) C_{\mathrm{FDC}}(i) \tag{2.5}$$

where G_{FDC} is the antigen concentration in a single fragment of the FDC. Similar calculation is followed separately for each fragment of FDC. First term denotes the association of antibodies and antigen that happens with an association rate constant of k_{on}. Second term denotes the dissociation of antibodies from antigen with a rate constant of k_{off}. Formation of immune complex is assumed to decrease the concentration of free antigen while the dissociation increases the concentration of free antigen. Concentration of antibodies is assumed to be much higher than the antigen, hence, the decrease in concentration of antibodies due to immune complex formation is neglected.

2.2.8 Correction of artifacts in the lattice

Lattice discretization leads to artifacts in the simulations of ABMs. One typical lattice artifact is the aggregation of cells. This is prevented by using the exchange algorithm with a probability 0.5. If a cell is unable to move to the neighboring site due to the presence of another cell that attempts to move in the opposite direction, the lattice positions of the two cells are exchanged.

2.2.9 Simulation setup

At the beginning of the simulation, no B cells are present and Tfh cells are randomly positioned in the lattice. FDCs are randomly placed in the LZ region and the antigen is distributed on different fragments. Steady state concentrations of CXCL12 and CXCL13 calculated for each lattice position is used. Consumption of chemokines and feedback on the chemokine gradient was considered elsewhere [13] and neglected in this thesis. B cells enter the GC at a fixed rate for a certain time duration. Simulation is run for approximately 21 – 40 days and each time step correspond to a time interval of 2 x

10^{-3} hours. At every time step, properties of all the cells present are evaluated in a randomized sequence. The model described was further extended for the work presented in this thesis. The extensions are explained in detail in the following Chapters, which includes an extension of antigen presentation in the FDCs where antigen cycling was incorporated to account for the dynamic antigen presentation in Chapter 4. In addition, model of single GC presented here was extended to a network of asynchronous GCs and interaction among the simulated GCs due to the soluble antibodies which is described in Chapters 5 and 6.

Chapter 3

Role of soluble antibodies in GC shutdown

3.1 Abstract

Soluble antibodies act as important regulators of the humoral immune response. This Chapter focuses on the regulation of GCs by soluble antibodies secreted from plasma cells. Previously, it has been hypothesized that soluble antibodies might promote shutdown of GCs by masking the antigen on FDCs, thereby limiting antigen access of GC B cells. As antigen limitation might also be capable of improving affinity maturation due to increased selection pressure, it is unclear to what extent endogenous soluble antibodies impact GC kinetics and affinity maturation. We addressed this question using the agent-based model described in Chapter 2, by varying the antibody feedback strength and also by exploring the impact of soluble antibodies from early initialized GCs on a late formed GC as a consequence of asynchronous GC onset. Simulations suggested that soluble antibodies might promote earlier termination of GCs. Despite the higher selection pressure and potential for faster affinity maturation with high antibody feedback, the affinity maturation was largely impaired due to earlier termination of the GCs. This suggested that antibody feedback can impair the efficiency of GCs by promoting earlier termination.

3.2 Regulation of immune response by antibodies

Soluble antibodies are involved in the regulation of antibody responses. Depending on the isotype and experimental settings, antibodies can enhance or suppress the immune response by several folds [64, 65]. Antibody mediated regulation is clinically employed in the suppression of immune responses against Rh factors [24]. Extensive investigations by several research groups suggest that antibodies can regulate the humoral response via numerous mechanisms [64]. IgM has been found to enhance the immune response in a complement dependent manner [63]. Enhancement by IgG antibodies has been reported to occur by the ligation of Fc receptors on dendritic cells, thus promoting efficient antigen uptake resulting in enhanced activation of T cells [54]. Further, it has been shown that Fc mediated enhancement is IgG subtype dependent [54]. Antibody mediated enhancement has also been proposed to occur due to co-ligation of BCR and complement receptor on B cells [64]. On the other hand, suppression of immune response by antibodies can occur by the masking of antigen epitopes thereby preventing the antigen uptake by B cells, ligation of inhibitory FcγRIIB receptors on B cells and clearance of immune complexes by enhanced phagocytosis [65]. Epitope masking has been demonstrated as a convincing mechanism

of suppression by IgG soluble antibodies and it could even be non-specific under high-epitope density conditions [177, 11]. FcγRIIB mediated suppression is believed to control antibody production to maintain homeostasis rather than imposing suppression of normal immune response [64].

3.3 Antibody feedback on GCs

As the primary sites of humoral immune response are the GCs, soluble antibodies also regulate humoral response by modulating the GCs. Maternal antibodies suppress the infant's response towards vaccination by affecting GC responses [165].

Experiments by Zhang and Meyer-Hermann et al., suggested that passively administered antibodies are able to enter the GCs as they are found to be deposited on the FDC network and this impacted the GC size and affinity maturation [178]. In this study, the influence of endogenous soluble antibodies on the GC kinetics was demonstrated using mice that lack the ability to produce soluble antibodies. This suggested that endogenous antibodies might be involved in the regulation of magnitude of the GC response and might even be a potential signal that terminates GCs when the antibody concentration is high enough. Mathematical modeling supported this hypothesis and suggested that antibody feedback might induce the termination of GC reactions [178]. In this context, it has been suggested in earlier studies that when the antibody production by plasma cells leaving GCs rise high enough, then immune bridges are formed and the antigen is protected deep in the immune complexes [78].

As multiple GCs are formed in response to immunization, soluble antibodies might mediate intercommunication between GCs that are spatially separated [178]. GCs form asynchronously as seen in the kinetics of GC formation [126, 151] and hence, the impact of soluble antibodies on different GCs might not be the same and a higher impact on late initialized GCs might be expected. However, the precise impact of endogenous antibodies on GCs initialized at different time points is unknown.

3.4 Computational methods

GC model described in Chapter 2 was used and the evolution of GC was simulated for a time period of 21 days. For the antibody feedback, plasma cells produced from the simulated GCs secrete antibodies with a rate of 10^{-17} mol/h per plasma cell [133]. Antibodies undergo degradation and are assumed to have a half-life of 30 days. Further, antibodies are classified into 11 bins with different affinities. Dissociation constant of the bins are varied between $10^{-5.5}$ and $10^{-9.5}$ M.

It is also assumed that the antibodies produced are spread over the circulatory system of the organism under consideration and hence, the antibody concentration is homogenous. Binding and unbinding of antibodies, to and from the antigen was modelled by chemical kinetics as described in detail in Chapter 2.

Two different simulation set ups were used to study the role of endogenous soluble antibodies in GC regulation (schematically shown in Figure 3.1). In the first set up (shown in Figure 3.1 A), simulated GCs experience feedback by the soluble antibodies produced. N (scaling factor) is varied to scale up the antibodies produced from simulated GCs and subsequently the strength of antibody feedback, to study the impact of varying antibody feedback strength. Value of N could also be interpreted as the number of synchronous GCs. Hence, the higher the value of N, the higher is the overall antibody production and

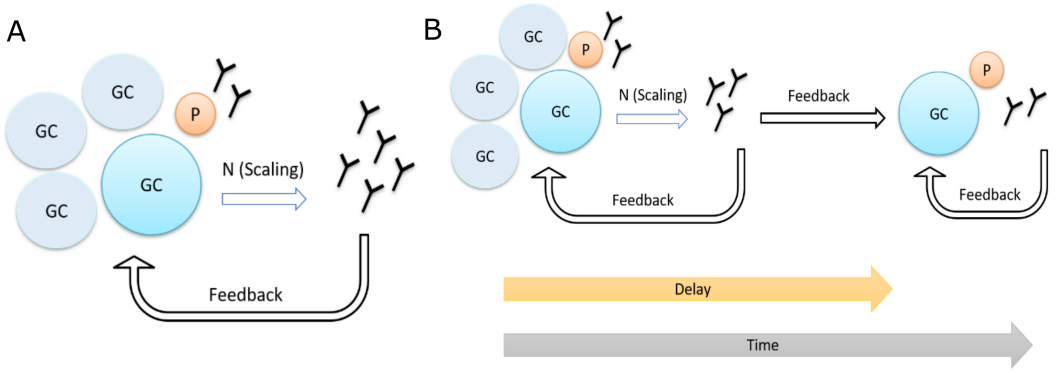

Figure 3.1: Schematic representation of the simulation set ups used in this study. In the set up shown in (A) antibody feedback strength is varied by changing the value of N (scaling factor) which influences the antibody production. In set up (B) impact of antibodies from early GCs on a late initialized GC is simulated. GC: Germinal centre.

the feedback strength on simulated GCs. This set up follows the simulations performed in [159] where an ODE-based model of GC reaction was used.

In the second set up shown in Figure 3.1 B, the impact of soluble antibodies from early initialized GCs on a late formed GC was simulated. In this case, early GCs are simulated as in set up shown in (A) and the antibodies produced from early GCs was used as an input while simulating the late initialized GC. The antibody concentration profile from the simulated early GCs was shifted depending on the delay in initialization of the late GC. Hence, the late GC simulated is under feedback by the self-produced antibodies and the antibodies produced by the early formed GCs. In the simulation of early initialized GCs, value of N was set to 300. The impact of antibodies from late initialized GC on the early ones was neglected.

In order to quantify the efficiency of GC reaction, we calculate a quantity termed immune power (IP) [159] which combines the quality and quantity of the GC output. It is defined as the fraction of antigen bound, when antibodies produced by the GC (without the scaling by N) is allowed to bind to a given concentration of test antigen. This is comparable to the Enzyme-linked Immunosorbent Assay (ELISA), where the presence of antigen specific antibodies in a given sample is detected and quantified using antigen coated wells. $G_{\text{bound}}(i)$ is the amount of antigen bound to the soluble antibodies in bin i and is calculated using the following steady state assumption

$$G_{\text{bound}}(i) = A(i)G/(K(i) + G) \tag{3.1}$$

where G is the amount of test antigen considered, $A(i)$ is the concentration of antibodies in bin i and $K(i)$ is the dissociation constant of bin i. Subsequently, Immune power IP is calculated as follows

$$IP = \sum_{\text{i}} G_{\text{bound}}(i)/G \tag{3.2}$$

3.5 Varying strength of antibody feedback

We varied the value of N from 1 to 300, to increase the concentration of antibodies produced which in turn determines the antibody feedback strength on the GCs. With lower feedback strength, fraction of antigen masked by soluble antibodies gradually increases and reaches a value of 0.65 on day 21 [Figure 3.2 A]. With increasing feedback strength, this fraction quickly reaches 1 and induces antigen limitation of the GC B cells [Figure 3.2A]. This enhances the apoptosis of GC B cells and also reduces average antigen uptake. As the number of cell divisions after selection by Tfh cells is assumed to depend on the amount of antigen collected, antigen limitation also impacts the maintenance of GCs by decreasing the number of divisions of selected cells.

Changes in apoptosis and GC B cell divisions are reflected in the volume kinetics of the GC reaction. Maximum size attained by the GCs is approximately similar with different antibody feedback strength [Figure 3.2B]. But at a later phase when the GC is contracting, GC volume decreases faster in the case of higher feedback strength. Hence, increased feedback strength promotes early termination of GCs and reduces the duration of the GC reaction.

Due to the reduced GC volume, production of output/plasma cells from the GC is remarkably reduced [Figure 3.2C]. Affinity of plasma cells produced is also slightly reduced with higher feedback strength [Figure 3.2D]. However, the effect of varying antibody feedback strength on affinity maturation is relatively weak when compared to the impact on GC volume kinetics and termination.

Due to the decreased antibody production (Figure 3.3A) and the small decrease in affinity, it is evident that the efficiency of GC reaction would be reduced with higher antibody feedback strength. To quantify the decrease in efficiency of the reaction, we calculated the IP (Immune power) using equation 3.2, as explained in section 3.4. Lower IP suggests a lower efficiency and as expected, the antibody feedback has decreased the efficiency of the GC reaction by impacting both the GC kinetics and the affinity maturation [Figure 3.3B]. These simulations show that the impact of antibody feedback on the GC B cell selection pressure is mostly detrimental for the GC reaction.

3.6 Delayed initiation

In the previous case, the impact of antibody feedback is higher after the GC reaches a peak volume as the feedback promoting antibodies are produced by the simulated GC itself. However, in a primary immune response, GCs are not formed in a synchronous manner and some late formed GCs might experience high antibody feedback at a very early phase as previously formed GCs would have already produced antibodies. To test the impact of antibodies from early GCs on a late formed GC, we performed simulations with varying extent of delay (varied from 0 – 120 hours) between the early and late GCs [Figure 3.4].

Similar to increasing antibody production, increasing the delay of initiation of late GC with respect to the early GC would result in an enhanced antibody feedback as more soluble antibodies are already produced when the late GC is initiated. As a result, the impact of antibody feedback on late GC is similar to the results in the previous section but was enhanced quantitatively.

With increasing delay of late GC initiation, duration of GC reaction is reduced as the late GC terminates earlier and there is also a decrease in the production of plasma cells [Figure 3.4B and C]. As opposed to the previous set up, the peak size attained by the GC is greatly reduced [Figure 3.4 B]. Mean affinity of plasma cells show a small increase

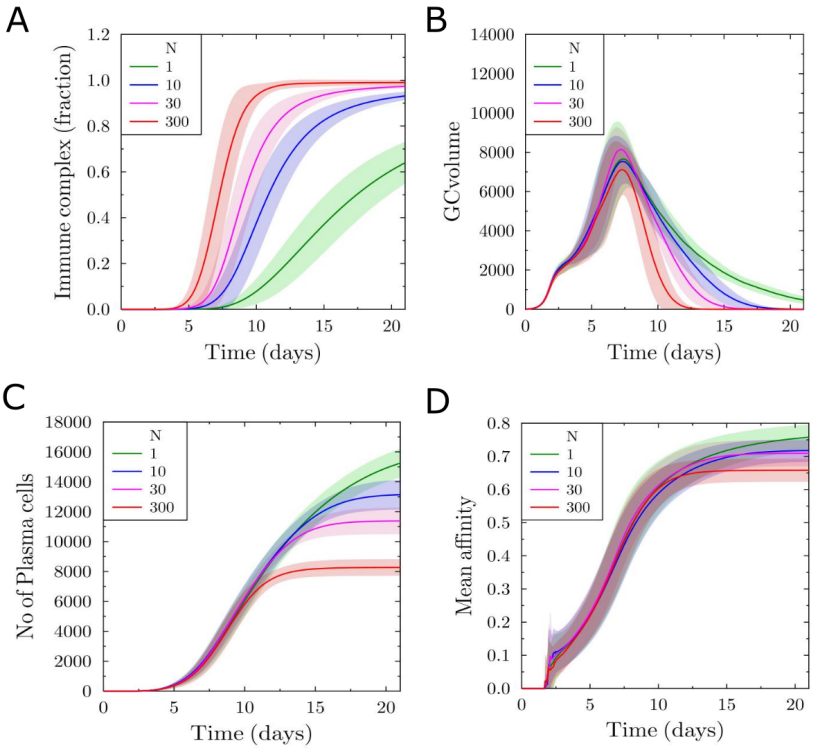

Figure 3.2: Impact of varying antibody feedback strength on the GC reaction. A) Fraction of FDC antigen bound by soluble antibodies, B) GC volume kinetics calculated as number of GC B cells, C) Number of plasma cells produced, D) Affinity of plasma cells produced. Solid line and the shaded area represent mean and standard deviation of 30 simulations. These simulations follow the setup shown in Figure 3.1 A. Figure reproduced from [7]. GC: Germinal centre; FDC: Follicular dendritic cell.

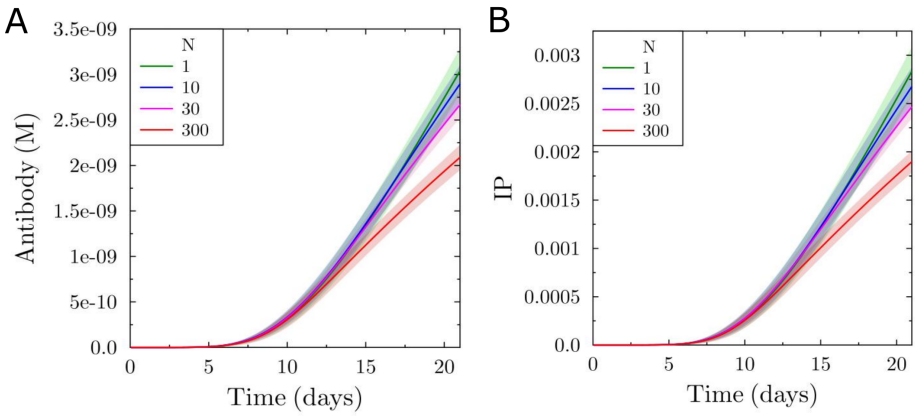

Figure 3.3: Antibody production (without considering scaling by N) and efficiency of GC in simulations with varying antibody feedback strength. A) represents antibodies produced from individual GCs and (B) shows the IP (Immune power), which is a measure of the efficiency of the GC reaction. Solid line and the shaded area represent mean and standard deviation of 30 simulations. Figure reproduced from [7]. GC: Germinal centre.

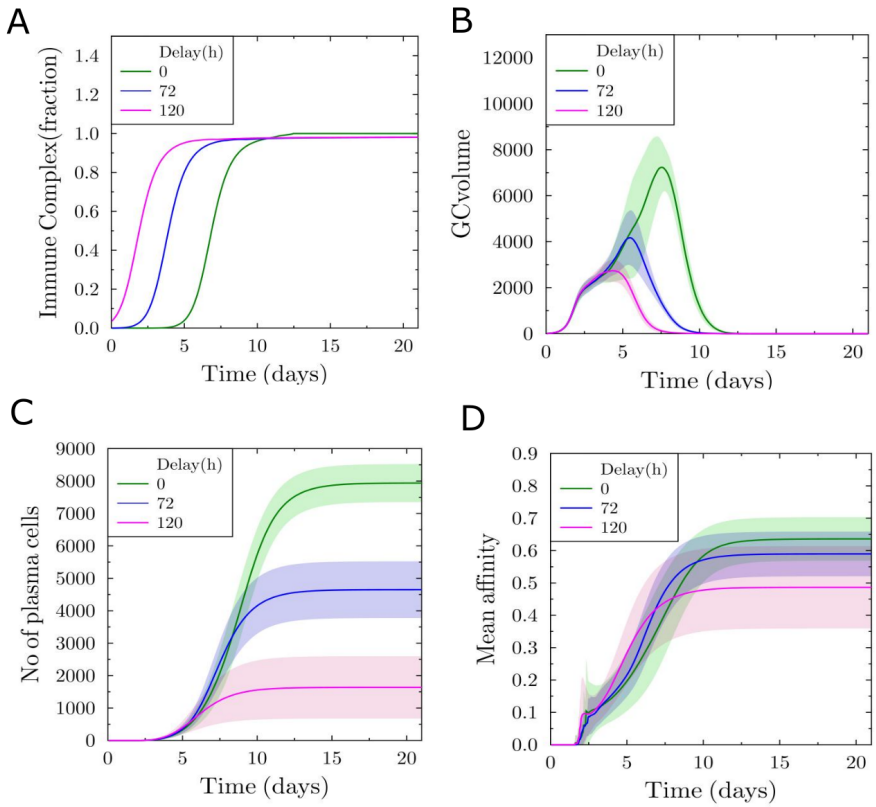

Figure 3.4: Impact of late initialization of a GC with respect to other GCs. A) Fraction of antigen bound by soluble antibodies, B) GC volume kinetics, C) Plasma cells produced and D) Mean affinity of plasma cells. These simulations follow the setup shown in Figure 3.1B. Solid line and the shaded area represent mean and standard deviation of 30 simulations. Figure reproduced from [7]. GC: Germinal centre.

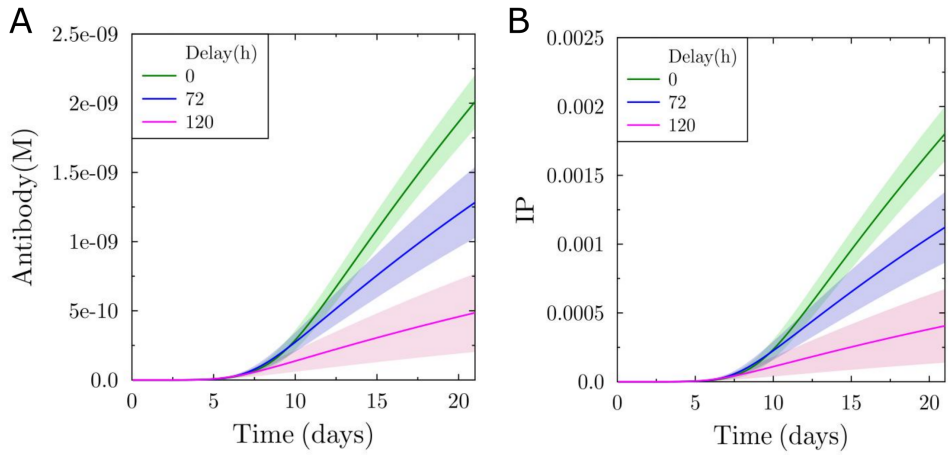

Figure 3.5: Antibody production (A) and efficiency of late initialized GC (B) in simulations corresponding to set up Figure 3.1B. Solid line and the shaded area represent mean and standard deviation of 30 simulations. Figure reproduced from [7]. GC: Germinal centre; IP: Immune power.

at early time points which is due to accelerated affinity maturation brought about by increased selection pressure due to the mild antigen limitation [Figure 3.4D]. However, the enhancement in affinity maturation doesn't persist longer because the GC reaction itself is terminated earlier. As a result, affinity of plasma cells observed at later time points is lower when the initiation is delayed. Consequently, the lower affinity and production of antibodies [Figure 3.5A] lead to a lower IP or efficiency of late initialized GC [Figure 3.5 B].

3.7 GC simulations with a large range of parameters

Results discussed in the previous sections showed that antibody feedback has a detrimental effect on the efficiency of GC reaction despite the small enhancement in affinity maturation seen at early time points. In order to test the validity of these findings over a large range of parameter values, we varied the N or scaling factor of early initialized GC and the delay of the late GC with respect to early GCs [Figure 3.6]. Plasma cell affinity of late GC showed different behavior on day 5 and day 21 as predicted in earlier simulations [Figure 3.6A and B]. On day 5, with increasing feedback strength on late GCs (higher N and higher delay), binding probability of plasma cells was increased by 50 % [Figure 3.6A]. On day 21, this trend was reversed and higher feedback strength resulted in 50 % reduction in binding probability [Figure 3.6B].

In order to check the impact on efficiency of late GC, we calculated the IP at different time points. As opposed to the mean affinity of plasma cells, IP or efficiency was consistently lower on day 5 and day 21 [Figure 3.6C and D]. Importantly, the small enhancement in affinity maturation was insufficient to improve the efficiency of the GC reaction.

3.8 Conclusions

Simulation results predict that antibody feedback might be detrimental for the efficiency of GC reaction due to earlier termination, despite the small enhancement in affinity mat-

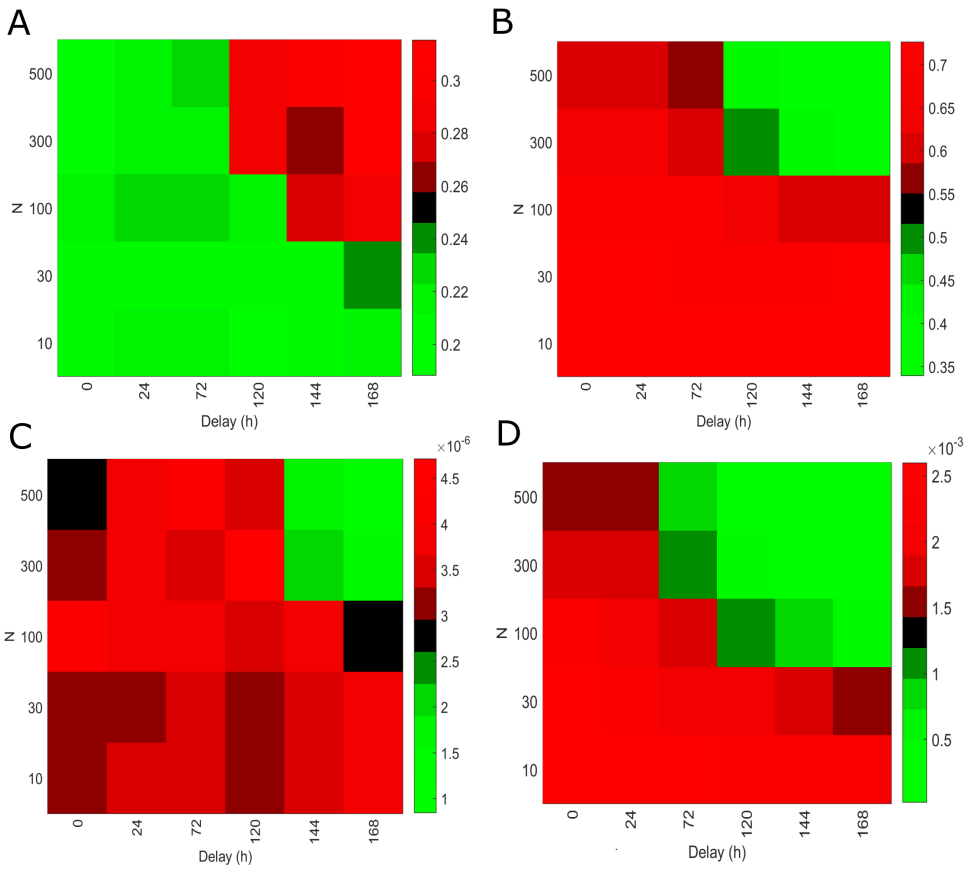

Figure 3.6: Affinity of plasma cells produced and efficiency of GC reaction with varying feedback strength and delay in initialization with respect to other simulated GCs. A) and B) are the affinity of plasma cells on day 5 and day 21 respectively. C) and D) are the efficiency (IP) of the GC on day 5 and 21 respectively. N represents the scaling factor used for the simulation of early GCs. Delay is the time delay in initialization of late GC with respect to the early GCs in hours. The readouts correspond to the late initialized GC in setup Figure 3.1B. Figure reproduced from [7]. GC: Germinal centre; IP: Immune power.

uration. This result contradicts with the expectation that antibody feedback might also accelerate and promote affinity maturation in a long term. It remains to be explored under what conditions antibody feedback can promote better affinity maturation despite the early termination.

Antibody mediated suppression of GC response was higher on a late initialized GC suggesting that the extent of synchronization of GCs would influence the overall GC response, if the GCs interact and influence each other by the production of soluble antibodies. Moreover, high antibody feedback at a late phase hardly impacted affinity maturation of B cells in the GCs. On the other hand, antibody feedback has a higher impact if the GC experiences high antibody feedback at early phases as in the case of a late initialized GC under feedback by antibodies from early initialized GCs. Among the two cases simulated here, the impact of antibody feedback on the GC of interest was different and the suppression was higher for a late initialized GC. This suggests that the response of GC to antibody feedback could vary depending on the phase of the GC reaction and the feedback strength.

A limitation of this study is that only the influence of early GC derived antibodies on late GC was explored and the impact of late GC produced antibodies on early GCs was neglected. This assumption is justified here as the antibody production from early initialized GCs was much higher than the late initialized GC. This could be interpreted as the impact of several early synchronously initialized GCs on a late initialized GC. However, the impact of soluble antibodies on individual GCs in a system of asynchronously developing GCs is unknown and will be addressed in Chapter 6.

Chapter 4

Immune complex cycling in FDCs

4.1 Abstract

Follicular dendritic cells (FDCs) are stromal cells present in primary and secondary B cell follicles including GCs. FDCs are known for their specialized ability to trap native antigen in the form of immune complexes (ICs) and retain the acquired ICs intact for a long period of time. As FDCs constantly supply B cells with ICs, they are considered crucial for the maintenance of GC reactions. Heesters et al., have shown that ICs in FDCs undergo cycling and suggested that this mechanism can extend the half-life of antigen in FDCs. Mechanism of IC cycling and its implications on GC reaction are unknown. To further characterize IC cycling, the time scale of cycling was estimated here. Although, periodic internalization might protect the ICs from degradation, it is not known how efficiently the ICs can be protected as extracellular presentation is also critical for IC uptake by GC B cells. To address this question, in this study, GC simulations were performed in the presence of antigen cycling and the impact of changes in antigen cycling kinetics on the GC dynamics and shutdown was also investigated. Simulation results predict that the extent of antigen protection and impact on GC kinetics vary with the antigen cycling kinetics. Further, blocking antigen cycling was able to terminate GC reactions suggesting that it could be a potential therapeutic target to disrupt pathologic GCs.

4.2 Characteristics of FDCs

FDCs originate from perivascular precursor cells or marginal reticular cells [74, 81] and form an extensive network in the B cell follicles and the GCs [30]. They have extended dendrite like structures [21] that make them resemble neurons of the nervous system. FDCs host antigen in the form of ICs which is non-uniformly distributed on the FDC surface [93]. Phan et al., discovered complement mediated transport of ICs where subcapsular sinus macrophages acquired the ICs and transferred them to the follicular B cells that bind ICs via the complement receptors [122]. Subsequently, FDCs acquired the ICs from the B cells [62, 122]. However, studies have shown that the mechanism of transport of antigen particles into the B cell follicles vary depending on nature and size of the antigen particles [50, 49, 85].

ICs in FDCs are considered important for efficient antibody and memory responses [79]. On the other hand, FDCs are also capable of producing various signaling molecules and hence, role of FDCs other than IC trapping have also been recognized [79]. FDCs supply B cells with the cytokine BAFF [52], that enhances the survival of B cells. FDCs have also been shown to maintain the follicular structure [167]. FDCs express an array of surface

markers such as CD23, ICAM-1 and VCAM-1, whose expression changes during the course of the GC reaction [18, 38, 45]. Maintenance of FDC network has been found to depend on the lymphotoxin signaling via B cells [39, 48, 14]. In the GCs of Peyer's patches, FDCs have also been shown to sense environmental stimuli such as bacterial products and respond by changes in gene expression profile and cytokine production [150].

4.3 Immune complex cycling in FDCs

Cycling of ICs in FDCs was demonstrated by Heesters et al., using a series of *ex vivo* experiments [62]. The authors showed that blocking the internalization of antigen in FDCs impaired the antigen uptake from B cells. Further, treatment with cytochalasin, an actin inhibitor resulted in blockade of the cycling process [62]. However, the exact mechanism of IC cycling is unknown. Although, cycling of ICs in FDCs was first discovered in murine FDCs, it was later confirmed with human FDCs [61]. FDCs from human patients infected with HIV harbored HIV virions in the cycling compartments [61] which suggests that HIV virions can be protected by the cycling mechanism of FDCs. This finding further highlighted the clinical importance of understanding the mechanisms that control antigen cycling to target these pathogenic agents.

Zhang et al., studied the distribution of antigen tagged nanoparticles of varying sizes in the FDCs and found that larger size particles mostly localized on the surface of FDC dendrites [179]. On the other hand, comparatively smaller particles were distributed between the interior and surface of FDCs [179]. This suggested that antigen retention and localization varied with the size of antigen particles and antigen presentation kinetics likely varies for different antigen particles. Hence, knowledge of the implications of antigen cycling on GC responses would be invaluable for designing antigen particles to enhance the GC responses towards vaccination.

4.4 Estimation of IC cycling times

A two-state model [Figure 4.1A], where antigen particles undergo transition between two states was used to estimate the time scale of the cycling process in FDCs. Surface and interior are the two states considered in the model that represent the surface and interior of FDCs. t_{surface} and t_{interior} are the residence time of antigen particles in the states surface and interior, respectively. t_{surface} and t_{interior} are sampled from Gaussian distributions $N(\mu_{\text{s}}, \sigma_{\text{s}})$ and $N(\mu_{\text{i}}, \sigma_{\text{i}})$. *In silico* simulations were performed following the *ex vivo* experimental protocol in [62] to identify the parameters μ_{s}, μ_{i}, σ_{s} and σ_{i} that best reproduces the experimental data.

In silico simulations and the corresponding experimental protocol are explained in detail below.

Sequential staining simulation

In sequential staining experiments, the authors used antibodies (labelled green, blue and red) to stain the IC particles on the surface of FDCs [62]. In the simulation, each staining antibody was added for a time period of 5 minutes sequentially following the experimental protocol. The staining periods were separated by intervals of 60 min duration where no antibody was added. During the staining periods, the antigen particles in the state surface acquired the corresponding color of the antibody added. Hence, the binding probability of staining antibodies were assumed to be 1. At the end of the staining steps as done in the experiment, the color combination of the individual IC particles was examined and classified based on the colors acquired.

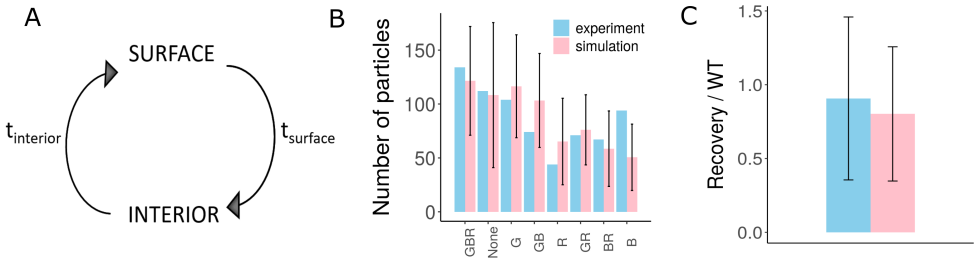

Figure 4.1: A) Schematic representation of the model used to estimate cycling times. t_{surface} and t_{interior} represent the residence times of antigen particles in the states surface and interior, respectively. B and C) Comparison of experimental data with simulation results for the parameter set with lowest cost compared to experimental data from [62]. B) Outcome of the sequential staining simulation where FDCs were sequentially treated with different staining antibodies. Readouts represent the number of IC particles stained with antibodies leading to the color combination shown below the bars (G-Green, B-Blue and R-Red). C) Results of acid wash simulations that follow the experiments where FDCs were briefly treated with acid to remove surface bound IC particles followed by recovery. Readout represents the recovery of surface antigen after acid wash followed by a recovery period, normalized with WT where no acid wash was performed. MFI from acid wash and recovery sample from the experimental data was normalized with the MFI from control experiment. Each simulation was repeated 100 times. IC: Immune complex; WT: Wild type; MFI: Mean Fluorescence Intensity; FDC: Follicular Dendritic Cell.

Acid wash simulation

Heesters et al., performed experiments where the cultured FDCs loaded with ICs were treated with acid buffer briefly to remove the surface bound IC particles [62]. Following a recovery period of 30 minutes, the reappearance of ICs from the interior to the FDC surface was monitored by quantifying the mean fluorescence intensity MFI [62]. In the simulations, acid wash was performed by removing antigen particles in the state surface. The system was allowed to recover for the next 30 minutes after which the number of antigen particles in the surface and interior of FDCs were quantified.

Parameter selection

Residence times were varied for the above-described simulations and the cost of the simulation results (S_{k}) with respect to the experimental data (E_{k}) was calculated for each parameter set as follows.

$$cost = \sum_{\text{k}=1}^{\text{n}} ((E_{\text{k}} - S_{\text{k}})/E_{\text{k}})^2 \tag{4.1}$$

where n is the cumulative number of experimental data points. Parameter sets were ranked based on the calculated cost. Parameter set with average residence times 36 and 21 minutes in the FDC interior and surface, had the lowest cost among the parameter combinations tested. The simulation results for this particular parameter set are shown in Figure 4.1B and C. There was a small deviation in the simulation prediction with respect to the mean of the number of particles labelled only by the blue antibodies (B). However, it could not be improved by the other variations of the model tested such as a bimodal distribution for residence times in state interior, changes in initial distribution of antigen

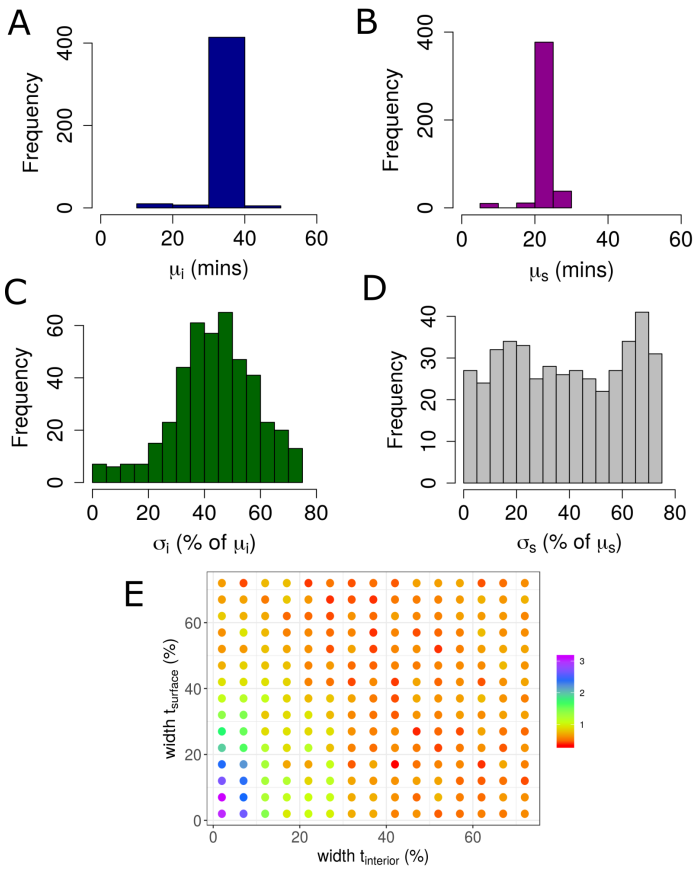

Figure 4.2: Distribution of estimated parameters. A) Average residence time of antigen in the interior μ_{i}, B) Average residence time on the surface μ_{s}, C) Width of the distribution for residence time in FDC interior σ_{i}, D) Width of the distribution for residence time on FDC surface σ_{s} and E) Cost of the best parameter set obtained when width of distribution of the residence times are varied. Cost is calculated with respect to the experimental results using equation 4.1. FDC: Follicular Dendritic Cell.

particles in the states surface and interior or binding probability of staining antibodies. ΔAIC (Akaike information criterion) value of each parameter set with respect to the lowest cost parameter set was calculated and the parameters sets with $\Delta AIC < 2$ were chosen as the final estimates. The distribution of parameters that satisfied this criterion is shown in Figure 4.2A-D. Variability in transition times was necessary to reproduce the data as the data could not be fitted with σ_{s} and $\sigma_{\mathrm{i}} = 0$. However, cost of the parameter sets estimated were similar when σ_{s} and σ_{i} were $> 40\%$ of the corresponding mean [Figure 4.2E].

4.5 Model of GC reaction with antigen cycling in FDCs

GC model described in Chapter 2 was extended by incorporating the dynamic antigen presentation in FDCs. In the GC model, FDCs consist of different fragments that occupy multiple lattice sites. In the absence of antigen cycling, antigen is distributed in each fragment of the FDC and the antigen concentration is constant unless it is reduced due to the consumption by B cells. In the new representation with antigen cycling, only a portion of antigen at a particular site is available for the GC B cell and the rest of the

antigen is in an internalized state. Surface antigen amount A_{surface} on FDCs changes due to the periodic internalization and externalization and is calculated using the following equation.

$$dA_{\text{surface}}/dt = k_{\text{ext}}(A_{\text{Total}} - A_{\text{surface}}) - k_{\text{int}}A_{\text{surface}} \tag{4.2}$$

A_{Total} is the total antigen amount on each FDC which includes surface and internalized antigen. The internalization and externalization rates (k_{int} and k_{ext}, respectively) were calculated using the average residence times estimated in section 4.4. Calculated surface antigen amount is distributed between the different sites of each FDC at every time step. When a B cell consumes antigen, surface antigen and total antigen amount in the FDC are reduced by one unit.

4.6 Simulations with antigen cycling

To study the impact of dynamic antigen presentation on GCs, simulations were performed in the presence and absence of cycling [Figure 4.3]. The different scenarios compared are schematically shown in Figure 4.3G. In the simulations labelled 'No cycling', entire fraction of total antigen is displayed on the FDC surface and remain available to the GC B cells at every time point. After the initial distribution of antigen among different FDC sites, the antigen remains within the same FDC site. However, antigen concentration at a given FDC site can decrease due to the consumption of antigen by GC B cells. In the simulations with label 'Cycling', antigen cycling is considered. Thus, depending on the rate constants of internalization and externalization, only a portion of antigen is displayed on the FDC surface. Moreover, the antigen is redistributed between the different sites of the same FDC at every time step. In order to distinguish the effects due to redistribution of antigen and due to changes in the surface antigen concentration, a control simulation 'No cycling (redist)' was performed, that is similar to the 'No cycling' simulations but the antigen is redistributed (redist) at every time step among the different sites of the same FDC.

Despite the reduced surface antigen concentration in GC simulations with cycling ('cycling') [Figure 4.3B], there was an increase in GC volume at the peak of the reaction and at later time points [Figure 4.3A]. Further, in the presence of antigen cycling, the plasma cell production was enhanced when compared to the absence of antigen cycling [Figure 4.3D]. However, control simulation with no cycling but with redistribution of antigen 'No cycling (redist)' was very similar to the simulation results of antigen cycling 'Cycling', suggesting that the enhancement in GC volume and plasma cell production seen in the case of antigen cycling is due to the redistribution of antigen on the surface of FDCs. This suggests that the decrease in surface antigen concentration, due to antigen cycling does not directly impact the GC reactions. However, the redistribution of antigen on the surface of FDCs due to internalization and reappearance on surface might enhance the GC reaction and increase the plasma cell production.

4.7 Simulations with different cycling rates

Impact of changes in antigen cycling kinetics on GC reactions was tested by choosing different cycling times as follows

1) I-10 S-50: Average residence time of antigen in the interior (I) and surface (S) are 10 and 50 minutes, respectively. In this case, proportion of antigen is higher on the surface at any time point [Figure 4.4A].

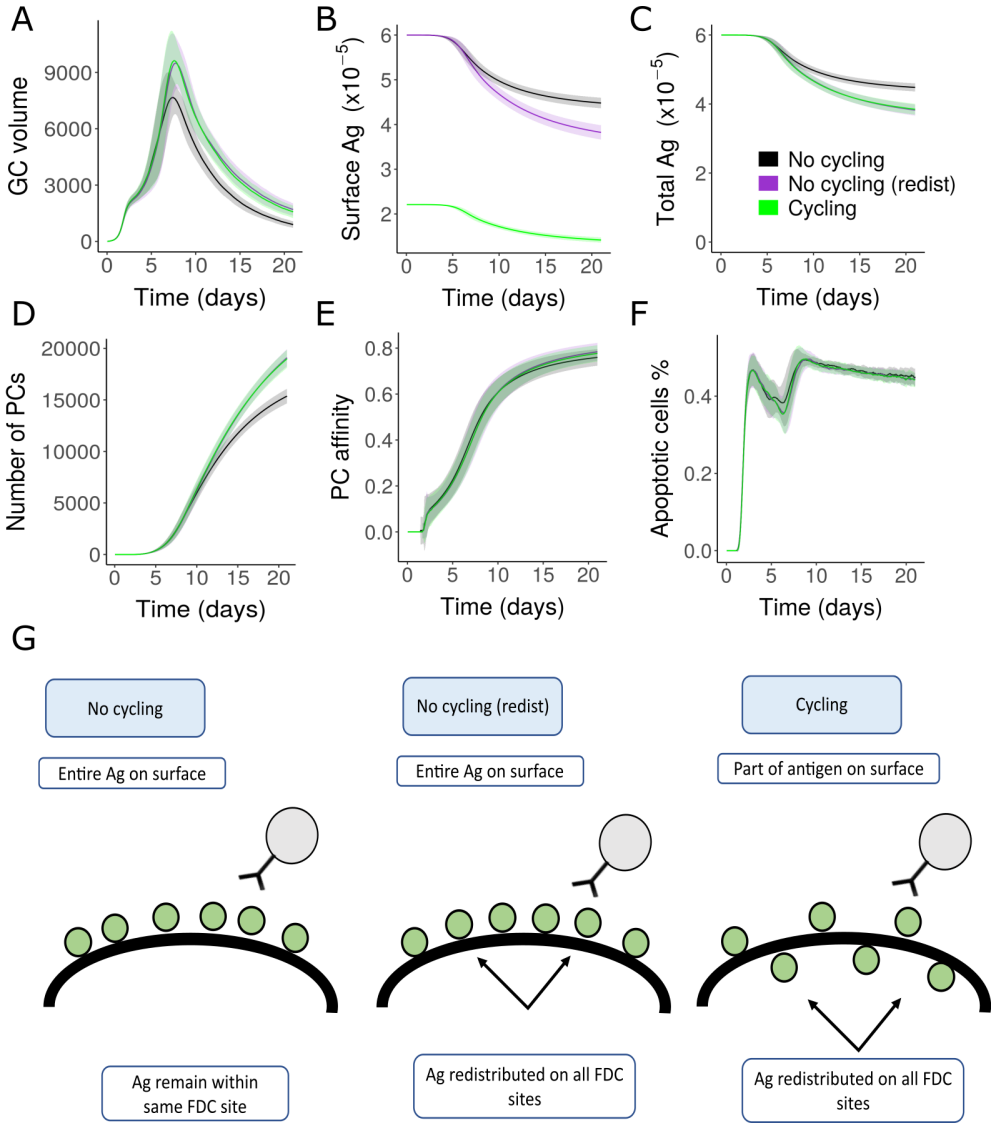

Figure 4.3: Comparison of GC simulations with and without antigen cycling. A) GC volume B) Surface antigen amount from all FDCs C) Total antigen amount on FDCs. This includes both internalized and surface antigen amount. D) Number of plasma cells E) Affinity of plasma cells and F) Percentage of apoptotic cells. Schematic representation of the antigen distribution and localization in the different scenarios compared are shown in (G).Total antigen amount in each FDC is 3000 antigen portions. Solid line and the shaded area represent mean and standard deviation of 100 simulations. GC: Germinal centre; FDC: Follicular dendritic cell; Ag: Antigen; PC: Plasma cell.

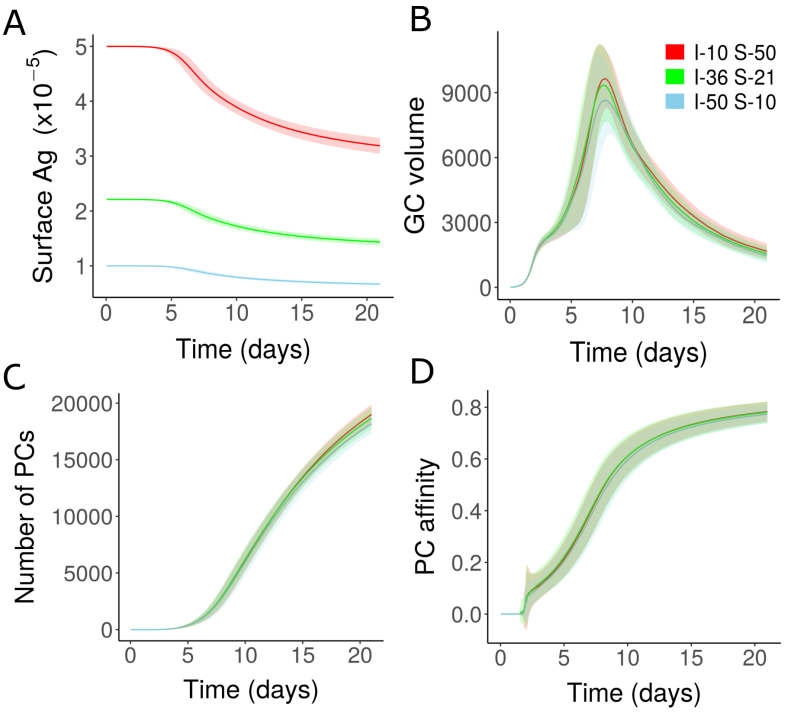

Figure 4.4: Effect of varying cycling kinetics on GC reactions. A) Surface antigen amount B) GC volume kinetics C) Number of plasma cells produced and D) Mean affinity of plasma cells. Cycling times are shown in the inset. I represent the average residence time of antigen in the FDC interior in minutes and S represents the average residence time on FDC surface. Total antigen amount in each FDC is 3000 antigen portions. Solid line and the shaded area represent mean and standard deviation of 100 simulations. GC: Germinal centre; FDC: Follicular dendritic cell; PC: Plasma cell; Ag: Antigen.

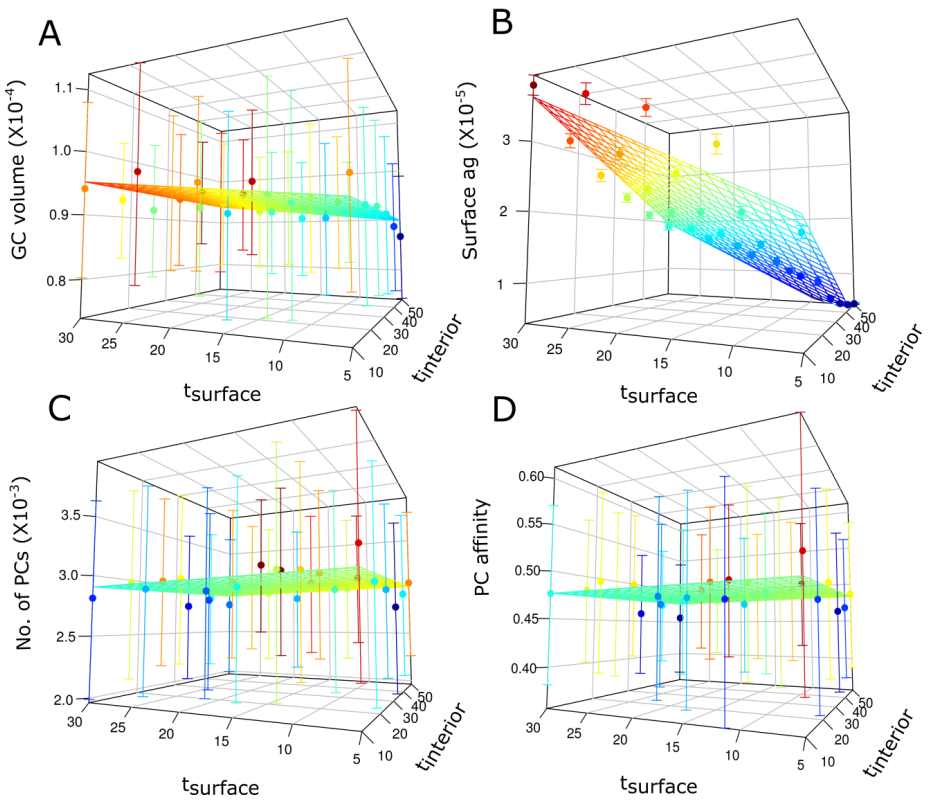

Figure 4.5: GC simulation readouts on day 8 for the estimated range of cycling kinetics. A) GC volume B) Surface antigen amount C) Number of plasma cells produced and D) Affinity of plasma cells. Simulation mean is shown as dots and the error bar is the standard deviation. Each simulation was repeated 100 times. Surface represents the regression plane calculated using the simulation readouts and the color represents the value of corresponding GC readouts in vertical axis. t_{surface} and t_{interior} are shown in minutes. Total antigen amount in each FDC is 3000 antigen portions. GC: Germinal centre; FDC: Follicular dendritic cell; PC: Plasma cell; Ag: Antigen.

2) I-36 S-21: This follows the average residence times estimated from the PE-IC data. Average residence time of antigen particles is slightly longer in the interior (36 minutes) when compared to the time spent on the FDC surface (21 minutes).

3) I-50 S-10: Average residence time in the interior (50 minutes) is higher than the residence time on FDC surface (10 minutes).

Consistent with the results in the previous section, changes in cycling kinetics did not directly impact the GC reactions [Figure 4.4B-D], although there were large changes in surface antigen concentration [Figure 4.4A].

These findings were verified over a larger range of parameters by varying the cycling times in the range estimated in section 4.4. Despite the large changes in surface antigen concentration there were only small differences in the GC volume, number and affinity of plasma cells at day 8 and day 21 of the GC reaction [Figure 4.5 and Figure 4.6]. A similar analysis was performed with lower antigen concentration on FDCs [Figure 4.7]. With lower antigen concentration, there were small differences in GC readouts with different cycling kinetics. In this case, plasma cell production from the GC was higher if the surface antigen concentration was higher [Figure 4.7C]. This is likely because with limiting antigen concentration, antigen uptake by GC B cells is impaired if the externalization of antigen

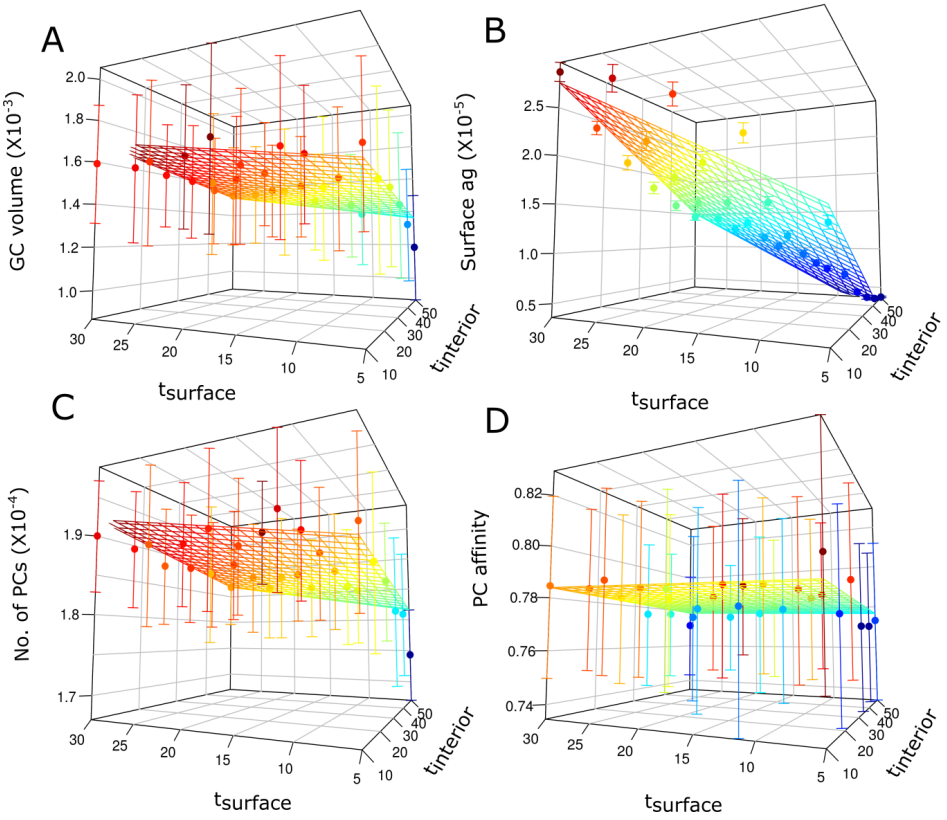

Figure 4.6: GC simulation readouts on day 21 for the estimated range of cycling kinetics. A) GC volume B) Surface antigen amount C) Number of plasma cells produced and D) Affinity of plasma cells. Simulation mean is shown as dots and the error bar is the standard deviation. Each simulation was repeated 100 times. Surface represents the regression plane calculated using the simulation readouts and the color represents the value of corresponding GC readouts in vertical axis. t_{surface} and t_{interior} are shown in minutes. Total antigen amount in each FDC is 3000 antigen portions. GC: Germinal centre; FDC: Follicular dendritic cell; PC: Plasma cell; Ag: Antigen.

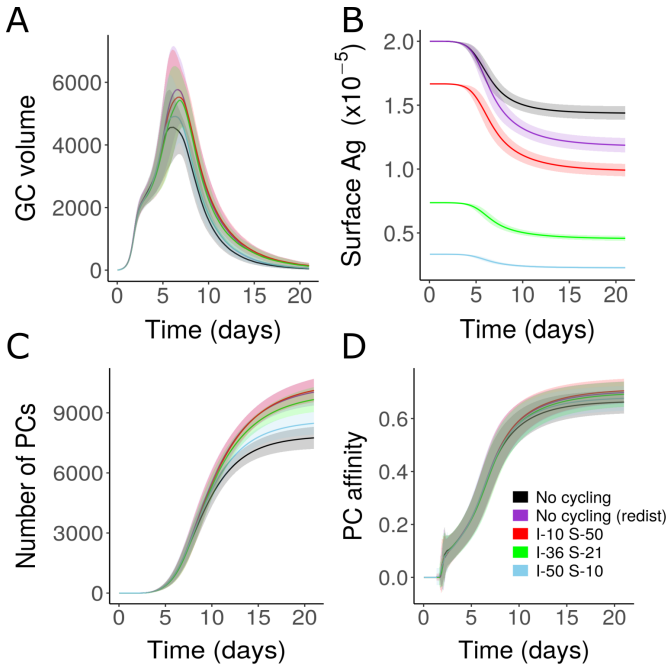

Figure 4.7: GC simulations with varying cycling times as in Figure 4.4 but with limiting antigen concentration. A) GC volume B) Surface antigen amount C) Number of plasma cells and D) Affinity of plasma cells. Inset shows the cycling times. Antigen amount on each FDC was 1000 antigen portions. Solid line and the shaded area represent mean and standard deviation of 100 simulations. GC: Germinal centre; FDC: Follicular dendritic cell; PC: Plasma cell; Ag: Antigen.

happens at a slower pace. However, cycling dynamics does not have any direct impact on the GCs if the antigen concentration is not limiting.

4.8 GC simulations with antigen degradation

As the antigen on extracellular surface of FDCs might not be stable, surface antigen was assumed to be prone to degradation, and the ability of antigen cycling to efficiently protect antigen without impairing antigen uptake of GC B cells, was tested. Surface antigen was assumed to undergo degradation with a fixed rate determined by the half-life chosen as follows.

$$dA_{\text{surface}}/dt = -k_{\text{deg}} A_{\text{surface}} \tag{4.3}$$

where degradation rate constant $k_{\text{deg}} = \ln 2/t_{\text{deg}}$ and t_{deg} is the half-life of antigen. When the half-life of antigen was fixed to 8 days, the extent of antigen degradation varied with the cycling kinetics as the surface antigen concentration varies [Figure 4.8 A and B]. Degradation was higher, when the average residence time of antigen on the surface was higher. Hence, depending on the cycling kinetics, antigen can be protected from degradation by minimizing surface exposure. In such cases, when antigen spends a longer time in interior, GC volume and plasma cell production are higher and GC shutdown is delayed [Figure 4.8].

In similar simulations with lower surface antigen concentration, GC output was slightly higher when the cycling times were 36 minutes on FDC interior and 21 minutes on the

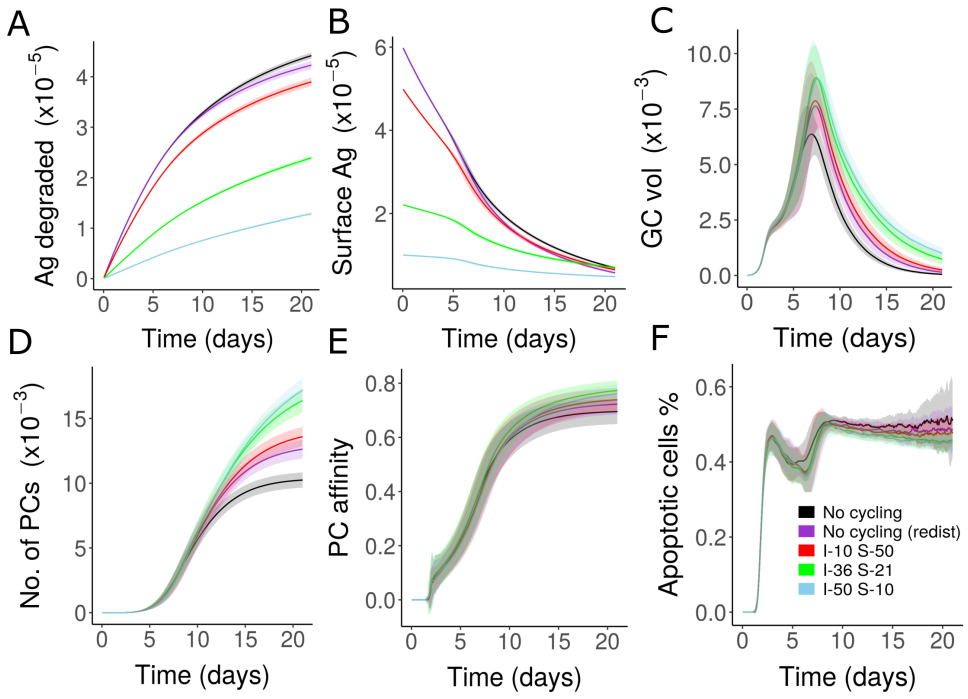

Figure 4.8: GC simulations with antigen degradation for varying cycling kinetics A) Amount of antigen degraded B) Surface antigen amount C) GC volume kinetics D) Number of plasma cells E) Affinity of plasma cells and F) Percentage of apoptotic cells. Inset shows the cycling times. Solid line and the shaded area represent mean and standard deviation of 100 simulations. GC: Germinal centre; PC: Plasma cell; Ag: Antigen.

surface [Figure 4.9D] as opposed to the previous case with higher antigen concentration [Figure 4.8D]. This is because with low antigen concentration, if a large proportion of antigen is in the interior, this negatively impacts the GC reaction due to reduced antigen uptake by GC B cells despite a better protection of antigen from degradation.

4.9 GC simulations with varying antigen half-lives

When antigen half-lives were varied, the GC output and volume were higher in the case where the antigen residence time in the interior is longer [Figure 4.10A-C]. However, this is not consistently the case in the presence of low antigen concentration [Figure 4.10D-F]. These results suggest that there is a trade-off between extracellular and intracellular antigen localization, that influences the GC reaction by affecting the balance between antigen protection from degradation and availability for GC B cells.

4.10 *In silico* antigen cycling blockade

To predict the impact of antigen cycling blockade, an *in-silico* blockade was performed, where the internalization and externalization of antigen were blocked [Figure 4.11]. This blockade was performed at different time points and the influence on GC kinetics and output were monitored. Blockade of antigen cycling resulted in earlier termination of the GC reaction [Figure 4.11A]. There was also a reduction in the plasma cell production [Figure 4.11C] and a small decrease in the affinity of plasma cells produced [Figure 4.11D].

Instead of blocking both externalization and internalization of antigen, if only the externalization of antigen is blocked [Figure 4.12], GC termination occurred earlier than in

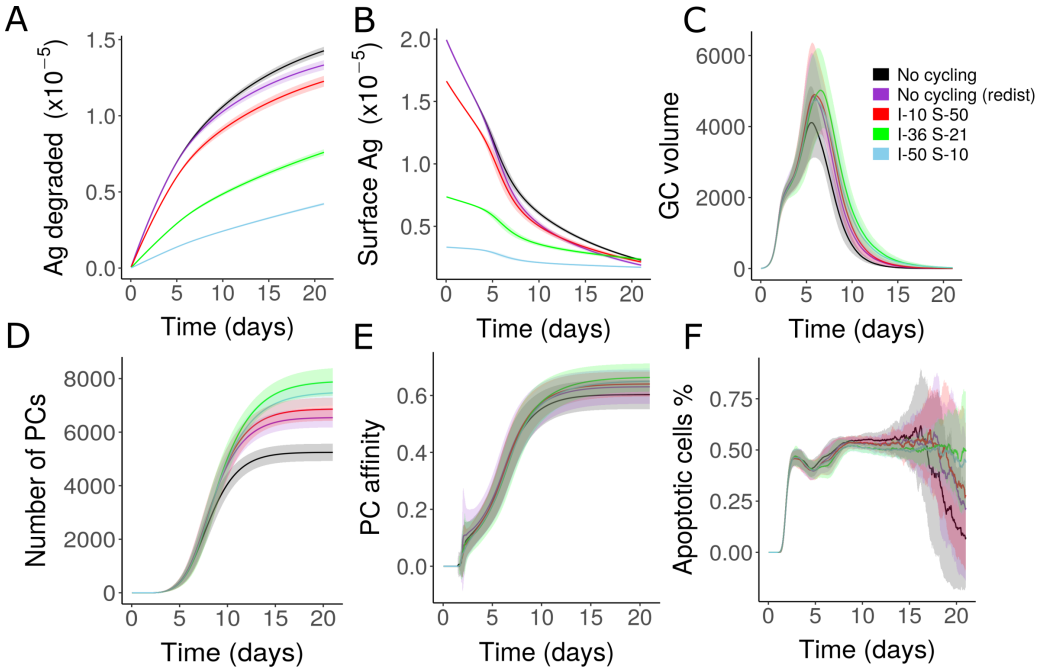

Figure 4.9: GC simulations with antigen degradation for varying cycling kinetics as in Figure 4.8 but with lower antigen concentration (1000 antigen portion per FDC) A) Amount of antigen degraded B) Surface antigen amount C) GC volume kinetics D) Number of plasma cells E) Affinity of plasma cells and F) Percentage of apoptotic cells. Inset shows the cycling times. Solid line and the shaded area represent mean and standard deviation of 100 simulations. GC: Germinal centre; FDC: Follicular dendritic cell; PC: Plasma cell; Ag: Antigen.

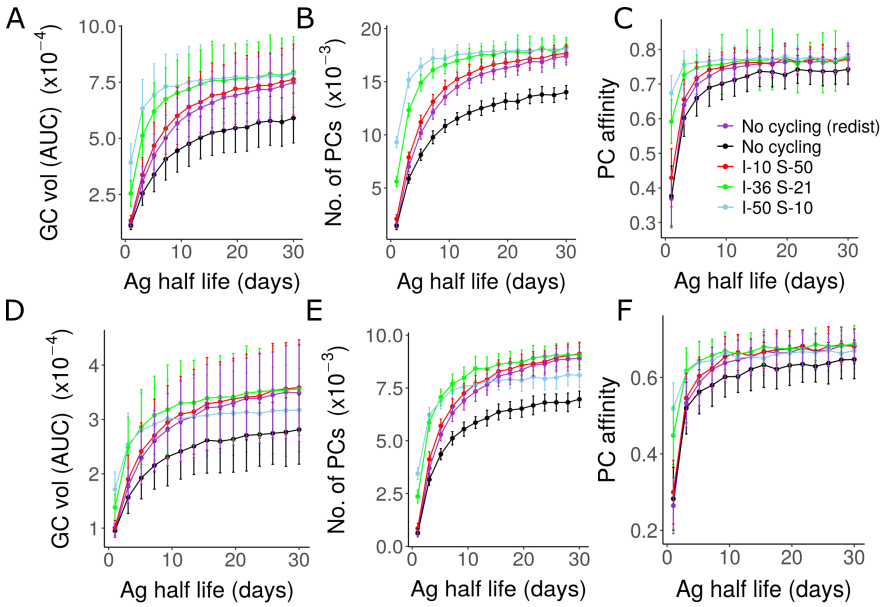

Figure 4.10: GC simulation readouts for varying antigen half-lives and cycling kinetics. Two different antigen concentrations were used (3000 and 1000 antigen units per FDC for A-C and D-F, respectively). A and D) AUC of GC volume kinetics, B and E) Number of plasma cells produced, C and D) Affinity of plasma cells. Each simulation was repeated 100 times. Inset shows the cycling times. GC: Germinal centre; FDC: Follicular dendritic cell; PC: Plasma cell; AUC: Area under curve.

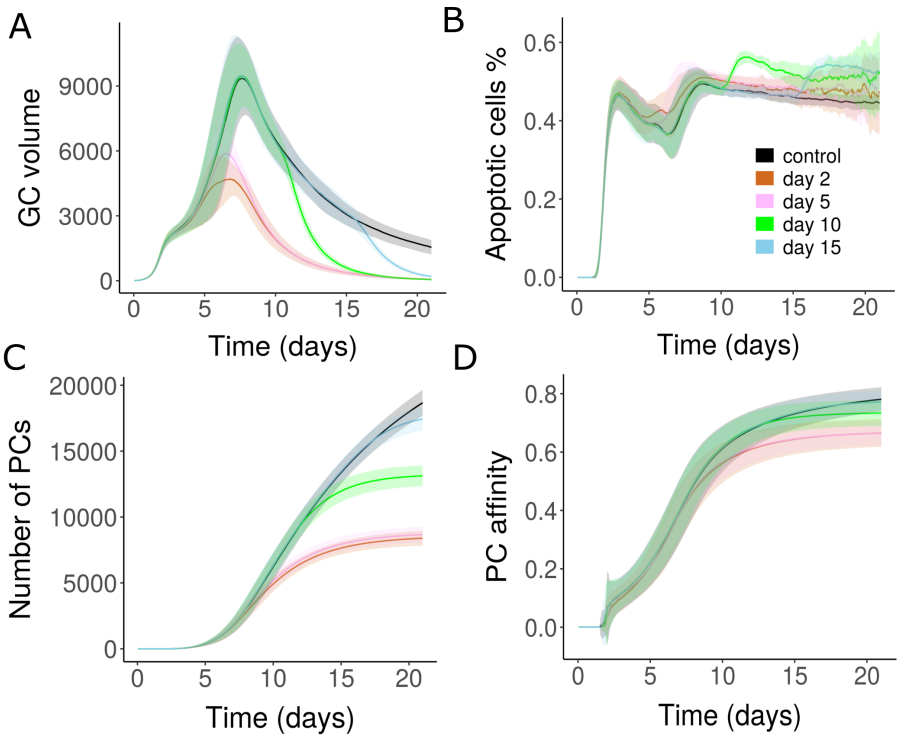

Figure 4.11: Impact of blocking antigen internalization and externalization in FDCs on the GC reactions A) GC volume kinetics B) Percentage of apoptotic cells C) Number of plasma cells and D) Affinity of plasma cells. Antigen cycling was blocked at different time points as indicated in the inset. Solid line and the shaded area represent mean and standard deviation of 100 simulations. GC: Germinal centre; FDC: Follicular dendritic cell; PC: Plasma cell.

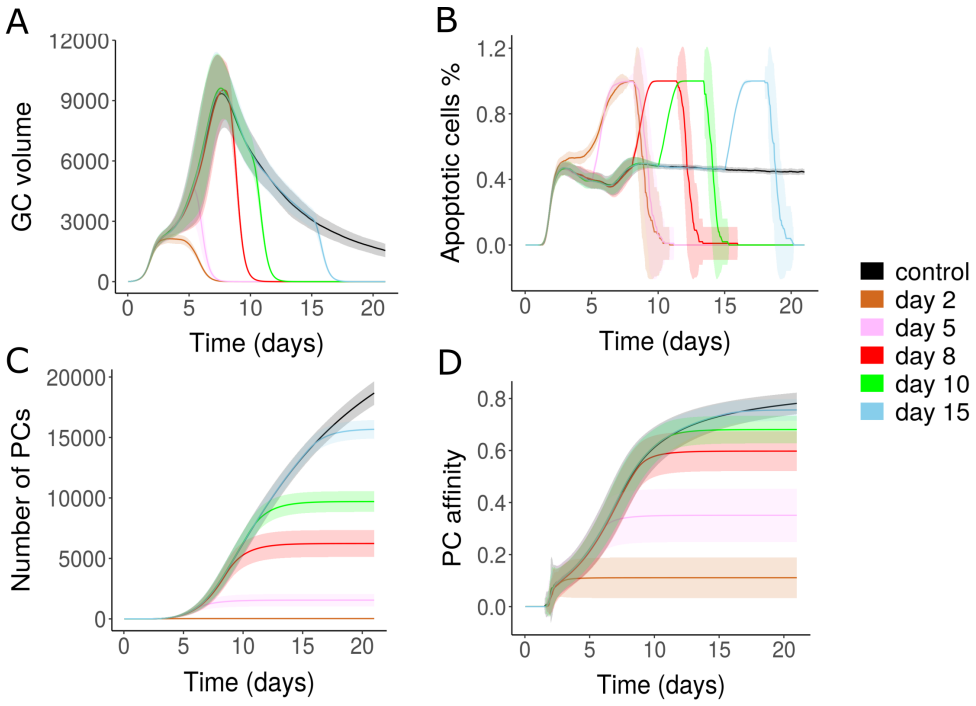

Figure 4.12: Impact of blocking antigen externalization in FDCs on the GC reactions A) GC volume kinetics B) Percentage of apoptotic cells C) Number of plasma cells and D) Affinity of plasma cells. Antigen externalization was blocked at different time points as indicated in the inset. Solid line and the shaded area represent mean and standard deviation of 100 simulations. GC: Germinal centre; FDC: Follicular dendritic cell; PC: Plasma cell.

Figure 4.11 [Figure 4.12]. Blocking antigen externalization results in the fast accumulation of antigen in the interior of FDCs leaving no extracellular antigen that the B cells can consume. Hence, the B cells undergo apoptosis due to the lack of antigen and the GC reaction is terminated. Earlier termination [Figure 4.12A] also decreased the plasma cell production and the affinity maturation resulting in reduced affinity of plasma cells [Figure 4.12C and D].

4.11 Conclusions

This Chapter investigates the impact of antigen presentation dynamics of FDCs on the GC reaction. Previous studies have shown that antigen delivery strategy can be altered to modulate the GC responses [22, 153]. Based on the simulation results, it can be proposed that antigen presentation dynamics within FDCs could also be a target to modulate the GC responses.

Although the exceptional antigen retention capacity of FDCs was known long ago, the mechanism behind this observation was unclear [93]. Discovery of IC cycling in FDCs by Heesters et al., suggested that antigen cycling might be the reason behind the extended half-life of antigen in FDCs [62]. Simulations in the presence and absence of antigen cycling suggested that antigen cycling is capable of efficiently protecting antigen from degradation without impairing antigen uptake of GC B cells.

Simulation results also suggested that changes in surface antigen concentration might not directly impact GC reaction if the antigen concentration is not limiting. However, if the

antigen is assumed to be unstable on the extracellular surface, then cycling kinetics influenced the shutdown and output of GCs by influencing the protection of antigen from degradation. These results are expected to have implications in designing and engineering antigen particles in enhancing GC responses towards vaccination. Considering the recent advances in mRNA vaccine development [118], it would be interesting to study how mRNA delivery impacts antigen presentation on FDCs. Simulations predicted that blocking antigen cycling can terminate the GC reactions. This suggests a potential role of modulation of antigen presentation in GC shutdown. Further, it also suggested a way to block ectopic or pathologic GC reactions.

Mechanism of IC cycling in FDCs is currently unknown. It is also not clear what determines the fate of internalized antigen in FDCs and whether a degradative pathway in addition to the non-degradative pathway also exists for internalized antigen as in the case of dendritic cells [12]. In this context, Zhang et al. showed that antigen particles with small size are internalized and cleared from FDCs [179]. Future studies are needed to investigate the mechanism and regulation of FDC IC cycling.

Estimation of PE-IC cycling time scale suggested that one complete cycle of PE-IC particles between the FDC surface and interior takes approximately 1 h on average. Future studies need to explore whether the cycling kinetics varies depending on the antigen used and the experimental settings. Cycling kinetics was assumed to be the same throughout the course of the GC reaction in this study. However, FDCs have been shown to undergo changes such as changes in surface markers and morphology [18, 38, 45, 160]. Further, it has also been shown that the contractility of FDCs can be influenced by cytokines. IL-10 has been shown to decrease the contractility of FDCs while IL-2 increases the contractility [112]. Hence, it can be speculated that the IC cycling kinetics might vary depending on the activation state of the FDCs or the cytokine milieu. The potential role of modulation in antigen presentation dynamics on the GC shutdown is discussed in Chapter 7.

Chapter 5

Analysis of lifetime of GCs

5.1 Abstract

Lifetime of GCs is a critical factor that influences the quantity and quality of memory/plasma cells, that ultimately determine the efficiency of antibody responses. Extending the lifetime of GCs has a potential application in enhancing vaccination responses. Several studies have quantified the lifetime of GC reaction in entire lymphoid organ but the lifetime of individual GCs is unknown. In this Chapter, lifetime of individual splenic GCs formed in response to primary immunization with model antigens was analyzed. Simulations of multiple asynchronously initiated GCs suggested that lifetime of GCs within the same lymphoid organ might be largely variable and hence, potential mechanisms that can lead to lifetime variability are identified and are consistent with the experimental data. Differences in antigen availability and founder cell specificities among individual GCs were able to independently explain the variability in GC lifetimes according to the data. Recent findings have highlighted several differences in the characteristics of individual GCs such as size and clonal diversity. Results discussed in this Chapter suggest that lifetime of GCs might also be heterogenous, in addition to the differences in other characteristics. Mechanisms and factors identified to explain the variability in lifetime are expected to promote future studies in investigating the shutdown of individual GCs.

5.2 Kinetics of GC reaction

GC kinetics is typically analyzed histologically and flow cytometrically using different measures such as the number of GC B cells or PNA+ area in a section of lymphoid organ. In this way, GC reaction kinetics of the entire lymphoid organ that in turn comprises multiple GCs is frequently investigated. Depending on the immunization conditions such as the antigen, route of administration and animal model used, the kinetics and lifetime of GC responses vary [1, 10, 59]. Adjuvant used for immunization can also influence the kinetics and lifetime of GC responses [75, 119].

In addition, number of GCs in a lymphoid organ dynamically changes over time. Asynchronous onset of GCs has been observed in several cases where GCs continue to be formed over an extended period of time [126, 151]. Kinetics of GCs investigated by Rao et al., suggest that GCs continue to be formed for at least the first 12 days after immunization [126]. Although the reason for the asynchronous onset and differences in initiation times are unknown, GCs can be made more synchronous by priming with a carrier protein that initiates a T cell response.

5.3 Characteristics of individual GCs

Multiple GCs are present in a lymphoid organ. For instance, hundreds of GCs are seen in spleen and around 10-16 GCs in the case of a single lymph node [66, 149]. Kinetics of individual GCs is difficult to study due to technical challenges. Despite this, differences in characteristics of individual GCs have been recognized by several studies. Individual GCs show large heterogeneity in the clonal diversity and pace of clonal evolution [154]. Size of individual GCs were also observed to be largely variable [149]. Differences in antigen specificities of B cells among individual GCs have also been observed. For instance, when two different hapten-carrier complexes were used for immunization, a proportion of GCs formed had cells specific to either hapten only, while other GCs had cells specific to both haptens [87]. Further, it was observed that after immunization with KLH or PHA, new follicles with GCs are formed in the spleen [69]. Induction of new follicles with GCs were seen for an extended period of time and the newly formed follicles had weak IC trapping capacity at the time of formation of GCs leading to notable differences in the IC trapping ability of different follicles [69]. Such studies suggested the importance of analyzing single GCs which is increasingly becoming popular following the technical advances [43].

GC reaction in a lymphoid organ lasts for approximately 3 weeks. However, the lifetime of individual GCs and whether all GCs undergo shutdown within the same period of time remain unexplored. Understanding the mechanisms controlling GC lifetime can also help identify factors that regulate the shutdown of individual GCs.

5.4 Simulation of multiple asynchronous GCs

The model described in Chapter 2 was extended to simulate multiple asynchronously formed GCs. The extended version includes similar features of single GC simulation but involves simulating GCs initialized at different time points. Two experimental data sets on number kinetics of GCs were used to analyze the lifetime of individual GCs [2, 126]. Further, the overall GC volume corresponding to number kinetics from Rao et al, was assumed to follow the data from [67] and [169] and were used for comparison with simulation.

Initiation of GCs was assumed to follow a Hill function that was fitted to the initial phase of the data as shown in Figure 5.1. In Figure 5.1A, it was assumed that new GCs are formed only for a restricted phase after immunization but we also explored an alternative scenario where the new GCs continue to be formed for an extended period of time (Figure 5.1B). The number of GCs at the initial phase follows

$$N(t) = N_{\max} t^{\mathrm{n}} / (T^{\mathrm{n}} + t^{\mathrm{n}}) \tag{5.1}$$

where $N(t)$ is the cumulative number of GCs formed until time t, $N_{\max}$ is the maximum number of GCs formed, T is the time point where $N(t) = N_{\max}/2$ and n is the Hill coefficient used. A threshold for number of GC B cells was considered to count the number of GCs and was arbitrarily set to 100. When the number of GC B cells decrease below 100, the GC is assumed to terminate.

For computational reasons, multiple GCs were approximated by a single representative GC. For this, the time period of GC initiation was divided into several intervals and a single representative GC was simulated for every time interval [Figure 5.1D-F]. This assumes that GCs initialized at similar timepoints (within the same time interval) are identical. The mid points of the time intervals were considered as the average initiation

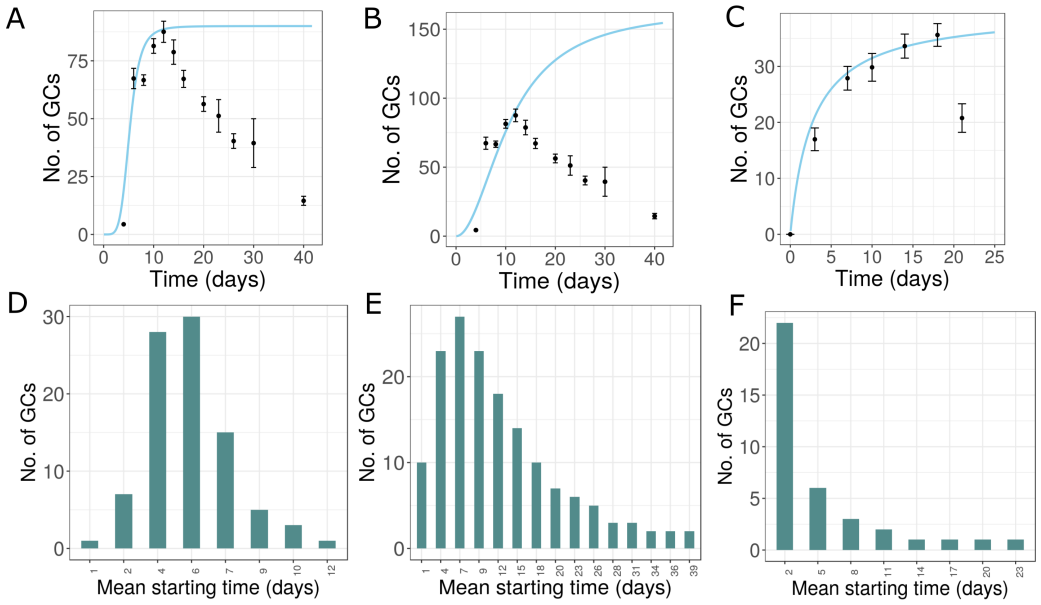

Figure 5.1: Hill function used to approximate the initial phase of GC number kinetics and the initiation times of the simulated GCs A) and D) With restricted formation of new GCs corresponding to data from [126], B and E) Extended formation of new GCs, C and F) Initiation criteria used for fitting data from [2]. GC: Germinal centre.

time of the simulated GCs. Some variability in the initiation time is also considered, hence, the initiation times are sampled from a Gaussian distribution with width of the distribution which was set to 24 hours.

To modulate the GC lifetime for fitting the data under different hypotheses, certain parameters were varied. The reference parameter set for these simulations are provided in Chapter 2 and any deviation from this parameter set is mentioned in figure captions of the corresponding simulations.

5.5 GCs with similar lifetimes

Simulations were performed to test whether the simulation results are consistent with data, if the GCs are assumed to have similar lifetimes. In order to adjust the lifetime, parameters were varied uniformly for all the simulated GCs. Due to similar characteristics, lifetime of individual GCs was similar on average except for some small variability due to the stochastic nature of the model [Figure 5.2B]. The data could not be fitted if formation of new GCs was restricted to first 12 days after immunization [Figure 5.2A], as GCs terminated in the simulation within a narrow period of time compared to the data [Figure 5.2A]. However, with longer GC lifetime, the initial decrease in number of GCs around day 12 cannot be explained. These results suggested that GCs might be formed for an extended period of time or GCs might have variable lifetimes.

Further simulations were performed to test whether GCs with similar lifetimes can fit the data if initiation dynamics of GCs is varied. GC formation was allowed for an extended period of time by varying the parameters of the Hill function [Equation 5.1] fitted to estimate the starting times of GCs [Figure 5.1B and E]. In this particular case, the reason for the extended contraction phase where the number of GCs slowly decline is because large number of GCs are formed at late time points and persist for a time period similar to the early formed GCs. Hence, the dynamics of termination of GCs is similar to the initiation

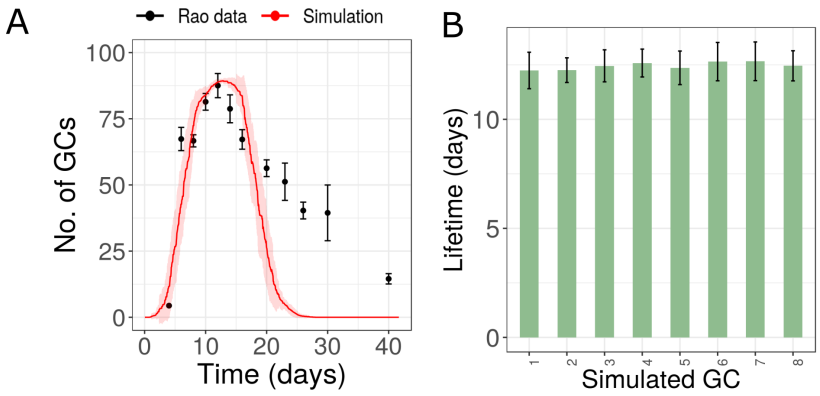

Figure 5.2: Simulation of GCs with similar lifetime A) Number kinetics of GCs B) Lifetime of simulated GCs. Number of GCs and initiation times used are shown in Figure 5.1A and D. Parameters used were same as the reference parameter set except for the following. Antigen concentration: 1500 units per FDC, Tfh selection threshold: 0.1 h, Number of antigen units consumed per interaction with FDC: 2. Solid line and the shaded area represent mean and standard deviation of 50 simulations. GC: Germinal centre; FDC: Follicular dendritic cell.

dynamics [Figure 5.3C and D]. Although, this was consistent with the experimental data [Figure 5.3A and B], new GCs needed to be initialized until very late time points [Figure 5.3C] which does not have any experimental evidence.

5.6 Parameters impacting GC lifetime

To test the hypothesis with variable lifetimes for GCs, potential causes of lifetime variability were identified by testing different parameters. Parameters identified to influence the GC lifetime considerably are shown in Figure 5.4. Parameters such as antigen concentration positively influenced the lifetime of GCs. When the antigen concentration was increased, the lifetime of GCs also increased [Figure 5.4 B]. Higher strength of antibody feedback decreases the lifetime of GCs as this induces antigen limitation [Figure 5.4C].

Stringency of GC B cell selection by Tfh cells, referred as the Tfh selection threshold, was also capable of influencing the GC lifetime. Higher selection threshold led to lower stringency of selection which in turn increased the longevity of GCs [Figure 5.4D]. Another critical factor influencing the maintenance of GCs is the recycling of selected GC B cells to the DZ where the cells undergo further rounds of cell divisions. The parameter recycling probability determines the proportion of cells recycling back to the DZ rather than directly differentiating to plasma cells and exiting the GC. Hence, with higher recycling probability lifetime of GCs were longer [Figure 5.4A]. Considerable variability in the lifetime of GCs was also achieved by varying the founder cell affinity of the GCs but the extent of variability was less [Figure 5.4E] when compared to the other parameters shown. Founder distance is the distance of founder B cells with respect to the optimal position in the shape space which can be interpreted as a measure for the affinity of cells. GC lifetime was relatively resistant to changes in mutation probability [Figure 5.4F]. These results suggested that parameters influencing the selection of GC B cells directly would have a large influence on lifetime of GCs.

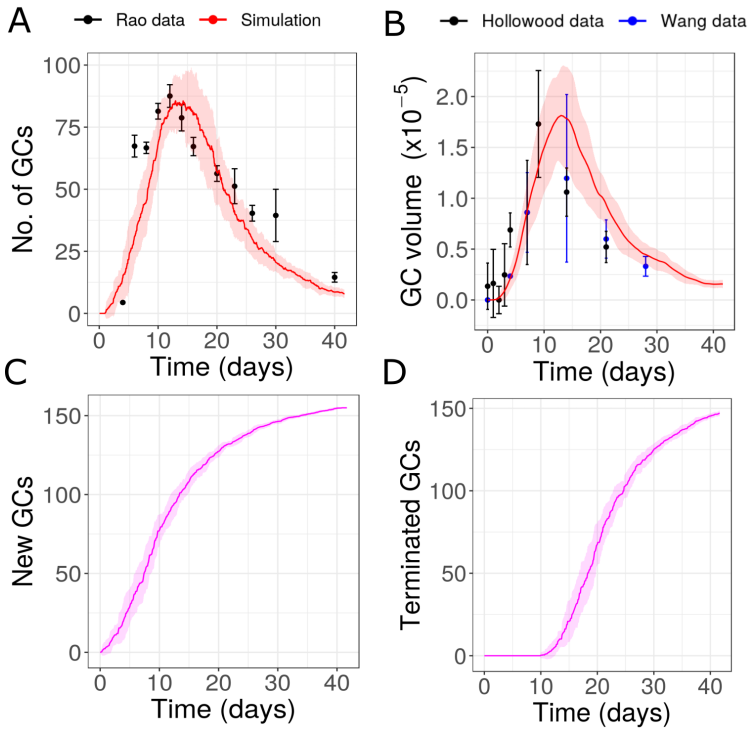

Figure 5.3: Extended formation of new GCs with similar lifetimes A) Number kinetics of GCs B) Overall volume kinetics of GCs C) Cumulative number of new GCs formed and D) cumulative number of terminated GCs. Parameters different from the reference set – Antigen amount per FDC: 800 portions, Tfh selection threshold: 0.1 h, Number of Tfh cells: 300 and Antigen consumed per interaction with FDC: 2 portions. GC: Germinal centre; FDC: Follicular dendritic cell; Tfh: T follicular helper cell.

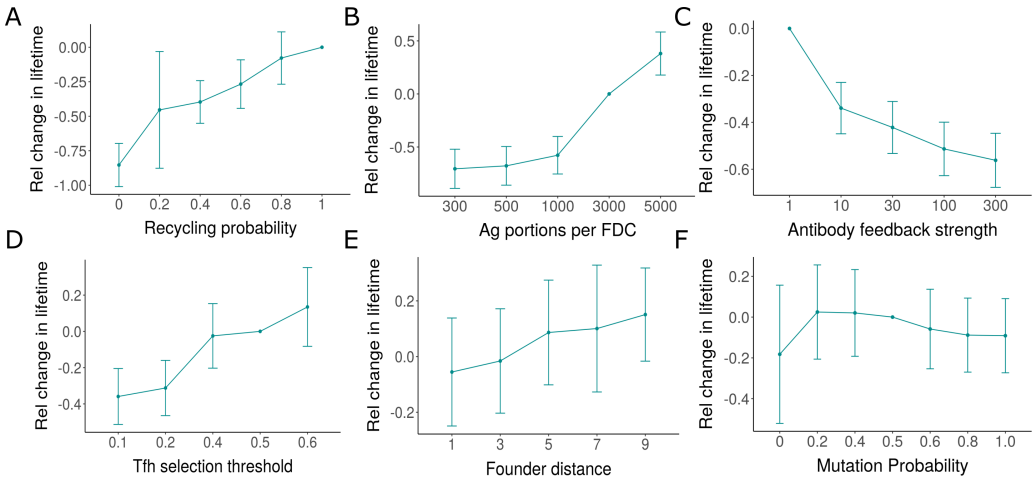

Figure 5.4: Impact of parameter changes on GC lifetime. Parameters varied are A) Recycling probability, B) Antigen concentration on FDCs, C) Strength of antibody feedback, D) Tfh selection threshold (in h), E) Founder cell affinity (distance from optimal position in Shape space) and F) Mutation probability. Lifetime is calculated with respect to the reference parameter set provided in Chapter 2. Each simulation was repeated 30 times. GC: Germinal centre; FDC: Follicular dendritic cell; Tfh: T follicular helper cell.

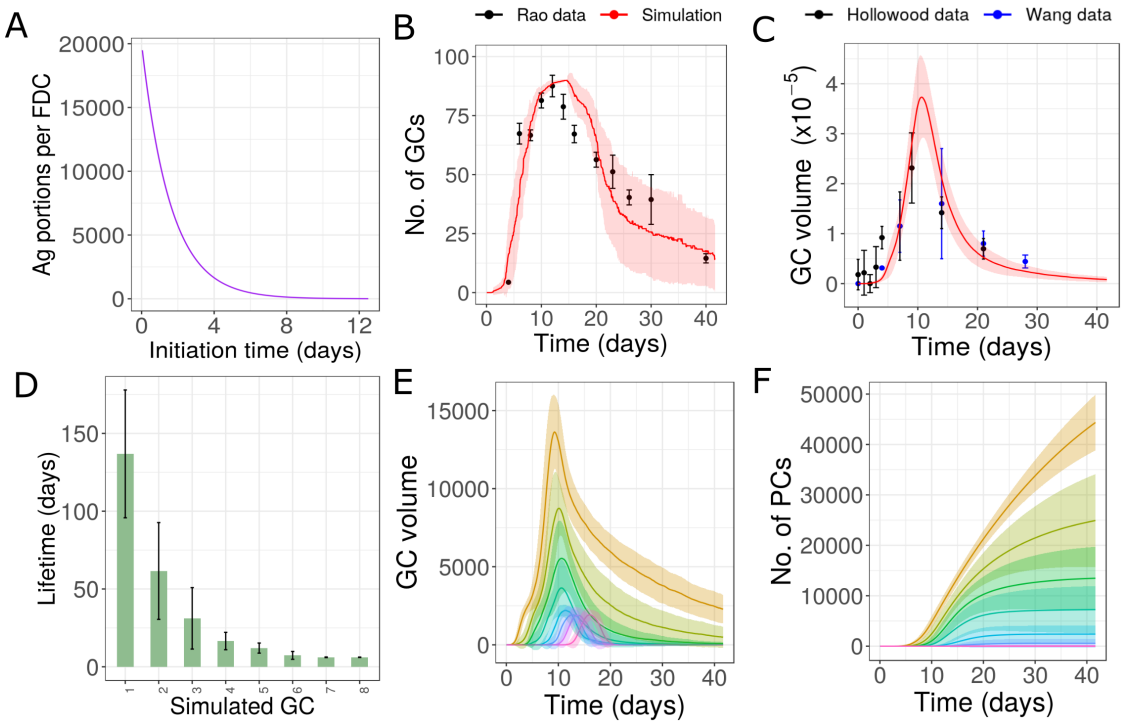

Figure 5.5: Simulations of GCs with varying antigen concentration A) Antigen concentration as a function of initiation time of GCs B) Number kinetics of GCs C) Overall GC volume D) Lifetime of simulated GCs E) Volume kinetics of simulated GCs and F) Number of plasma cells from simulated GCs. Individual simulated GCs are shown in different colors in panels E and F. Parameter values used in the exponential distribution shown in equation 5.2 were $A_0 = 20000$ and $k = 0.026$. Other parameters were similar to the reference parameter set in Chapter 2. Solid line and the shaded area represent mean and standard deviation of 60 simulations. GC: Germinal centre; PC: Plasma cell; Ag: Antigen.

5.7 Varying antigen concentrations

Next, GCs were assumed to acquire different amount of total antigen depending on the initiation times. Antigen acquired by a GC was modelled using the exponential function shown in Figure 5.5A, such that the antigen acquired decreases as the GC initiation is delayed. The exponential function used is as follows.

$$A(t) = A_0 e^{-kt} \tag{5.2}$$

where $A(t)$ is the total number of antigen portions per FDC, t is the initiation time of the GC and A_0 is the initial number of antigen portions at the time of immunization. Decreasing antigen amount is based on the observation that free antigen is rapidly cleared from the lymphoid organs [55, 156] unless it is trapped by the FDCs. This is because FDCs have an exceptional ability to trap and retain antigen in a stable form [93, 155] due to a protective cycling mechanism [62, 61] as discussed in Chapter 4.

This assumption was consistent with the experimental data of the number of GCs and the overall GC volume data as shown in Figure 5.5B and C. Lifetime of individual GCs showed a large variability from less than 10 days to more than 100 days [Figure 5.5D]. Early GCs had a longer lifetime and higher GC volume due to the higher concentration of antigen they had acquired. On the other hand, late formed GCs had a shorter lifetime and terminated

quickly due to antigen limitation. Consequently, early formed GCs span the entire lifetime of the overall GC response but the late ones that appear and vanish are inherently short lived [Figure 5.5E]. Further, the early formed GCs are the main contributors to the output production. Late formed GCs produced very few plasma cells and had a substantially less contribution to the plasma cell production [Figure 5.5F]. This hypothesis suggests that the GCs that terminate as early as 12 days after immunization are the late formed GCs that terminate due to antigen limitation and the extended contraction phase is due to the presence of early formed GCs that persist for a longer period of time. This mechanism also provides an explanation for why new GCs are formed only within a restricted time window after immunization depending on the availability of ICs.

5.8 Multiple epitopes and different founder specificities

In this hypothesis, founder cells of the different GCs were assumed to differ in the specificity towards different epitopes. As explained in Chapter 2, affinity of GC B cells is represented using a 4D shape space where a fixed position represents the optimal affinity towards the antigen. For multiple epitopes, many such optimal positions are considered. For simulations with multiple epitopes, the optimal positions were chosen far away in the shape space and could be interpreted as unrelated antigen epitopes. Affinity of founder cells for different GCs were chosen by specifying the shape space distance with respect to the optimal position corresponding to each epitope.

This could be expected because the immunization agent used to generate the data is Sheep Red Blood Cells (SRBCs) which are complex particles with several epitopes. Hence, GCs were assumed to have different lifetimes due to differences in the specificities of founder cells. Under this assumption, two different ways of distributing founder cells among individual GCs were considered. In the first case, early formed GCs had cells specific to all the epitopes present and the founder cells were randomly chosen anywhere in the shape space. Late formed GCs had founder cells specific to only one of the epitopes. As the epitopes were not considered in equal proportions, these GCs showed differences in the lifetime and was consistent with the data [Figure 5.6]. Such differences could arise due to the memory cells founding the late GCs.

In the second possibility, the distribution of founder cells were varied such that early formed GCs had more specific founders and late formed GCs were provided with more diverse founder cells. This possibility was also able to fit the data [Figure 5.7]. The basis for these assumptions could not be justified as the factors determining the founder cell characteristics of a given GC is unknown. However, it could be due to differences in the timing of activation of different B cell clones or due to competition within early stages of the GC that eliminates some of the clones.

5.9 Differences independent of initiation times

An alternate scenario was considered where the characteristics of GCs vary independently of the initiation time in a random manner. Antigen concentration was varied randomly such that there is a large variation in the total antigen amount acquired initially by the individual GCs. This resulted in large variability in the lifetime of GCs in single simulations [Figure 5.8D]. However, the average lifetime when many simulations were considered was the same for all simulated GCs as the antigen concentration is randomly sampled every time [Figure 5.8C]. Consequently, in this case, each individual GC is short-lived or long-lived and is determined randomly by the amount of antigen acquired. This possibility was also consistent with the data as it showed a fair fitting [Figure 5.8A and

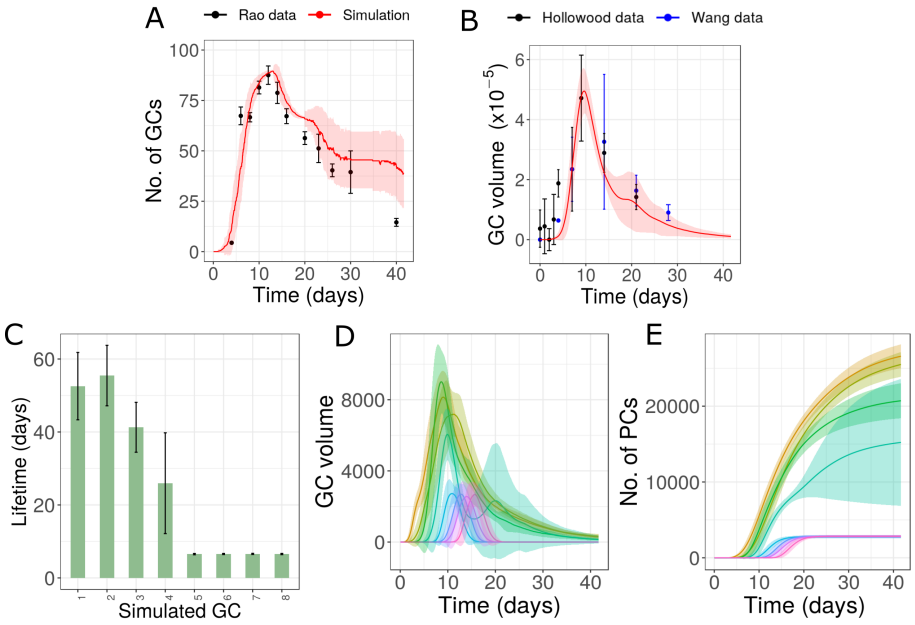

Figure 5.6: Simulations of GCs with multiple epitopes and different founder cell distribution A) Number kinetics of GCs B) Overall GC volume C) Lifetime of simulated GCs D) Volume kinetics of simulated GCs and E) Plasma cell production from simulated GCs. Three epitopes were considered at shape space positions 1111, 5555 and 8888 and the proportion of the epitopes were 5%, 25% and 70%, respectively. Founder cells of GC1 and 2 were randomly chosen, GC 3 were chosen at distance 1-3 from position 8888, GC 4 were chosen at distance 1-3 from position 5555 and GCs 5-8 were chosen at distance 1-3 from epitope 1111. Individual simulated GCs are shown in different colors in panels D and E. Solid line and the shaded area represent mean and standard deviation of 60 simulations. GC: Germinal centre; PC: Plasma cell.

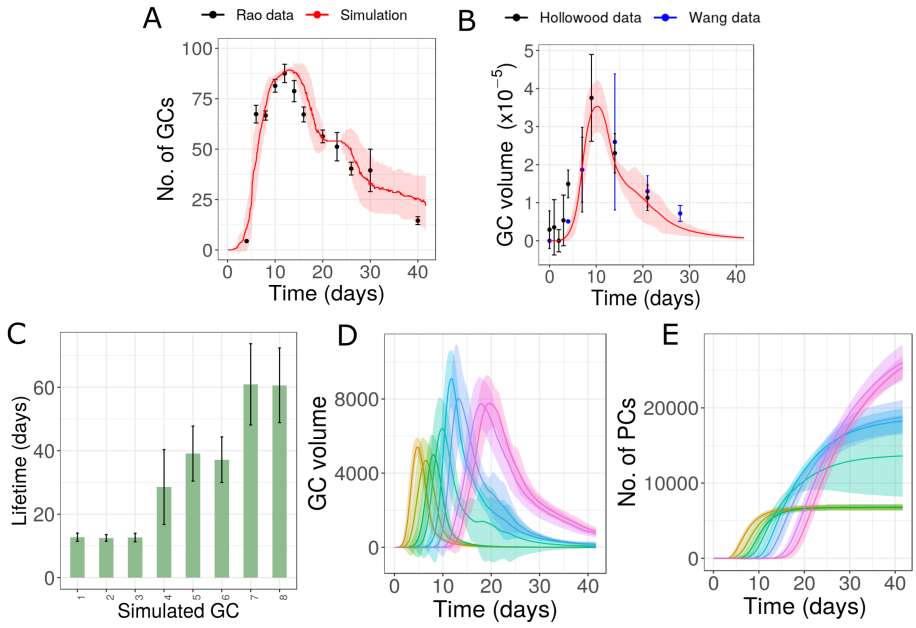

Figure 5.7: Simulations of GCs with multiple epitopes as in Figure 5.6 but with a different founder cell distribution A) Number kinetics of GCs B) Overall GC volume C) Lifetime of simulated GCs D) Volume kinetics of simulated GCs and E) Plasma cell production from simulated GCs. Three epitopes were considered at shape space positions 1111, 5555 and 8888 and the proportion of the epitopes were 15%, 30% and 55%, respectively. Founder cells of GCs 1-3 were chosen at distance 1-3 from position 1111, GC 4 were chosen at distance 1-3 from position 5555, GC 5 and 6 were chosen at distance 1-3 from position 8888 and GCs 7-8 were chosen randomly anywhere in the shape space. Individual simulated GCs are shown in different colors in panels D and E. Solid line and the shaded area represent mean and standard deviation of 60 simulations. GC: Germinal centre; PC: Plasma cell.

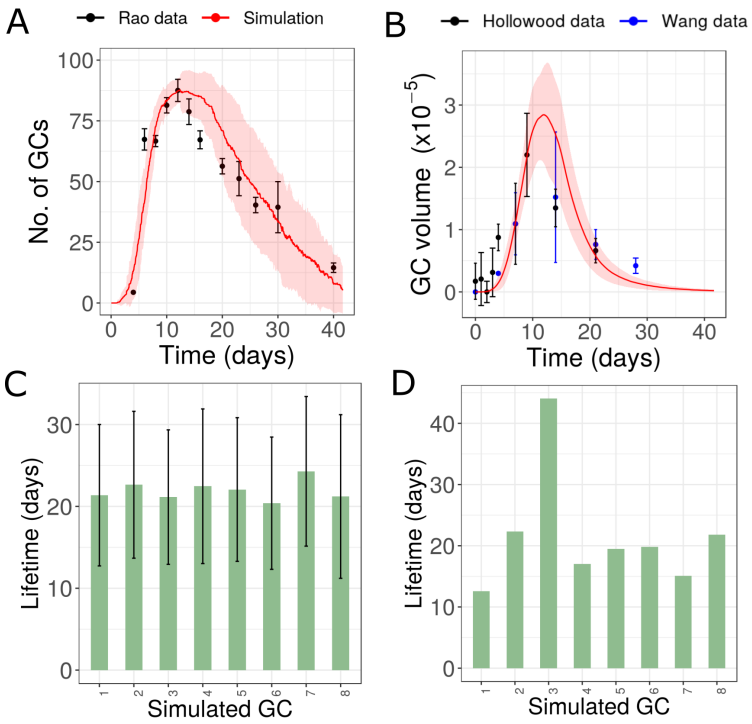

Figure 5.8: Multi-GC simulations with randomly varying antigen availability: A) Number kinetics of GCs B) Overall GC volume kinetics C) Lifetime of GCs from multiple simulations and D) Lifetime of simulated GCs from single simulation. Antigen amount of GC was sampled from Gaussian distribution with mean of 1300 antigen portions per FDC and standard deviation = 1100 antigen portions. Solid line and the shaded area represent mean and standard deviation of 60 simulations. GC: Germinal centre; FDC: Follicular dendritic cell.

B]. Accordingly, individual GCs within a lymphoid organ might have a large variability in lifetimes but the average lifetime of individual GCs from multiple lymphoid organs could be similar.

5.10 Antibody feedback

As the soluble antibodies secreted by plasma cells are capable of influencing the lifetime of GCs, simulations were performed to test whether interaction between individual GCs due to the exchange of soluble antibodies is capable of reproducing the experimental data without the need to introduce differences among other GC characteristics. Changes incorporated in the model to consider the antibody exchange are described in detail in Chapter 6. These simulations differ from Chapter 3 as a real network of multiple GCs is simulated here, rather than simply introducing early GC antibodies into late GC simulations. As the GCs are initialized in an asynchronous manner, individual GCs were not equally influenced and late GCs were particularly more impacted by the GC-GC interactions. However, the data could not be fitted [Figure 5.9] in the absence of differences in other parameters. Hence, antibody feedback cannot be the main reason behind the variability in lifetimes seen in the experimental data and there are likely other factors that contribute to the variability as predicted in the previous sections.

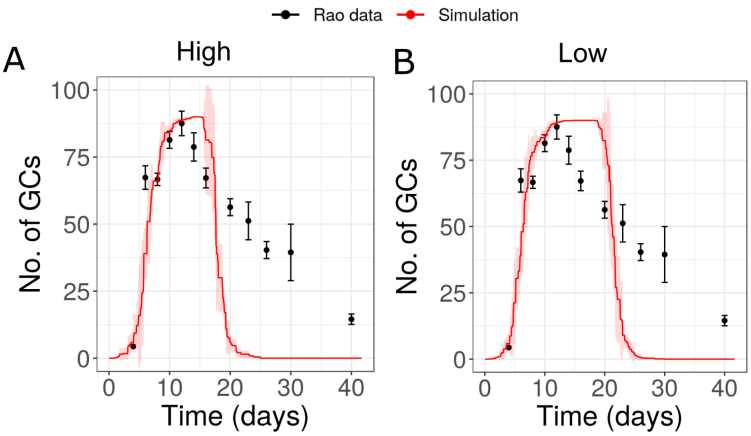

Figure 5.9: GCs interacting by exchanging antibodies with high (A) and low (B) antibody feedback strengths, respectively. Solid line and the shaded area represent mean and standard deviation of 10 simulations. Antibody production rates were 9e-18 (high) and 1e-18 (low) mol/h per plasma cell. GC: Germinal centre.

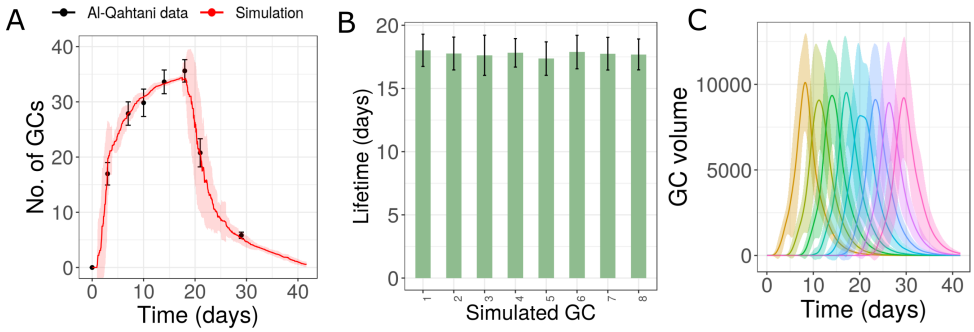

Figure 5.10: GCs with similar characteristics compared to data from [2] A) Number kinetics of GCs B) Lifetime of simulated GCs and C) Volume kinetics of simulated GCs. Individual simulated GCs are shown in different colors in panel C. Parameters different from reference set – Tfh selection threshold – 0.1 and Number of antigen units consumed per interaction with FDC: 2. Solid line and the shaded area represent mean and standard deviation of 50 simulations. GC: Germinal centre; Tfh: T follicular helper cell; FDC: Follicular dendritic cell.

5.11 GC kinetics with a different immunization condition

As previously discussed, GCs with different antigens or experimental settings have different overall kinetics. As the analysis in the previous sections were performed on a limited set of experimental data from SRBC primary immunization, to test the validity of the findings, GC number kinetics data from [2] was considered that differ in the immunization conditions. Antigen used for immunization is NP-CGG in [2]. As opposed to the previous data set, GCs with similar lifetime was able to fit the data as shown in Figure 5.10A. This was due to the short contraction phase in this data when compared to the previous data set with extended contraction phase. However, GCs with variable lifetimes were also consistent with the experimental data suggesting that GCs having variable lifetimes is also a possibility (Figure 5.11). As this data was consistent with all the possibilities tested, it was not possible to conclude whether the GC lifetimes are same or variable in this case. However, it suggested that if the lifetimes are variable then the extent of variability might depend on the immunization conditions.

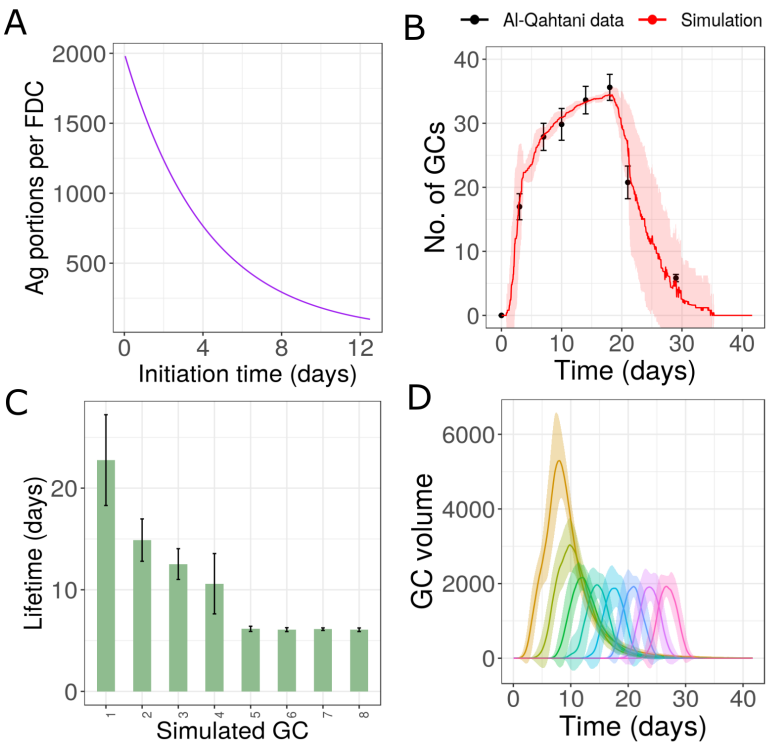

Figure 5.11: Initiation time dependent antigen availability: A) Exponential function used to calculate the antigen amount of GCs B) Number kinetics of GCs C) Lifetime of simulated GCs and D) Volume kinetics of simulated GCs. Individual simulated GCs are shown in different colors in panel D. Parameters different from reference set – Tfh selection threshold – 0.1 h and Number of antigen units consumed per interaction with FDC: 2. Antigen amount was varied following the exponential function $2000e^{-0.01t}$ where t is the starting time of GCs. Solid line and the shaded area represent mean and standard deviation of 55 simulations. GC: Germinal centre; Tfh: T follicular helper cell; FDC: Follicular dendritic cell.

5.12 Conclusions

In this study, lifetime of individual GCs and factors influencing the lifetime were analyzed, which suggested that GCs within the same lymphoid organ might have large heterogeneity in their lifetimes. When GCs were assumed to have similar lifetimes, simulation results were consistent with the data only if large number of new GCs were allowed to be initialized until the very end of the overall GC response. The reason behind the extended formation of new GCs is unknown and consequently, it is also not clear how long new GCs continue to be formed. Hence, factors influencing the initiation time of individual GCs need to be addressed by future studies. Until now there is no evidence showing that several new GCs can be formed at a late phase of the GC response.

Alternatively, assuming that the GCs have variable lifetimes was consistent with the data even if formation of most new GCs were restricted to initial phase of GC response. Tas et al., discovered that individual GCs in a lymph node show widely varying clonal diversity suggesting that GCs differ in their characteristics [154]. Consequently, indirect evidences and such heterogeneity seen among individual GCs suggest that GC lifetimes might also be heterogeneous. As the reason for such variability is not obvious, various parameters that can lead to heterogeneity in the lifetime of GCs were identified.

Decreased antigen trapping of late GCs when compared to early GCs was able to recapture the experimental data. As there is no direct evidence that GCs initiated at different time points might harbor different concentrations of antigen, this needs to be investigated experimentally. Indirect evidence comes from studies showing that follicles in spleen after KLH or PHA immunization show differences in the IC trapping capacity [69]. Although in this study [69] the follicles were newly formed, pre-existing follicles might show differences in IC trapping ability as the maturation state of FDC network influences IC trapping [33]. Alternate model that is able to explain the experimental data independently is the presence of multiple epitopes and a biased distribution of founder cells with different specificities among individual GCs. Simulation results predict that such differences in founder cell characteristics is also capable of generating variability in the lifetime of GCs. Antibody feedback was unable to explain the data in the absence of other differences. This suggested that GCs might have variable lifetimes due to differences in characteristics that are independent of the influence by soluble antibodies. Influence of GC intercommunication due to soluble antibodies on the lifetime of individual GCs will be addressed in chapter 6.

Due to limited availability of experimental data, the analysis was restricted to data from two different sources. As large differences are seen in the kinetics of GC reactions under different immunization conditions [1, 10, 59], it is unknown whether the GC lifetimes are variable under other immunization conditions or in the case of GCs present in a single lymph node. Moreover, GCs with similar and variable lifetimes were able to fit the data from [2], suggesting a need to perform further analysis. GC lifetime and the extent of variability needs to be analyzed under different conditions by future studies in order to understand how the individual GCs give rise to the overall GC response. It would be interesting to test how the number of GCs formed, their extent of synchronization and lifetime of individual GCs lead to differences in the overall GC reaction kinetics under different immunization conditions.

Chapter 6

Antibody mediated interaction of GCs

6.1 Abstract

Soluble antibodies have been shown to reenter GCs suggesting a mechanism of intercommunication between spatially separated GCs. In addition, given the potential role of soluble antibodies on GC shutdown, there is a possibility that GCs influence the shutdown of each other. Simulations in Chapter 3 predicted the impact of antibodies from early formed GCs on a late initialized GC. Conversely, the impact of late GC produced antibodies on early GCs was neglected in Chapter 3. Asynchronous onset and complex behavior of GCs discussed in Chapter 5 suggested the need to simulate a more realistic system of GCs, dynamically contributing to and influenced by antibodies, in order to predict the impact of intercommunication on the GC response. Therefore, *in silico* simulations were performed using a network of asynchronously initialized GCs interacting by the exchange of antibodies. Simulation results suggested that soluble antibodies could limit the magnitude of GC responses. Late initialized GCs were particularly more sensitive to antibody feedback but were able to partially overcome the inhibition in the presence of high affinity founder cells. In a GC response towards multiple antigen epitopes, intercommunication increased the diversity between individual GCs in terms of epitope specificity. Although the late GCs were short lived and had reduced production of plasma cells, soluble antibodies from early GCs also supported a better affinity maturation of rare epitope in late GCs. Moreover, depending on the founder cell composition, antibody feedback was able to shape the affinity maturation of different epitopes in interacting GCs. Such differences in the behavior of GCs might potentially be useful to probe the existence and strength of antibody-mediated interaction in experimental investigations.

6.2 Intercommunication by soluble antibodies

Endogenous and passively administered soluble antibodies have been shown to influence the shutdown and affinity maturation of GCs [178]. These findings led to the suggestion that GCs might intercommunicate by exchanging soluble antibodies [178]. *In silico* simulations have also predicted that administration of antibodies targeting immunodominant epitope can shift the focus of GCs from immunodominant to a subdominant epitope [102]. In Chapter 3, a simplistic case was considered where antibodies from a single simulated GC was scaled up to represent the contribution of multiple synchronous GCs. Similarly, to simulate the impact of early GC produced antibodies on a late GC, antibody concentration

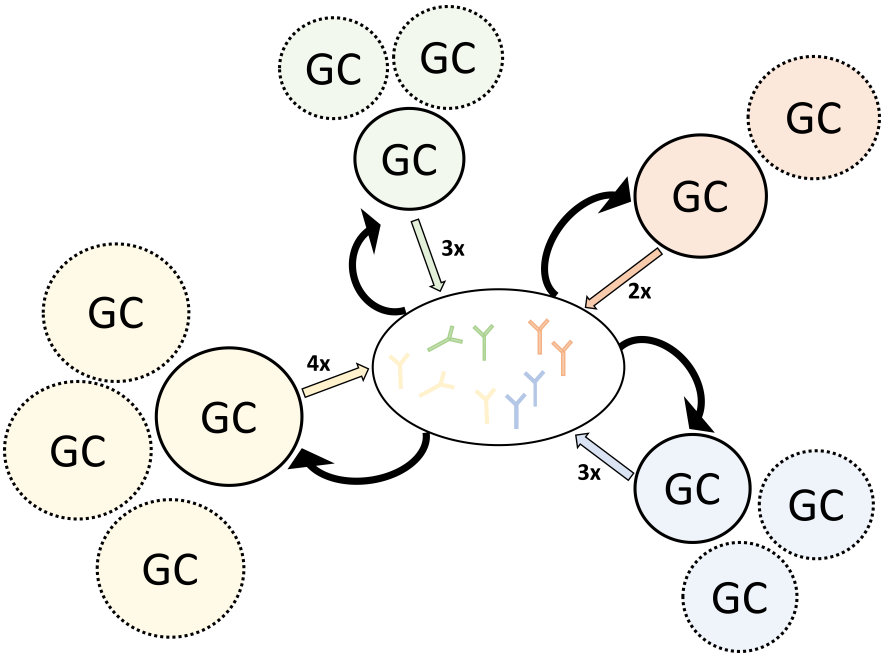

Figure 6.1: Schematic representation of multiple GC simulations and interaction of GCs via soluble antibodies. Simulated GCs (shown as colored circles with solid borders) are initialized asynchronously. Each simulated GC represents many identical synchronous GCs (shown by dotted circles, not explicitly simulated). Antibodies produced from each simulated GC (colored arrows) is scaled up to consider the contribution of identical GCs that are not explicitly simulated. Value of n in nx, adjacent to the colored arrows represent the number of identical GCs corresponding to each simulated GC. Antibodies contributed by the entire system of GCs in turn feedback on each simulated GC (shown by the black arrows).GC: Germinal centre.

profile of already simulated GCs was shifted by time and added to the simulation of late GC, thus neglecting the reverse feedback of late GC on early GCs. These results suggested that impact of antibody feedback might vary depending on the initiation time of GCs. As GCs might be formed asynchronously, the precise impact of such intercommunication is also hard to predict.Testing the existence of antibody-mediated interaction between GCs and the intensity of interaction remains challenging due to technical difficulties and hence, it remains a speculation that GCs influence the kinetics, affinity maturation and epitope specificity of interacting GCs. In general, the role of antibody feedback on GCs can be tested by blocking the endogenous production of soluble antibodies. However, lack of soluble antibodies might also impact processes such as the transport of antigen to FDCs and clearance of antigen from the GCs and the impact of these processes can hardly be disentangled. Hence, it would be beneficial to identify the characteristics of GCs that could help detect the existence of antibody mediated intercommunication.

6.3 Methods

Extended GC model described in Chapter 5 was used for simulating multiple GCs initialized at specified time points. Simulated GCs were assumed to intercommunicate by the exchange of soluble antibodies secreted from plasma cells (Schematically shown in Figure 6.1). As explained in Chapter 5, 8 GCs were simulated, each of which was assumed to represent several other GCs. Simulated GCs were initialized asynchronously or synchronously. In the former scenario, the initiation times and number of representative GCs follow Fig-

ure 5.1D. In the case of synchronous onset, 8 GCs were simulated (each representing 10 GCs) and all simulated GCs were synchronously initialized at the start of the simulation. In the simulation, starting time of GCs were sampled from Gaussian distribution with width 24 h and specified mean. Each initialized GC was iteratively evaluated at every timestep. Each simulated GC produces plasma cells that in turn secretes antibodies with a fixed rate. Concentration of antibodies resulting from each GC was calculated using the Equation 2.4. At the end of every time step, concentration of antibodies resulting from the entire system of GCs (A_{T}) was calculated as follows.

$$A_{\mathrm{T}}(i,t) = \sum_{\mathrm{n}=1}^{\mathrm{N}} X_{\mathrm{n}} A_{\mathrm{n}}(i,t) \tag{6.1}$$

where i is the antibody bin classified based on affinity, N is the number of simulated GCs, A_{n} is the concentration of antibodies produced by simulated GCs and X_{n} is the number of GCs represented by simulated GCs. Antibodies were assumed to distribute such that the concentration is homogeneous throughout the organism. Antibody production rate was varied to investigate the influence of different intensity of interaction. For the simulation with single epitope, shape space position 3333 was chosen to represent the antigen. For multiple epitope simulations, multiple positions were chosen in the shape space as described in Chapter 2.

6.4 Impact on overall GC response

Simulation results discussed in Chapter 3 show that antibody feedback is capable of decreasing the efficiency of individual GCs by promoting earlier termination. This suggests that intercommunication between GCs by soluble antibodies might influence the efficiency of individual GCs. However, due to asynchronous onset, response of individual GCs to soluble antibodies might differ as some GCs start producing plasma cells earlier when compared to the other GCs. To investigate the influence of intercommunication between GCs on the overall GC response, we simulated a group of asynchronously initiated GCs as described in section 6.3. Strength of GC-GC interaction was varied by changing the antibody production rate. With increasing antibody feedback strength, the overall GC response terminated earlier [Figure 6.2A] resulting in decreased plasma cell production [Figure 6.2B]. Affinity of plasma cells was also decreased due to earlier termination of affinity maturation process [Figure 6.2C]. Similar results were obtained when the GCs are initiated in a synchronous manner [Figure 6.2D-F] suggesting that intercommunication by soluble antibodies limits the overall GC response irrespective of the extent of synchronicity in GC initiation.

6.5 Impact on individual GCs

Individual GCs also terminated earlier in response to intense interaction by antibodies [Figure 6.3A]. Early and late initialized GCs showed differences in kinetics due to intercommunication [Figure 6.3A]. Late initialized GCs attained lower maximum size and were particularly more sensitive to the influence by GC-GC interactions [Figure 6.3B]. With high antibody feedback, production of plasma cells from individual GCs decreased consistently in the sequence of GC initialization suggesting that plasma cell production from early formed GCs can further decrease the efficiency of late formed GCs [Figure 6.3C]. There was also a decrease in affinity of plasma cells from individual GCs with high feedback [Figure 6.3D]. Similarly, in the case of synchronous onset, antibody feedback de-

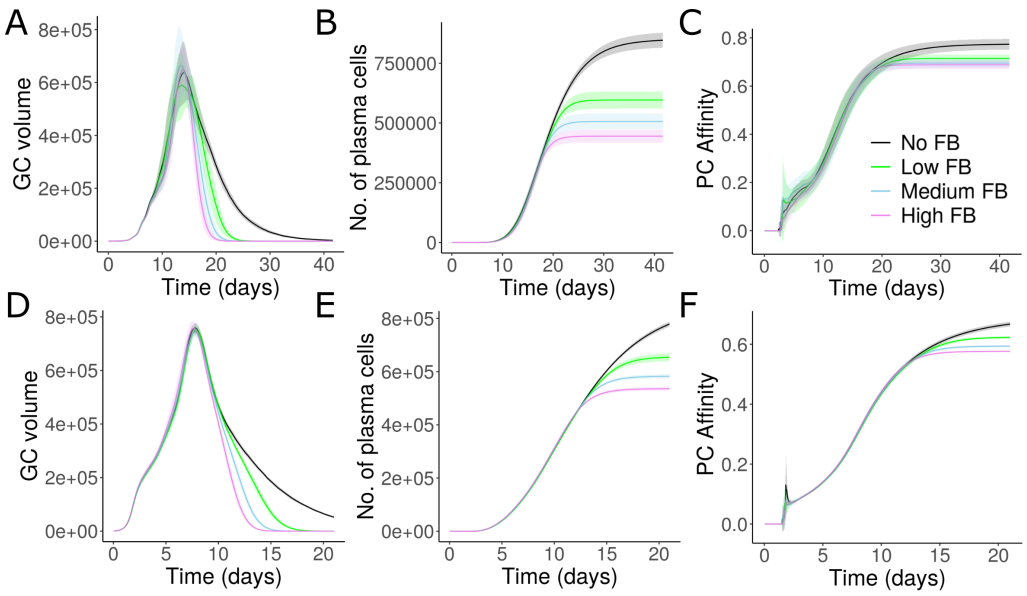

Figure 6.2: Effect of GC-GC interactions by soluble antibodies on overall GC kinetics and output. Colors represent the intensity of interactions. No interaction was considered between GCs in simulations labelled No FB (No Feedback). In panels A-C and D-F, GCs were initialized asynchronously and synchronously, respectively. A and D) Volume kinetics, B and E) Number of plasma cells produced and C and F) Mean affinity of plasma cells. These readouts correspond to the entire system of GCs including the GCs that were not explicitly simulated. Antibody feedback strength was modulated by varying the antibody production rate. Solid lines and shaded area represent mean and standard deviation of 10 simulations. GC: Germinal centre; PC: Plasma cell; FB: Feedback.

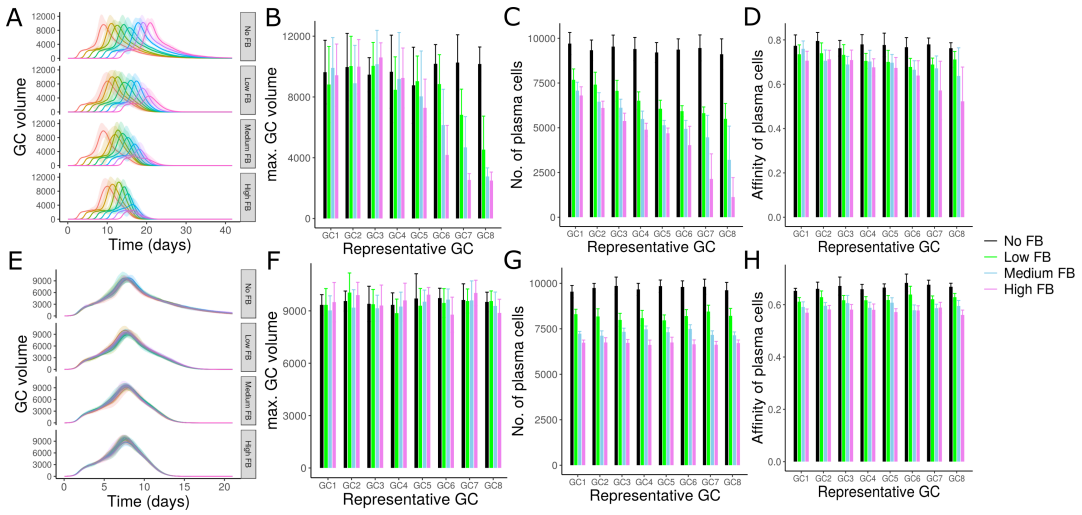

Figure 6.3: Effects of intercommunication on kinetics and output of individual GCs corresponding to Figure 6.2. GCs were initialized asynchronously (Panels A-D) or synchronously (Panels E-H). A and E) Volume kinetics of individual GCs. Different colors are used in A and E to represent individual simulated GCs. B and F) Grouped bar plots showing the maximum volume attained by individual GCs with different feedback strength. C and G) Number of plasma cells produced from individual GCs until the end of the simulation. D and H) Mean affinity of plasma cells from individual GCs calculated at the end of the simulation. Simulated GCs, GC1-GC8 are shown in the sequence of initialization from left to right. Color code in panels B-D and F-H represent different intensity of GC -GC interactions. Solid lines and shaded area represent simulation mean and standard deviation. Error bars in barplots represent standard deviation. Each simulation was repeated 10 times. GC: Germinal centre; FB: Feedback.

creased the production and affinity of plasma cells from individual GCs [Figure 6.3E-H]. However, with synchronous onset every individual GC was impacted similarly by soluble antibodies.

6.6 Late GCs with high affinity founders

Given the ability of certain memory cell subsets to participate in the secondary GC response [34], simulations were performed to test whether the late GCs can overcome antibody feedback mediated inhibition, if they are seeded by memory cells. With memory cells as founders, late GCs had a higher GC volume and plasma cell production [Figure 6.4D and E]. However, this was insufficient to overcome the inhibition of overall GC response by GC-GC interactions due to soluble antibodies [Figure 6.4A-C]. Simulations suggest that the extent of inhibition of late GCs compared to early GCs would be lower if high affinity cells seed the late GCs. Future experimental investigations are needed to test the capability of memory B cells to participate in a primary GC response and whether the late formed GCs are seeded by recently activated B cells as the early formed GCs or by memory cells arising from early GCs.

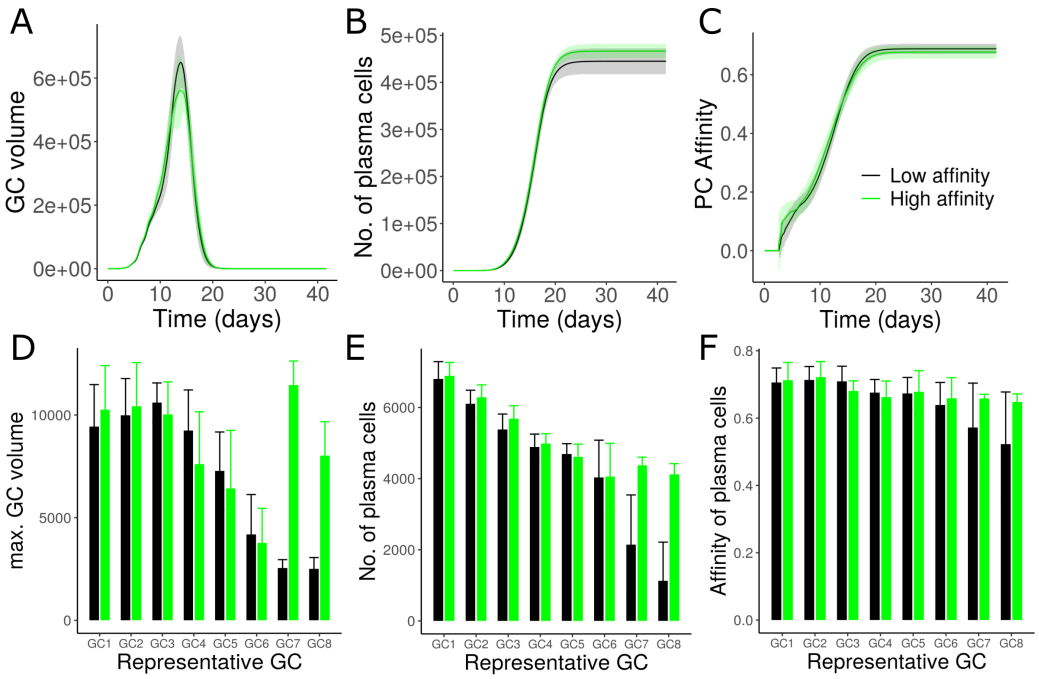

Figure 6.4: Simulation of GCs with high affinity founder cells. GCs were simulated asynchronously with high antibody feedback strength. In simulations labelled low affinity, founder cells of all GCs were chosen randomly (anywhere in the shape space) resulting in average low affinity. In simulations labelled High affinity, founder cells of late GCs, GC7 and GC8 were chosen to have relatively high affinities (Distance of 2 in shape space from optimal position). A-C) and D-F) represent the overall and individual GC readouts, respectively. Solid lines and shaded area represent simulation mean and standard deviation. Error bars in bar plots represent standard deviation. Each simulation was repeated 10 times. GC: Germinal centre; PC: Plasma cell.

6.7 Simulation of GC-GC interactions with multiple epitopes

Simulations were performed with two epitopes to test the validity of the above-described findings in the context of multiple epitopes. Shape space position of the two epitopes were chosen as 3333 and 5555 and the GC seeder cells were chosen randomly anywhere in the shape space. Despite the presence of two epitopes (in equal proportion), with increasing intensity of interaction, the overall GC response and individual GC response were inhibited by soluble antibodies [Figure 6.5]. Plasma cell affinity towards the two epitopes in the overall GC response were similar suggesting similar extent of affinity maturation towards both the epitopes [Figure 6.5C and D].

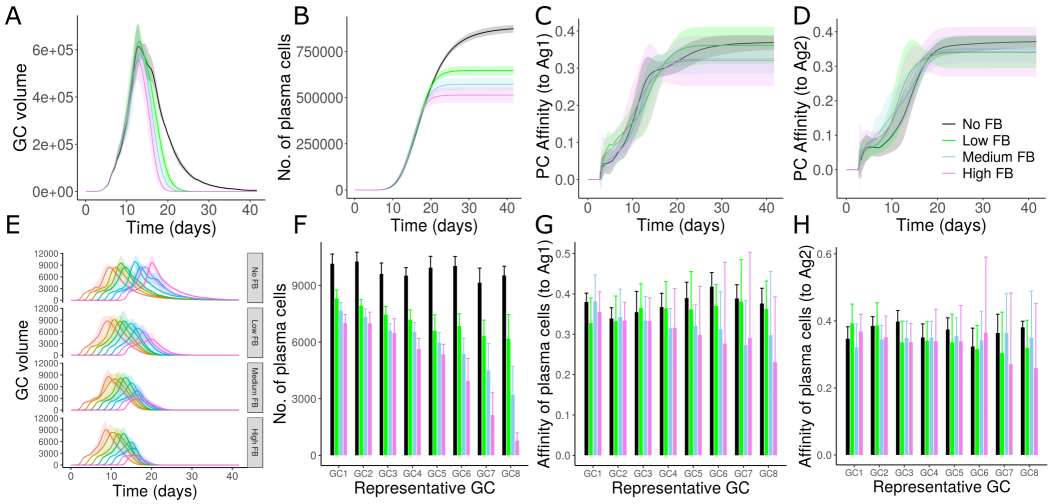

Figure 6.5: GC simulations with two antigen epitopes in equal proportions (Shape space position of antigens 3333 and 5555). A-D) Overall GC readouts. E-H) Individual GC readouts. A and D) GC volume kinetics, B and F) Number of plasma cells produced, C and G) Affinity of plasma cells towards the epitope with shape space position 3333 and D and H) Affinity of plasma cells towards the epitope with shape space position 5555. Colors in A-D and F-H represent different strength of antibody feedback. In E, each individual GC is shown in a different color. Founder cells were chosen randomly anywhere in the shape space. Solid lines and shaded area represent simulation mean and standard deviation. Error bars in bar plots represent standard deviation. Each simulation was repeated 10 times. GC: Germinal centre; PC: Plasma cell; Ag: Antigen; FB: Feedback.

Individual GCs in single simulations showed similar affinity maturation towards both epitopes with low feedback [Figure 6.6A and D]. Unexpectedly, there were marked differences in affinity maturation of GCs towards different epitopes with medium and high feedback [Figure 6.6B, E, C and F]. Affinity of early formed GCs were similar towards both the epitopes. However, the late GCs showed a preference towards one of the epitopes. Hence, such differences in affinity maturation among GCs in the presence of equally dominant epitopes could also be a consequence of antibody feedback.

6.8 GC response towards two epitopes in unequal proportions

Previous study has shown that the soluble antibodies have a tendency to shift the focus of the GC towards the least dominant epitope during GC reaction [102]. Similar analysis was

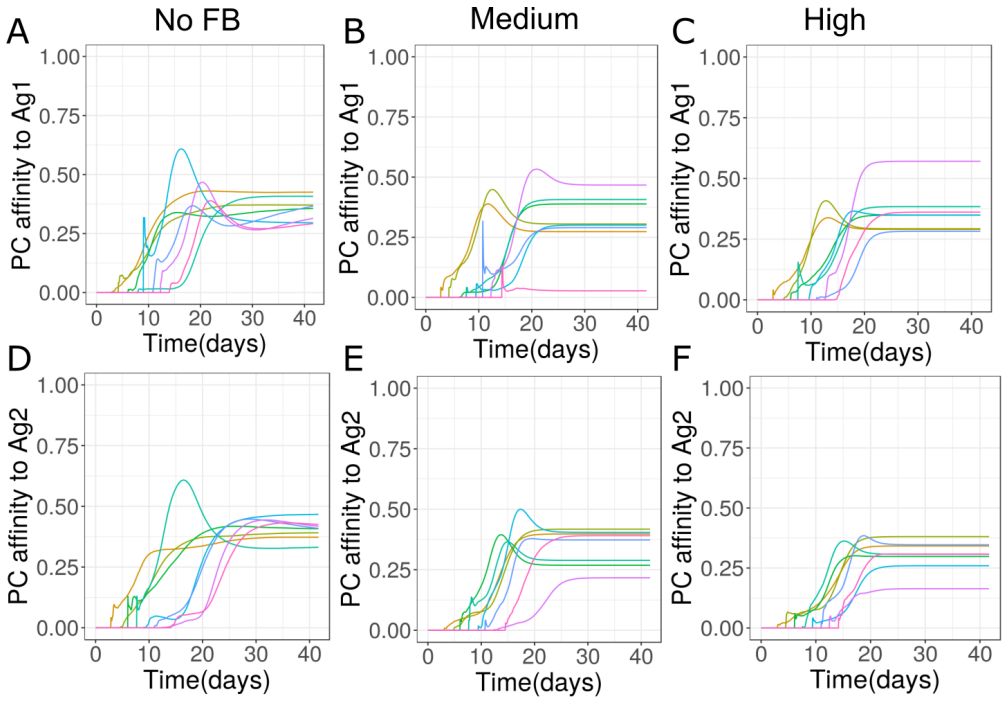

Figure 6.6: Plasma cell affinities towards different epitopes in GC simulations with two epitopes (Shape space positions 3333 and 5555) and different strength of antibody feedback. A and D) No interaction between GCs. B and E, C and F represent medium and high antibody feedback strengths respectively. Individual GCs are shown in different colors. Both the antigen epitopes were present in equal proportions. Founder cells were chosen randomly anywhere in the shape space. GC: Germinal centre; PC: Plasma cell; Ag: Antigen.

performed to test whether the antibody feedback is able to enhance the response towards least dominant epitope in the case of multiple asynchronous GCs. Two epitopes were considered in unequal proportion (90 % and 10 %) and the influence of GC-GC interaction was tested with different feedback strength. Founder cells were chosen randomly anywhere in the shape space, leading to approximately equal proportion of founder cells being specific to either epitope. With high antibody feedback, the affinity maturation of rare epitope was higher in late GCs when compared to early GCs [Figure 6.7H]. Hence, there is a tendency to focus on rare epitope as feedback strength increases. Late GCs are relatively short lived and produce less plasma cells [Figure 6.7E and F]. However, it is not sufficient to enhance overall plasma cell affinity (considering the plasma cells from all GCs) towards the rare epitope [Figure 6.7D]. Further, the efficiency (Immune power or IP) of the GC response to rare epitope was also unaltered [Figure 6.7 C]. Consequently, depending on the antibody feedback strength, late GCs might be observed to promote better affinity maturation for rare epitopes compared to early formed GCs.

6.9 GCs with different founder cell composition

Analysis in Chapter 5 suggested that individual GCs within the same lymphoid organ might also have differences that are not directly induced by antibody feedback such as differences in antigen availability or founder cell composition. Considering this result, the impact of intercommunication was tested in the presence of differences in founder cell composition of individual GCs. In simulations with two antigen epitopes (shape space position 2222 and 6666), founder cell composition was chosen such that a proportion of

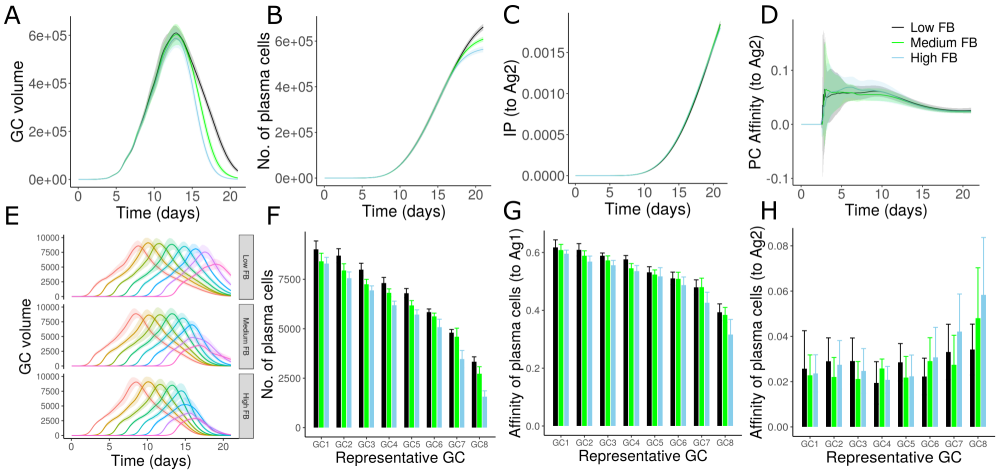

Figure 6.7: GC simulations with two epitopes (Shape space position of epitopes 3333 (Ag1) and 5555 (Ag2) in unequal proportions, 90 % and 10 % respectively). A-D) Overall GC readouts. E-H) Individual GC readouts. A and E) GC volume, B and F) Number of plasma cells, C) IP towards Ag2, G) Affinity of plasma cells to Ag1, D and H) Affinity of plasma cells to Ag2. Color code represents the strength of interaction. Colors in A-D and F-H represent different strength of antibody feedback. Colors in E represent individual simulated GCs. Founder cells were chosen randomly anywhere in the shape space. Solid lines and shaded area represent simulation mean and standard deviation. Error bars in bar plots represent standard deviation. IP was calculated using Equation 3.2. Each simulation was repeated 10 times. GC: Germinal centre; PC: Plasma cell; Ag: Antigen; FB: Feedback; IP: Immune power.

GCs were seeded by founder cells specific towards a single epitope while other GCs receive founders specific to both epitopes. Founders of GCs 1-3 were chosen anywhere in the space space and therefore includes B cells specific to both epitopes. Founder cells of GCs 4-8 were chosen at distance of 1 from shape position 2222. In this case, antibody feedback was able to alter the affinity maturation of individual GCs towards different epitopes. GCs 4-8 that focussed only on one of the epitope, were able to shift the focus of other GCs towards a different epitope [Figure 6.8]. So, depending on the outcome of other GCs, the affinity maturation is shaped by antibody feedback. These results show that similarity between the founder cell composition critically influences the impact of intercommunication.

6.10 Persistent antigen deposition

Simulations discussed previously mimic a system where a single dose of antigen is administered. Impact of persistent antigen deposition was tested to determine whether continuous antigen deposition can overcome the inhibition by antibody feedback. Therefore, a different antigen deposition dynamic was considered such that there is a persistent addition of antigen on FDCs at a constant rate. As expected, with fixed antibody feedback strength, depending on the deposition rate, the effects of antibody feedback were reversed [Figure 6.9] suggesting a mechanism by which GCs could overcome antibody feedback.

6.11 Conclusions

Soluble antibodies have been speculated to be involved in intercommunication between spatially separated GCs. Here, an *in-silico* approach was used to test the influence of

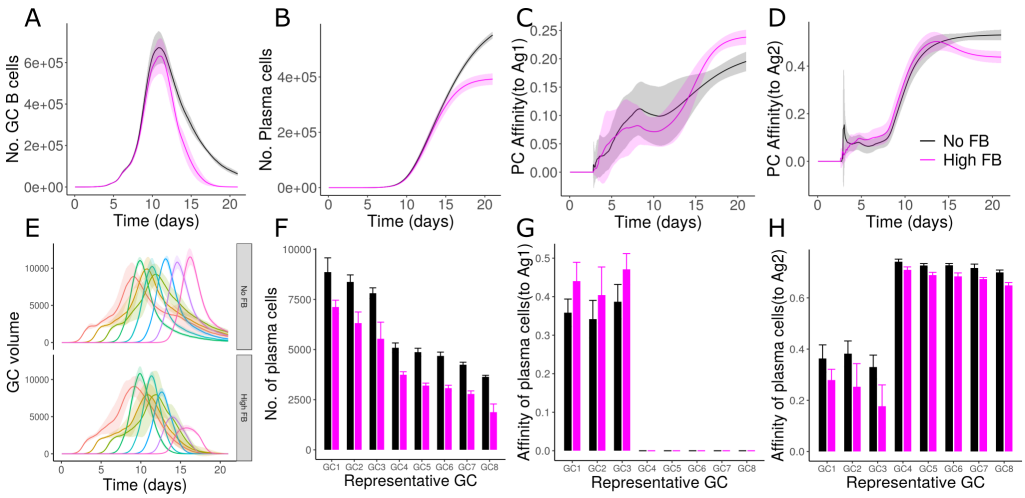

Figure 6.8: Simulation of GCs with different founder cell compositions. A-D) Overall GC readouts. E-H) Individual GC readouts. A and E) GC volume, B and F) Number of plasma cells, C and G) Affinity of plasma cells to Ag1, D and H) Affinity of plasma cells to Ag2. Color code represents the strength of interaction. Two epitopes with shape space positions 2222 and 6666, were considered in equal proportions. Founder cell composition of GCs 1 to 3 – were chosen randomly anywhere in the shape space, GCs 4 – 8 – Distance 1 from shape space position 2222. Solid lines and shaded area represent simulation mean and standard deviation. Error bars in bar plots represent standard deviation. Each simulation was repeated 10 times. GC: Germinal centre; PC: Plasma cell; FDC: Follicular dendritic cell; Ag: Antigen; FB: Feedback.

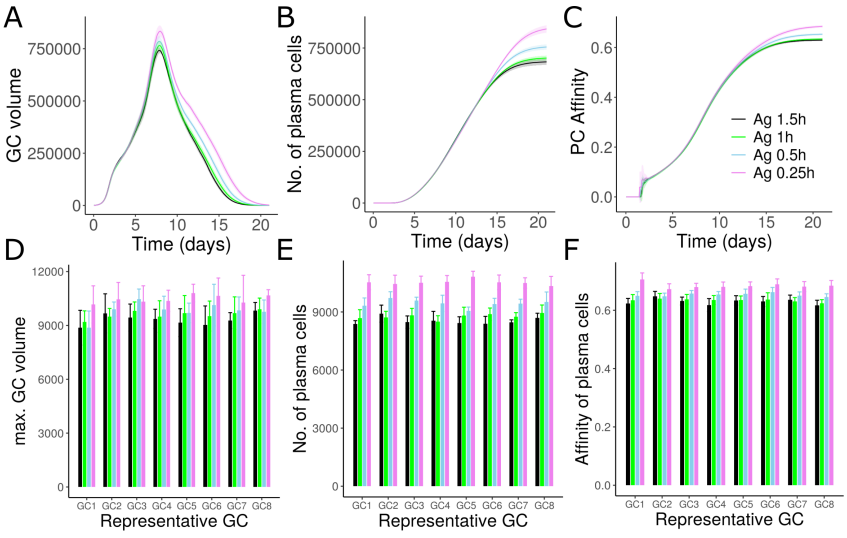

Figure 6.9: Simulation of GCs with persistent deposition of antigen at constant rate. A-C) Overall GC readouts. D-F) represent the individual GC readouts. A and D) Overall GC volume and maximum size attained by individual GCs, respectively. B and E) Number of plasma cells produced. C and F) mean affinity of plasma cells produced. Inset shows the time interval between subsequent antigen addition per FDC in hours. Individual GCs were synchronously initiated. In E and F) Number of plasma cells and mean affinity of plasma cells from individual GCs were calculated at the end of the simulations. Solid lines and shaded area represent simulation mean and standard deviation. Error bars in bar plots represent standard deviation. Each simulation was repeated 10 times.

soluble antibodies on overall GC response and individual GCs under a wide range of conditions. Predicted behavior of GCs due to interaction, might enable testing the existence of antibody feedback without altering the production of soluble antibodies. Simulations predicted that in general, antibody mediated interaction between GCs, minimizes the magnitude and output of overall GC response. In the context of individual GCs, late initialized GCs were relatively more impacted when compared to early formed GCs. Although there is evidence suggesting the asynchronous onset of GCs, the extent of synchronicity might vary depending on the experimental settings. Upon synchronous onset, the simulated individual GCs were similarly modulated by soluble antibodies. Hence, depending on the extent of synchronicity in GC initiation, influence of soluble antibodies on individual GCs varies as predicted in Chapter 3. Consequently, it would be expected that delayed onset with respect to other GCs would lead to a reduction in peak GC size and production of plasma cells due to antibody mediated intercommunication. However, the nature of late GCs and whether they also differ in characteristics other than those induced by antibody feedback are unknown and need future investigations. Alternatively, with the assumption that late GCs might predominantly be seeded by memory cells from early GCs, late GCs were partially able to overcome the inhibition in an immune response towards single antigen epitope. This suggests that in the presence of high antibody feedback, late GCs perform well when seeded by memory B cells compared to relatively low affinity naïve B cells. However, the extent of memory B cells participating in primary GC response remains unclear. In a recall GC response, only minimal participation of memory B cells has been observed [100]. Computational simulations have suggested that memory cells are likely excluded from participation in GCs due to the presence of antibody feedback in the context of secondary immunization [102].

In a GC response towards two equally dominant epitopes, pool of plasma cells produced from individual GCs had similar affinities towards both the epitopes in the absence of intercommunication. With increasing feedback strength, especially the late GCs produced plasma cells of high affinity predominantly towards a single epitope. When the proportion of two antigen epitopes were varied such that one of the epitopes is rare, the overall response towards rare epitope was lower as expected. However, late GCs had a better affinity maturation towards rare epitope compared to the early GCs. This is consistent with previous findings suggesting that antibody feedback tends to shift the focus of GCs from immunodominant to subdominant epitope during the GC reaction [102].

Results discussed in chapter 5 predict that individual GCs in a lymphoid organ might have different lifetimes that might be a consequence of various reasons including differences in founder cell composition. Although, interaction between GCs via soluble antibodies can also induce differences in GC behavior, the differences observed in the data were solely not explainable by antibody feedback suggesting the presence of antibody feedback independent variability. Hence, in this chapter, the influence of antibody mediated intercommunication was also tested with GCs having different founder cell composition. Diverse effects were observed when GCs had founder cells specific to different epitopes. Such intercommunication was able to direct the GCs to focus on one or the other epitope depending on the founder cell composition of other GCs. As discussed in Chapter 5, exact reason for heterogeneity seen among individual GCs is not known and antibody feedback might also be a contributing factor.

Impact of intercommunication was also tested with persistent antigen deposition on FDCs. Increasing deposition of antigen had the opposite effect of antibody feedback and hence, with similar antibody feedback strength, the effects of antibody feedback could be reversed by the deposition of more antigen. Therefore, mutant control of GCs by antibody feedback is particularly important in limiting the magnitude of GC response in a single shot

vaccination. Reversal of antibody mediated inhibition by persistent antigen deposition might also be a contributing factor for enhanced GC response seen in the case of slow delivery immunization [22, 153]. Precise effects of antibody feedback in the case of a viral infection where there is a persistent deposition of antigen variants need to be explored in the future. Moreover, the extent of antibody feedback critically depends on the plasma cell production and antibody secretion. Therefore, other mechanisms regulating differentiation of plasma cells and those that regulate secretion of antibodies from plasma cells need to be investigated to gain a better understanding of the role of soluble antibodies in the regulation of GC response.

Chapter 7

Mechanisms of GC shutdown

7.1 Abstract

In this Chapter, different mechanisms of GC shutdown were proposed and tested *in silico* to identify experiments that can distinguish these mechanisms. Hypotheses proposed suggest various causes of GC shutdown including antigen limitation, changes in Tfh signals and changes in B cell divisions independent of antigen or Tfh. Antigen limitation could be due to antigen consumption by B cells, feedback by soluble antibodies, morphological changes in FDCs or changes in antigen presentation kinetics. As these mechanisms were capable of terminating GCs independently, they might potentially contribute to GC shutdown at least under certain settings. Hence, various experiments were identified to test the existence of the mechanisms proposed. Depending on the mechanism and assumptions considered, GC shutdown is due to changes in number of recycling cells and/or due to decrease in average number of divisions. This finding suggests that it is important to reanalyze the factors determining number of cell divisions and dependence of Tfh signaling on pMHC presentation. Implication of GC shutdown on the quality and quantity of GC output were also examined.

7.2 GC shutdown

GCs are transient and undergo shutdown through an unknown mechanism. Various mechanisms have been hypothesized to be the potential cause of GC shutdown based on indirect evidences from experiments [77, 111]. Despite this, examining the mechanism of shutdown experimentally is a challenging task as defects in several factors can terminate the GCs but the alterations might not be physiological. This is further complicated by the fact that it is difficult to monitor GCs longitudinally for a long period of time. Moreover, it is not known whether GCs formed under different experimental settings or even GCs within the same lymphoid organ follow the same mechanism of shutdown.

One of the mechanisms that is believed to cause GC shutdown is the limitation of antigen. GC B cells acquire antigen from FDCs that could host native antigen in a stable form for a long period of time [93]. However, decrease in antigen access might occur due to masking by soluble antibodies [178], or changes in the morphology of FDCs [80]. Another hypothesis is that the changes in the state of FDCs/Tfh induces differentiation of late GC B cells and promote their exit from GC leading to shut down [111]. These changes occurring in the dynamics and behavior of different cell populations during the GC reaction are mostly unexplained and it is not clear whether they might be the cause of GC shutdown or just a consequence of contracting GC.

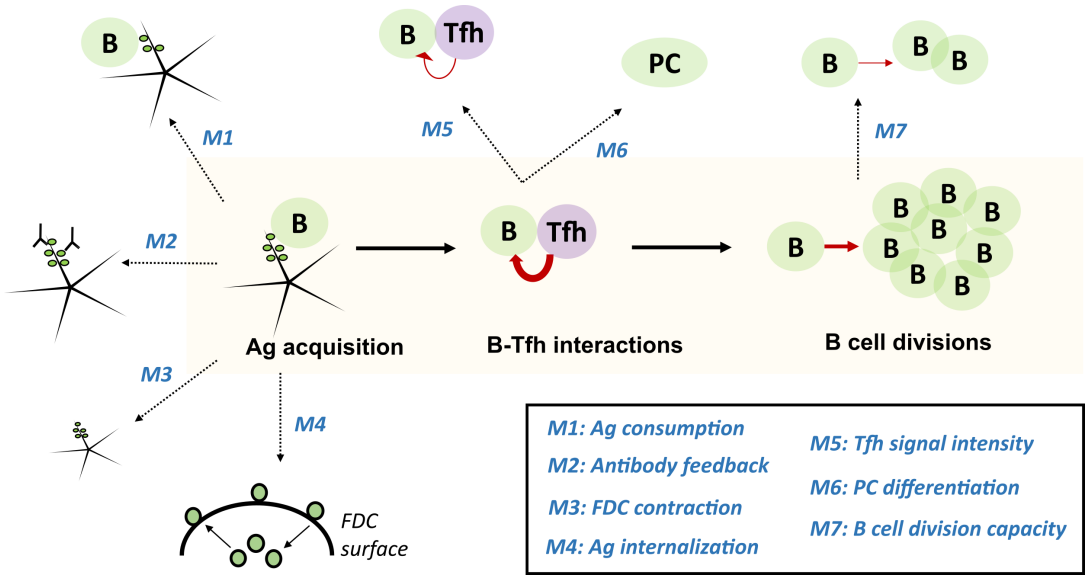

Figure 7.1: Summary of mechanisms proposed for the shutdown of GCs. In mechanisms M1–M4, consumption of antigen by B cells, binding of soluble antibodies, contraction of FDCs and increase in the fraction of FDC internalized antigen, respectively are assumed to decrease antigen availability or accessibility. M5-M7 are independent of antigen limitation. In M5, signaling capacity of Tfh cells is assumed to decrease as GC progresses. In M6, an increase in PC production leads to GC shutdown. In M7, division capacity of B cells is assumed to decrease as the GC matures. GC: Germinal centre; PC: Plasma cell; FDC: Follicular dendritic cell; Tfh: T follicular helper cell; Ag: Antigen; B: B cell

Despite the unclear knowledge about the mechanism of shutdown, experimental studies have suggested that GC response can be enhanced by extended provision of antigen via slow delivery immunization or by using a combination of TLR ligands [23, 75, 153, 22]. As GC lifetime is a critical factor that determines the state of B cell affinity maturation and quantity of GC output, understanding the mechanism of GC shutdown might help identify targets to efficiently modulate GC reactions.

7.3 Methods

Based on indirect evidences from experimental studies, mechanisms of GC shutdown were hypothesized (Figure 7.1) and tested *in silico* using the model described in Chapter 2.

Details of each mechanism is explained below

Antigen consumption (mechanism M1)

Acquisition of antigen by a B cell reduces the amount of antigen on FDC by 1 portion. Thus, there is a gradual decrease in antigen during the GC reaction. This mechanism hypothesizes that the GC shutdown is due to antigen limitation arising from consumption by B cells.

Antibody feedback (mechanism M2)

This hypothesis considers the antibody feedback as the mechanism of GC shutdown. Antibody feedback is implemented as described in Chapter 2.

FDC contraction (mechanism M3)

As there is considerable evidence that FDCs undergo remodeling during the GC reaction [18], this mechanism assumes that the GC shutdown is due to morphological changes in FDCs that limit antigen access of GC B cells. More specifically, it is assumed that the FDC network extends at early stages of the GC reaction and contracts after the GC reaches a maximum size, thus leading to GC shutdown. As the exact basis of the FDC morphological changes is unknown, it was modelled in a phenomenological way. Length of FDC dendrites at the start of the simulation was set to 5 µm. Dendrites are extended at a rate (k) corresponding to 24 h until time t (162 or 155 h) of the GC reaction. After time t, length of FDC dendrites is assumed to decrease leading to contraction of FDC network. However, number of FDCs (=200) is assumed to be constant throughout the GC reaction.

Extension and growth of FDC network at early stages could be due to interaction with B cells, as FDCs are known to be maintained by lymphotoxin signaling by B cells [39, 48]. Contraction of FDCs can be speculated to be due to changes in the nature of FDC-GC B cell interactions. Morphological changes in FDCs could also be due to the action of Tfr cells. Tfh/Tfr ratio is higher at late stages of GC reactions [166, 174] and Tfr cells act as a source of IL-10 [83, 19]. A study has shown that cytokines such as IL-10 can alter the contractility of FDCs [112], thus supporting the speculation that Tfrs alter the morphology of FDCs during the GC reaction.

Antigen internalization (mechanism M4)

This hypothesis assumes that the antigen presentation dynamics is modulated during the GC reaction and is the cause of GC shutdown. For the simulations of this hypothesis, implementation of dynamic antigen presentation by antigen cycling in FDCs described in Chapter 4 is used. Externalization rate (k_{ext}) of immune complex is decreased over time (t) following the equation.

$$k_{\text{ext}} = k_{\text{ext}}(0)(1 - t^{\text{n}})/(K^{\text{n}} + t^{\text{n}}) \tag{7.1}$$

GC simulation is started with immune complex cycling rates estimated using the PE-IC data from [62], $k_{\text{ext}}(0) = 1/(36\ \text{min})$. Hence, there would be a drop in the surface antigen concentration during GC reaction without any alteration in total antigen concentration of FDCs. While, cycling of immune complex has been demonstrated in both mouse and human FDCs [62, 61], it is not known whether the cycling rates are modulated during the GC reaction. However, changes in morphology and differentiation state of FDCs might lead to changes in antigen cycling dynamics.

Tfh signal intensity (mechanism M5)

In this hypothesis, it is assumed that the signaling strength of Tfh decreases over time. Signals delivered to B cells is reduced at constant rate k at every time step of the simulation. Tfh cells undergo changes during the GC reaction [170] but the implications of such changes in selection of GC B cells is unknown. However, Tfr cells seen in the GCs at late time points, are capable of suppressing Tfh cells [130, 136, 173] and might lead to such decrease in Tfh signaling intensity.

Increased Plasma cell (PC) differentiation (mechanism M6)

According to this hypothesis, shutdown of GCs is due to large proportion of cells exiting GC at late stages. Therefore, a fraction of Tfh selected cells is allowed to differentiate into PCs and exit the GC.

Different variants of this mechanism are tested

pMHC dependent PC differentiation

Probability of PC differentiation (F) was assumed to depend on pMHC presentation (p) of selected cell according to the equation

$$F = p^{\mathrm{n}}/(p^{\mathrm{n}} + K^{\mathrm{n}}) \tag{7.2}$$

Tfh signal dependent PC differentiation

Probability of differentiation into PCs (F) was assumed to depend on the amount of Tfh signals (T_{sig}) received until the time of selection and follows the equation

$$F = T_{\mathrm{sig}}^{\mathrm{n}}/(T_{\mathrm{sig}}^{\mathrm{n}} + K^{\mathrm{n}}) \tag{7.3}$$

Time dependent PC differentiation

Probability of PC differentiation (F) was assumed to increase in a time dependent manner and independent of antigen uptake or Tfh signals received. This follows the equation

$$F = 1 - e^{-\mathrm{kt}} \tag{7.4}$$

It has been widely accepted that cells receiving stronger Tfh signals preferentially exit the GC as PCs [71]. However, it might be possible that changes in Tfh signals or other mechanisms lead to preferential differentiation of GC B cells at late time points.

B cell division capacity (mechanism M7)

In this mechanism, B cells are assumed to undergo progressive changes during the GC reaction that leads to gradual loss of the proliferation capacity over time. It is assumed that the B cells that have undergone higher number of DZ-LZ cycles would divide less.

$$K = K_{\mathrm{min}} + (K_{\mathrm{max}} - K_{\mathrm{min}})N_{\mathrm{cyc}}^{\mathrm{n}}/(N_{\mathrm{cyc}}^{\mathrm{n}} + K_{\mathrm{K}}^{\mathrm{n}}) \tag{7.5}$$

Number of divisions is determined by Hill function shown in Equation 2.2 such that the number of divisions vary between 1 and 6. K is the amount of antigen or Tfh signals received by B cells that leads to half of the maximum number of divisions. In this scenario, K is assumed to vary as a function of total number of cycles the GC B cell has undergone between the LZ and the DZ, N_{cyc}. As a result, the value of K differs among B cells.

According to this mechanism, the B cell that has spent longer time in the GC has to receive higher amounts of antigen/Tfh signals in order to achieve half of the maximum number of divisions. Although, changes in antigen uptake and Tfh signals received, primarily influence the GC B cell fates and number of divisions of GC B cells, the basis for this assumption is the recent finding which shows that late GC B cells have an exhausted fatty acid reserve [171].

Exact determinants of Tfh signals received by a B cell and number of divisions that B cells undergo after selection by Tfh cells are unclear. Consequently, different assumptions were considered that vary in the extent of dependence on pMHC presentation and Tfh signals received (Table 7.1).

Alternate assumptions for selection by Tfh cells:

1) In the basic version of the model used, Tfh and B cell interact for a fixed duration, during which the Tfh may or may not polarize to the B cell. B cell receives a unit of signal from Tfh only if the Tfh polarizes towards it at a given time point. If a Tfh is bound to

Table 7.1: Summary of assumptions considered in the simulations for each shutdown mechanism. pMHC: peptide major histocompatibility complex; Tfh: T follicular helper cell; sig:signal.

Assumption	Tfh signals	No. of divisions
A1	pMHC independent	pMHC dependent
A2	pMHC dependent	pMHC dependent
A3	pMHC independent	Tfh sig. dependent
A4	pMHC dependent	Tfh sig. dependent

many B cells, then the Tfh polarizes towards the B cells with highest pMHC presentation. Thus, in this assumption, there is an indirect dependence of selection on the amount of antigen collected.

2) Tfh polarized to the B cell delivers signals dependent on the amount of antigen collected by the B cell.

Similarly, the number of divisions of selected GC B cells was assumed to depend either on pMHC presentation (antigen collected) or on the amount of Tfh signals received until the time of selection by Tfh. By combining these assumptions for selection by Tfh cells and number of divisions, four different set of assumptions were considered and are summarized in Table 7.1.

7.4 Potential mechanisms

Different mechanisms described in the methods section, were tested for their ability to terminate GCs independently. A reference model [black curves in Figure 7.2] where the GCs do not undergo shutdown, was used to test the ability of different mechanisms to terminate GCs. In the reference simulation, as no mechanism of shutdown is explicitly implemented, the GC volume saturates after reaching a maximum value due to the limiting number of Tfh. Although, limiting Tfh help is limiting the magnitude of GC reaction, it is unable to contract the GC to promote shutdown. Seven mechanisms were identified to shutdown GCs under certain conditions and are summarized in Figure 7.1.

Mechanisms M1-M4, led to antigen limitation and terminated GCs. Antigen consumption by GC B cells (M1), antibody feedback (M2) and antigen internalization (M4) were able to terminate GCs under all the 4 assumptions tested [Figure 7.2A-D for M1, Table 7.1 and 7.2]. FDC contraction model was able to terminate GCs in three of the assumptions [Figure 7.2E, F and H]. When the number of GC B cell divisions and Tfh signals received are not directly dependent on pMHC presentation of GC B cells, FDC contraction model was incapable of terminating the GC [Figure 7.2G].

Similarly, a reduction in the Tfh signaling intensity during the GC reaction can shutdown GCs irrespective of the assumption considered [Figure 7.3A-D]. This suggests that in the absence of antigen limitation, other mechanisms might exist that can terminate GCs. A reduction in B cell division capacity could also terminate GCs [Figure 7.3E-H]. Increasing PC differentiation was unable to terminate GCs, when PC differentiation was assumed to depend on the pMHC presentation or Tfh signals received by the B cells [Figure 7.4A and

Table 7.2: Ability of different mechanisms to shutdown GCs under different assumptions. Yes = can shutdown GCs, No = could not shutdown GCs (refer to Table 7.1 for A1-A4 and Figure 7.1 for M1-M7). PC: Plasma cell; GC: Germinal centre; Ag: Antigen; Ab: Antibody; FDC: Follicular dendritic cell; Tfh: T follicular helper cell.

Mechanism	**Assumption A1** **Tfh sig:** pMHC indep **divisions:** pMHC dep	**Assumption A2** **Tfh sig:** pMHC dep **divisions:** pMHC dep	**Assumption A3** **Tfh sig:** pMHC indep **divisions:** Tfh sig. dep	**Assumption A4** **Tfh sig:** pMHC dep **divisions:** Tfh sig. dep
M1: Ag consumption	Yes	Yes	yes	yes
M2: Ab feedback	yes	yes	yes	yes
M3: FDC contraction	yes	yes	No	yes
M4: Ag internalization	yes	yes	yes	yes
M5: Tfh signal intensity	yes	yes	yes	yes
M6: PC differentiation	yes	yes	yes	yes
M7: B cell division capacity	yes	yes	yes	yes

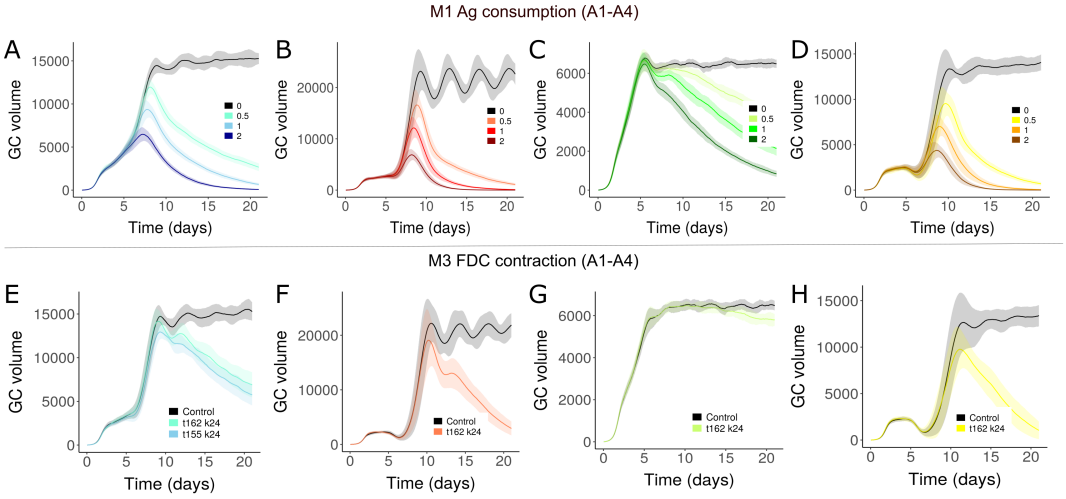

Figure 7.2: GC dynamics for mechanisms M1 (Ag consumption) and M3 (FDC contraction) with different assumptions (Table 7.1). Black curves represent reference simulations where the GC does not terminate. A-D) Mechanism M1. Inset in A-D show the amount of antigen (in portions) consumed by a B cell per FDC encounter. E-H) Mechanism M3. Insets in E-H show the values of t (time until when FDC dendrites extend in h) and k (Rate of extension or contraction of FDC dendrite per lattice constant in h^{-1}). Color code represent the assumptions considered. A-D and E-H correspond to assumptions A1-A4. Solid lines and shaded area represent mean and standard deviation of 10-30 simulations. GC: Germinal centre; FDC: Follicular dendritic cell; Ag: Antigen.

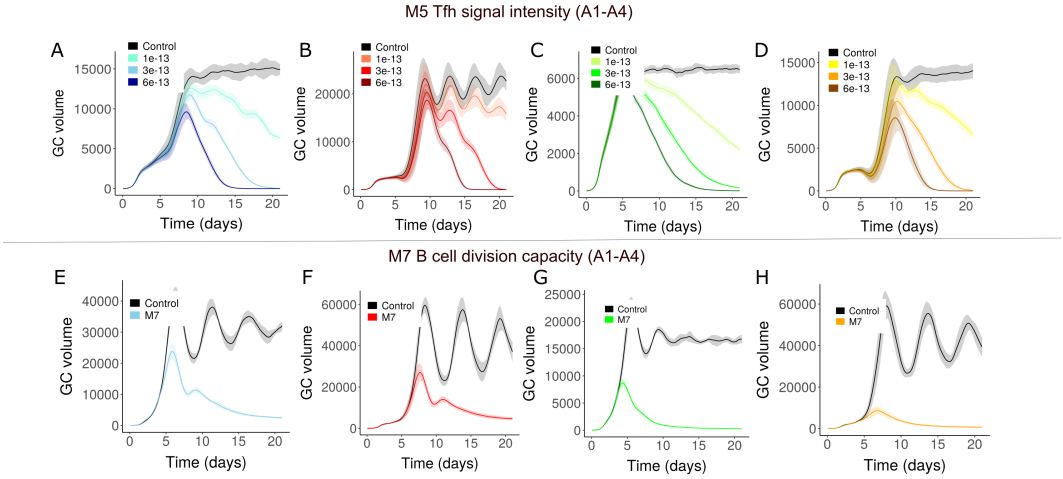

Figure 7.3: GC dynamics for mechanisms M5 (Tfh signal intensity) and M7 (B cell division capacity). A-D) Mechanism M5. Insets in A-D show the rate of decrease in Tfh signals in every time step of the simulation. E-H) Mechanism M7. Black curves represent reference simulations where the GC does not terminate. Color code represent the assumptions considered. A-D and E-H correspond to assumptions A1-A4. Solid lines and shaded area represent mean and standard deviation of 10-30 simulations. GC: Germinal centre; Tfh: T follicular helper.

B]. In this case, either the GCs could not contract or the GC was prematurely terminated at a very early stage. This suggests that either such PC differentiation might not lead to GC shutdown or there could be additional factors that control the differentiation to PCs. Alternatively, a time dependent increase in PC differentiation independent of pMHC presentation or Tfh signals received was capable of terminating GCs under all the four assumptions tested [Figure 7.4C and Table 7.2].

7.5 GC shutdown under different hypotheses

As mentioned previously, identified mechanisms terminated GCs due to antigen limitation, Tfh signal limitation, reduced B cell divisions or faster terminal differentiation and exit from GC. These hypotheses were further examined to investigate the mechanistic details of GC shutdown. Exact cause of GC shutdown varied depending on the assumptions considered [Table 7.3], and suggest the need to clarify these assumptions [Table 7.1] under different experimental conditions.

Antigen limitation due to antigen consumption in M1 decreased the antigen uptake of GC B cells after the peak of the GC volume compared to the reference simulations [Figure 7.5A]. When the number of divisions after selection by Tfh was assumed to depend on the antigen uptake of GC B cell, the antigen limitation led to gradual decrease in average divisions [Figure 7.5B]. On the other hand, when the number of divisions was determined by the Tfh signals received, there was no decrease in average divisions [Figure 7.5D], instead the fraction of cells selected to recycle back to the DZ to undergo further divisions was decreased [Figure 7.5C]. In this mechanism, reduced Tfh signals increased the fraction of GC B cells undergoing apoptosis. Depending on the assumptions considered, there can be a decrease in average divisions as well as decrease in number of selected cells compared to the reference model [Table 7.3]. Hence, GC shutdown due to antigen limitation is due to reduced number of divisions of selected cells and/or decreased fraction of selected cells. Similar results were obtained for other antigen limitation models [Figure 7.5 and Table

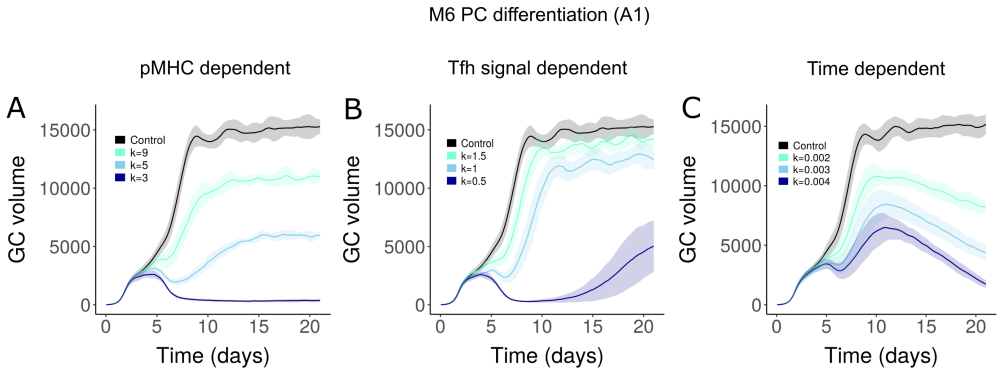

Figure 7.4: GC dynamics for mechanism M6 (PC differentiation) considering assumptions A1 (Table 7.1). A) pMHC dependent PC differentiation. Value of K used in Equation 7.2. is shown in the inset. B) Tfh signal dependent PC differentiation. Value of K used in equation 7.3 is shown in the inset. C) Time dependent PC differentiation. Inset shows the value of k used in equation 7.4. Black curves represent reference simulations where the GC does not terminate. Solid lines and shaded area represent mean and standard deviation of 10-30 simulations. GC: Germinal centre; Tfh: T follicular helper; PC: Plasma cell; pMHC: peptide major histocompatibility complex.

Table 7.3: GC shutdown in different mechanisms (Figure 7.1) under different assumptions (Table 7.1). PC: Plasma cell; GC: Germinal centre; Ag: Antigen; Ab: Antibody; FDC: Follicular dendritic cell; Tfh: T follicular helper cell.

Mechanism	**Assumption A1** **Tfh sig:** pMHC indep **divisions:** pMHC dep	**Assumption A2** **Tfh sig:** pMHC dep **divisions:** pMHC dep	**Assumption A3** **Tfh sig:** pMHC indep **divisions:** Tfh sig. dep	**Assumption A4** **Tfh sig:** pMHC dep **divisions:** Tfh sig. dep
M1: Ag consumption	**Reduced av. divs**	**Reduced av. divs** **Reduced sel. cells**	**Reduced sel. cells**	**Reduced sel. cells**
M2: Ab feedback	**Reduced av. divs**	**Reduced av. divs** **Reduced sel. cells**	**Reduced sel. cells**	**Reduced av. divs** **Reduced sel. cells**
M3: FDC contraction	**Reduced av. divs**	**Reduced av. divs** **Reduced sel. cells**	**Cannot shutdown**	**Reduced sel. cells**
M4: Ag internalization	**Reduced av. divs**	**Reduced av. divs** **Reduced sel. cells**	**Reduced sel. cells**	**Reduced av. divs** **Reduced sel. cells**
M5: Tfh signal intensity	**Reduced sel. cells**	**Reduced sel. cells**	**Reduced av. Divs** **Reduced sel. cells**	**Reduced av. Divs** **Reduced sel. cells**
M6: PC differentiation	**More exit**	**More exit**	**More exit**	**More exit**
M7: B cell division capacity	**Reduced av. divs**	**Reduced av.divs**	**Reduced av.divs**	**Reduced av.divs**

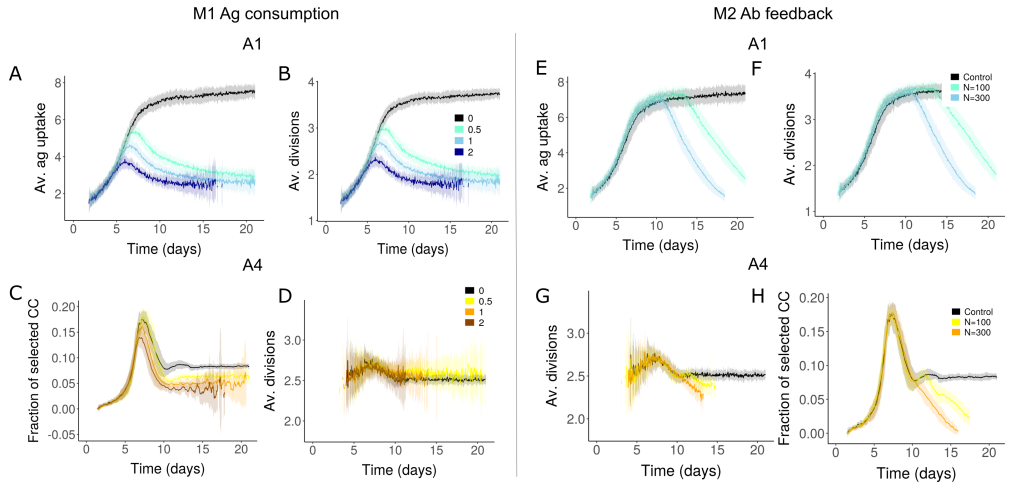

Figure 7.5: Mechanistic details of GC shutdown in mechanisms M1 (Ag consumption, panels A-D) and M2 (antibody feedback, panels E-H). Results are shown for assumptions A1 and A4. Color code represent the assumptions considered. A and E) Average antigen uptake of recycling cells. B and F) Average divisions of Tfh selected GC B cells, C and G) Average divisions of Tfh selected GC B cells and D and H) Fraction of selected centrocytes. Insets in M1 show the amount of antigen consumed by GC B cell per interaction with FDC. Insets in M2 show the value of N used to scale the production of antibodies and reflect different strength of antibody feedback. Black curves represent reference simulations where the GC does not terminate. Solid lines and shaded area represent mean and standard deviation of 10-30 simulations. GC: Germinal centre; Ag: Antigen; Tfh: T follicular helper; Ab: Antibody; CC: Centrocyte; FDC: Follicular dendritic cell.

7.3]. These models show a decrease in average antigen uptake, that could be detected in the experiments by measuring the average pMHC presentation of GC B cells at different stages of GC reaction. Antigen limitation is expected to decrease the pMHC presentation when the GC starts contracting. Results of different hypotheses are summarized in Table 7.3.

In the FDC contraction model, when the number of divisions and selection by Tfh were not directly influenced by pMHC presentation, there was no decrease in average divisions but only a very small decrease in fraction of selected cells which was unable to terminate the GCs [Figure 7.2G]. As there is no direct experimental evidence suggesting that FDC network contracts when the GC is terminating, it could be tested by measuring the FDC area in the GCs [Figure 7.6B]. Moreover, this mechanism leads to antigen limitation by decreasing the fraction of FDC encounters rather than the decreased antigen amount on FDCs. Hence, in the absence of limitation in antigen amount, presence of this mechanism can be tested by monitoring the fraction of B cell-FDC encounters that lead to successful antigen uptake. As the affinity of GC B cells increase during the GC reaction, the fraction of successful antigen uptake events simply increases or saturates in this hypothesis [Figure 7.6D]. However, under the action of other antigen limitation mechanisms such as consumption of antigen by B cells, masking by soluble antibodies and increased antigen internalization, the fraction of successful antigen uptake events decreases at late time points.

Changes in antigen cycling dynamics and internal accumulation of antigen leads to decreased antigen uptake [Figure 7.7A] as in the other mechanisms. As this mechanism decreases the fraction of antigen presented on FDC surface [Figure 7.7C], measuring the amount of internalized and surface presented antigen might be considered as a test for

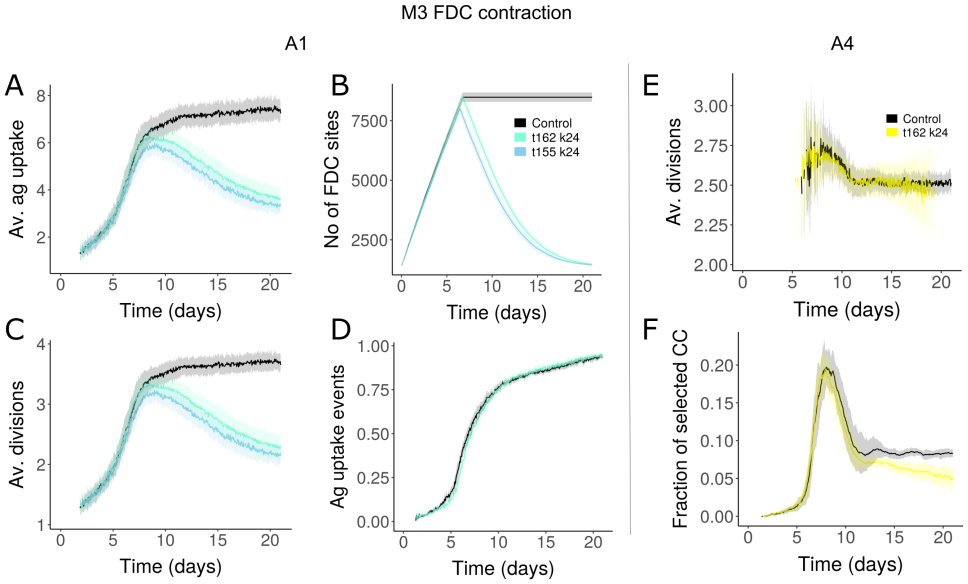

Figure 7.6: GC shutdown in mechanism M3 (FDC contraction). Color code represent the assumptions considered. Results are shown for assumptions A1 (A-D) and A4 (E-F). A) Average antigen uptake of recycling GC B cells. B) Number of lattice sites occupied by FDCs. C and E) Average divisions of Tfh selected cells. D) Fraction of B cell - FDC encounters with successful antigen uptake. F) Fraction of selected centrocytes. Insets show the values of t (time until when FDC dendrites extend in h) and k (Rate of extension or contraction of FDC dendrite per lattice constant in h^{-1}). Black curves represent reference simulations where the GC does not terminate. Solid lines and shaded area represent mean and standard deviation of 10-30 simulations. GC: Germinal centre; FDC: Follicular dendritic cell; Ag: Antigen; CC: Centrocyte; Tfh: T follicular helper cell

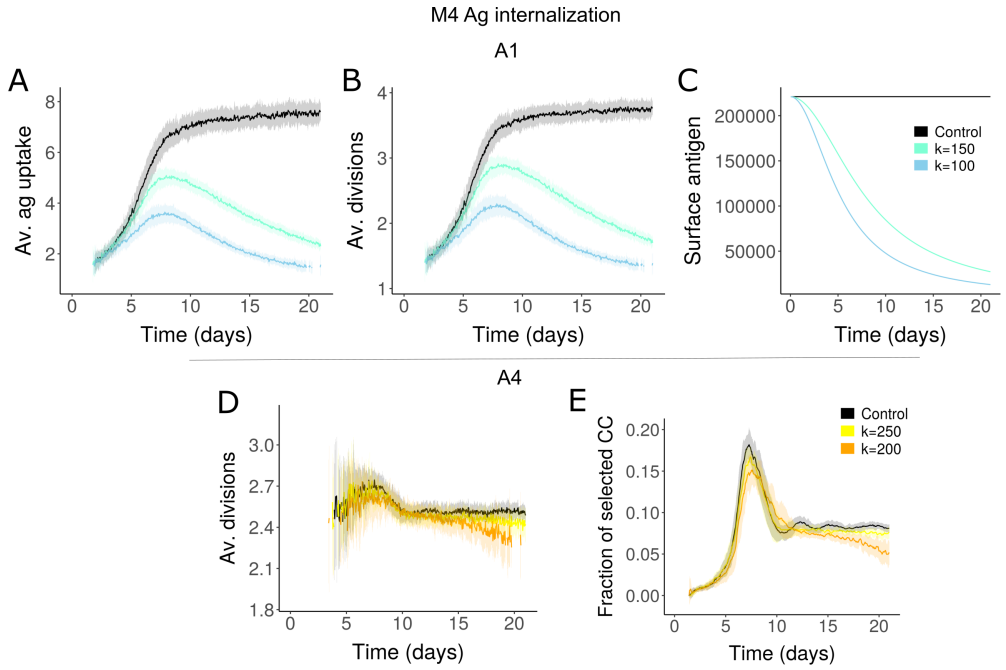

Figure 7.7: GC shutdown in mechanism M4 (Ag internalization). Color code represent the assumptions considered. Results are shown for assumptions A1 (A-C) and A4 (D and E). A) Average antigen uptake of Tfh selected GC B cells, B) Average divisions of Tfh selected GC B cells with A1, C) Surface antigen on FDCs, D) Average divisions of Tfh selected GC B cells with A4 and E) Fraction of selected centrocytes with A4. Inset shows the value of K used in equation 7.1. Black curves represent reference simulations where the GC does not terminate. Solid lines and shaded area represent mean and standard deviation of 10-30 simulations. GC: Germinal centre; Ag: Antigen; CC: Centrocyte; Tfh: T follicular helper cell.

modulation of antigen cycling dynamics.

Decrease in Tfh signaling capacity primarily leads to reduced Tfh signals [Figure 7.8A] in selected GC B cells. Strength of Tfh signals received by GC B cells can be tested by quantifying the levels of signaling molecules such as c-Myc. However, antigen limitation can also lead to decreased Tfh signals when the Tfh signals are directly dependent on pMHC presentation.

In the mechanism M6, fraction of selected GC B cells that express differentiation markers increases during the GC reaction [Figure 7.9C]. In the presence of limitation in the B cell division capacity, the distribution of GC B cell divisions shifts to lower values despite sufficient pMHC presentation and Tfh signal induction [Figure 7.10C]. Hence, high affinity cells at late time points are expected to divide less compared to earlier time points. All the mechanisms identified ultimately influence the ability of GC B cells to proliferate.

7.6 Implication on GC output

Implications of GC shutdown on the output production and affinity maturation were also tested *in silico*. In general, shutdown of GC leads to decreased PC production and affinity maturation compared to a functional long-lasting GC. However, it might be possible that the mechanisms proposed might accelerate the production of output or affinity maturation at early stages before they terminate. Such a situation might be beneficial for quick

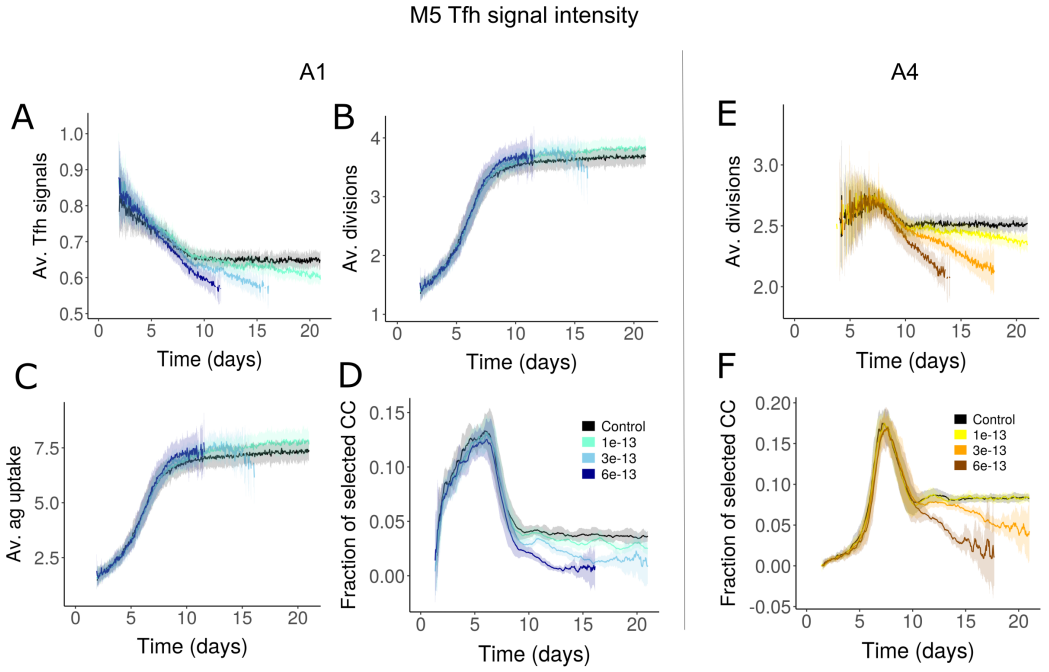

Figure 7.8: GC shutdown in mechanism M5 (Tfh signaling intensity). Color code represent the assumptions considered. Results are shown for assumptions A1 (A-D) and A4 (E and F). A) Average Tfh signals in selected GC B cells, B and E) Average divisions of Tfh selected GC B cells, C) Average antigen uptake of Tfh selected GC B cells, D and F) Fraction of selected centrocytes. Inset shows the rate of decrease in Tfh signals at every time step of the simulation. Black curves represent reference simulations where the GC does not terminate. Solid lines and shaded area represent mean and standard deviation of 10-30 simulations. GC: Germinal centre; Ag: Antigen; CC: Centrocyte; Tfh: T follicular helper cell

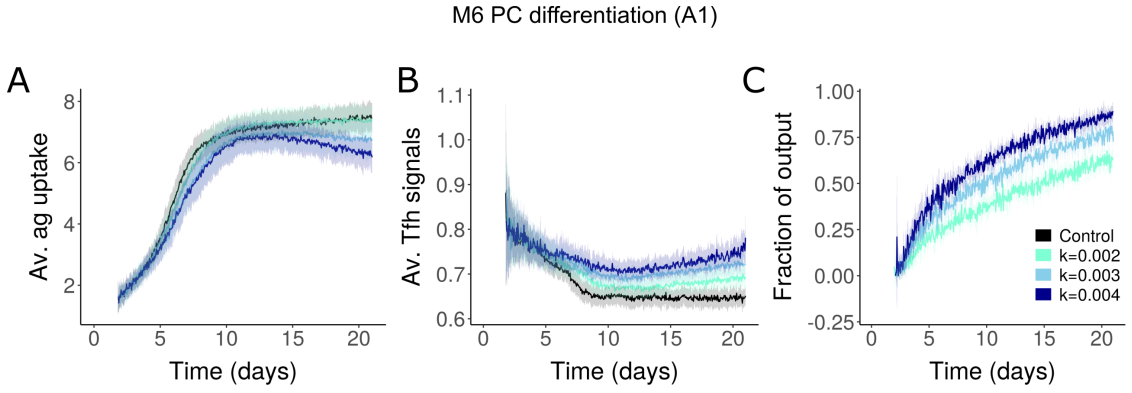

Figure 7.9: GC shutdown in mechanism M6 (PC differentiation) with assumption A1. A) Average antigen uptake of recycling cells, B) Average Tfh signals received by selected cells, C) Fraction of selected cells differentiating to output. Inset shows the value of k used in equation 7.4. Black curves represent reference simulations where the GC does not terminate. Solid lines and shaded area represent mean and standard deviation of 10-30 simulations. GC: Germinal centre; Ag: Antigen; PC: Plasma cell; Tfh: T follicular helper cell.

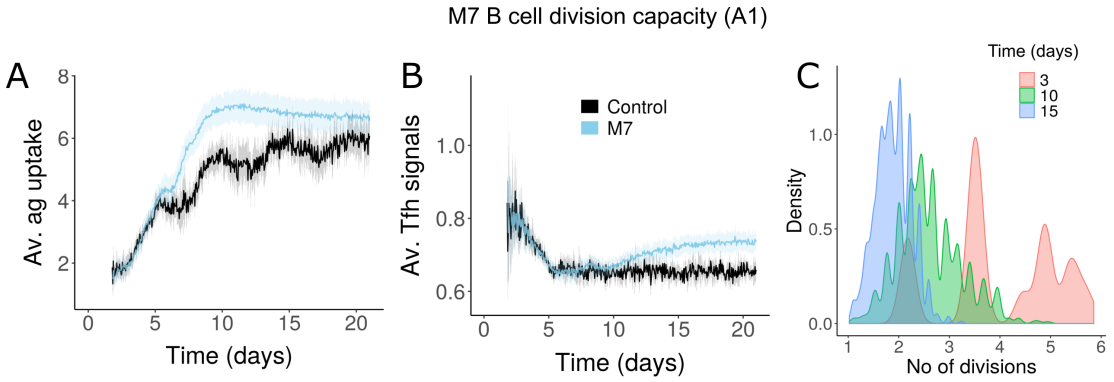

Figure 7.10: GC shutdown in mechanism M7 (B cell division capacity) with assumption A1. A) Average antigen uptake of recycling cells, B) Average Tfh signals received by selected cells, C) Distribution of number of divisions of selected cells. Black curves represent reference simulations where the GC does not terminate. Solid lines and shaded area represent mean and standard deviation of 10-30 simulations. GC: Germinal centre; Ag: Antigen; Tfh: T follicular helper cell.

pathogen clearance. Although, the outcome varied depending on the assumptions, under most cases the shutdown of GC did not accelerate the PC production except the increased PC differentiation model and B cell division capacity model [Table 7.4, Figure 7.11]. In M6, shutdown due to earlier PC differentiation leads to accelerated production of PCs. Affinity of PCs produced was enhanced in M7. In the other mechanisms, increased longevity of GCs might be critical for higher affinity maturation [Table 7.5]. It can be speculated that depending on the conditions, shutdown of GC might be controlled by different processes leading to differences in output and affinity maturation to meet the specific requirements.

7.7 Conclusions

As it is technically challenging to test the cause of GC shutdown, an *in-silico* analysis was performed to identify mechanisms that can terminate GCs independently. In total, seven mechanisms were capable of terminating GCs at least under certain assumptions. Furthermore, for each mechanism, different assumptions were considered as the factors determining the number of divisions of GC B cells and the intensity of Tfh signals received are not clearly understood. GC B cell divisions were assumed to depend either on the amount of antigen collected or on the signals received from Tfh cells. Similarly, the amount of Tfh signals received was assumed to be a function of pMHC presentation or depend on pMHC only to a limited extent as in the case of GC B cells competing for Tfh signals. These assumptions resulted in slightly different results suggesting that studies on further clarifying the validity of these assumptions under different experimental conditions is necessary.

Antigen limitation due to various reasons was able to cause GC shutdown. Small decrease in antigen due to consumption by B cells is predicted to decrease the average number of divisions over time or decrease the number of selected cells and lead to GC termination. Alternatively, masking of antigen by soluble antibodies is also predicted to lead to antigen limitation and terminate GCs. Such antigen limitation could be identified by a decrease in density of pMHC presentation of GC B cells during the GC reaction. Decrease in the surface area of FDCs can also decrease the antigen uptake of GC B cells. However, this mechanism was unable to shut down GC independently, when amount of Tfh signals received and number of divisions were not directly dependent on pMHC presentation.

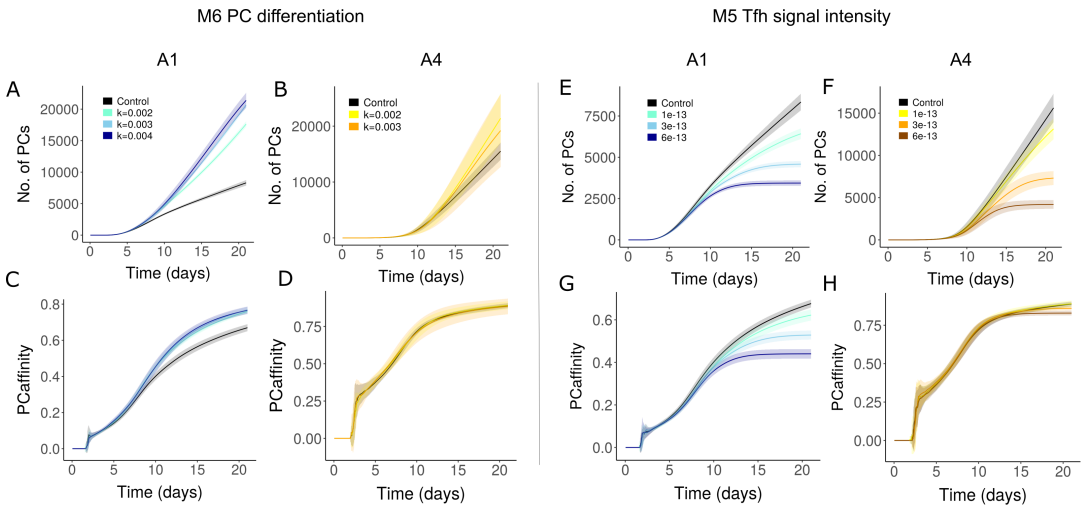

Figure 7.11: Changes in output and affinity maturation due to GC shutdown in M6 (PC differentiation) and M7 (Tfh signal intensity). Results are shown for assumptions A1 and A4. A and B) Number of PCs in PC differentiation mechanism (M6) under assumptions A1 and A4, respectively. Corresponding PC affinities are shown in C and D, respectively. E and F) Number of PCs produced in Tfh signal intensity mechanism (M5) under assumptions A1 and A4, respectively and the corresponding PC affinities are shown in G and H. Insets in M6 show the value of k used in equation 7.4. Insets in M5 show the rate of decrease in Tfh signaling intensity at every time step of the simulation. Black curves represent reference simulations where the GC does not terminate. Solid lines and shaded area represent mean and standard deviation of 10-30 simulations. GC: Germinal centre; PC: Plasma cell; Tfh: T follicular helper cell.

Table 7.4: Changes in PC production due to GC shutdown. PC: Plasma cell; GC: Germinal centre; Ag: Antigen; Ab: Antibody; FDC: Follicular dendritic cell; Tfh: T follicular helper cell.

Mechanism	**Assumption A1** **Tfh sig:** pMHC indep **divisions:** pMHC dep	**Assumption A2** **Tfh sig:** pMHC dep **divisions:** pMHC dep	**Assumption A3** **Tfh sig:** pMHC indep **divisions:** Tfh sig. dep	**Assumption A4** **Tfh sig:** pMHC dep **divisions:** Tfh sig. dep
M1: Ag consumption	Increase	Decrease	Decrease	Decrease
M2: Ab feedback	Increase	Decrease	Small decrease	Decrease
M3: FDC contraction	Increase	Decrease	**Cannot shutdown**	Decrease
M4: Ag internalization	Increase	Decrease	Decrease	Decrease
M5: Tfh signal intensity	Decrease	Decrease	Decrease	Decrease
M6: PC differentiation	Increase	Increase	Increase	Increase
M7: B cell division capacity	Increase	Increase	Increase	Increase

Table 7.5: Changes in PC affinity due to GC shutdown. PC: Plasma cell; GC: Germinal centre; Ag: Antigen; Ab: Antibody; FDC: Follicular dendritic cell; Tfh: T follicular helper cell.

Mechanism	Assumption A1 **Tfh sig:** pMHC indep **divisions:** pMHC dep	Assumption A2 **Tfh sig:** pMHC dep **divisions:** pMHC dep	Assumption A3 **Tfh sig:** pMHC indep **divisions:** Tfh sig. dep	Assumption A4 **Tfh sig:** pMHC dep **divisions:** Tfh sig. dep
M1: Ag consumption	Increase	Decrease	Decrease	Decrease
M2: Ab feedback	Increase	Small decrease	No change	Small decrease
M3: FDC contraction	Increase	No change	Cannot shutdown	No change
M4: Ag internalization	Increase	Small increase	No change	No change
M5: Tfh signal intensity	Decrease	Decrease	Decrease	Decrease
M6: PC differentiation	Increase	Small increase	Decrease	No change
M7: B cell division capacity	Increase	Increase	Decrease Increase until day 10	Increase

Such changes can be determined by quantifying the surface area of FDCs during the GC reaction. Modulation of antigen cycling kinetics is another mechanism that might induce antigen limitation and could be detected by quantifying the proportion of FDC antigen displayed on FDC surface.

Tfh cells undergo dynamic changes over time that can be observed as changes in cytokines and surface marker expression [170]. Although there is no experimental evidence, assuming that Tfh cells signal less over time was sufficient to terminate GC reactions. As in the case of antigen limitation, GC B cells undergo reduced number of divisions over time or there is reduced number of selected GC B cells depending on the assumptions. It is questionable whether Tfh cells signal less over time, however such an assumption could be justified due to the potential suppressive activity of Tfr cells [130, 136, 173] that appear late in the GCs.

Differentiation and exit of GC B cells was unable to promote GC shutdown when the differentiation probability was assumed to depend on antigen collected or Tfh signals received. This suggests that either this mechanism might not be responsible for GC shutdown or there are additional factors influencing differentiation fate decision such as the changes in nature of Tfh over time. Moreover, increasing differentiation of GC B cells in a manner independent of antigen or Tfh signals was able to cause GC shutdown as expected. Hence, time course studies determining the fraction of recycling and differentiating cells can address questions related to GC shutdown. Tfh cells have been shown to undergo selection in a way similar to B cells [99]. Such Tfh selection needs interaction with B cells and Tfh with high affinity towards the pMHC presented by B cells are selected [99]. As a result, higher affinity Tfh cells likely persist at the end of the GC reaction and it can be speculated to drive the differentiation of GC B cells into PCs and contribute to GC shutdown as larger proportion of cells start to exit the GC reaction. Future work, is needed to address whether the selection of Tfh cells play a role in GC shutdown. Furthermore, unknown mechanisms might lead to changes in the nature of GC B cells during GC reaction. This was modelled by a decreased division capacity of GC B cells over time in a manner independent of antigen acquisition or Tfh signals.

In summary, mechanisms tested led to GC shutdown due to a reduction in number of recycling cells or the average number of divisions of GC B cells. However, as the exact basis of mechanisms modelled here are unknown, only a phenomenological approach was considered. Experiments suggested can test the existence of different mechanisms, as simulations suggest that these mechanisms if they exist are capable of acting independently as a mechanism of shutdown under certain conditions. However, future investigations are necessary to identify the primary mechanism of GC shutdown or contribution of different mechanisms when multiple mechanisms act together. Moreover, these mechanisms might not be completely independent of each other and this needs to be improved in the future to incorporate potentially missing cross talks. Nevertheless, future investigation along the directions pointed by this study are expected to promote a better understanding of GC shutdown.

Chapter 8

GC dysregulation by *BTG1* mutation in B cells

8.1 Abstract

GC B cell program and fate decisions are tightly regulated to ensure efficient affinity maturation and production of plasma and memory cells. Failure in the regulation of GC B cell program is associated with pathological GCs that can lead to autoantibody production or lymphomagenesis. *BTG1* (B cell translocation gene 1) mutation is associated with lymphoma development and experimental analysis by Mlynarczyk et al., suggested that *BTG1* mutation enhances the anabolic programming of GC B cells and promotes competitive advantage over the wild type GC B cells. *In silico* analysis predicted that *BTG1* mutation leads to increased number of cell divisions and faster transition between the GC zones. These results suggest the importance of cell cycle regulation in preventing lymphomagenesis in addition to the control of GC maintenance and termination discussed in Chapter 7. This work was done in collaboration with Coraline Mlynarczyk and Ari Melnick from Weill Cornell Medical College.

8.2 GC-derived B cell lymphoma

It is well recognized that the unique characteristics of GC B cells needed for efficient affinity maturation such as high proliferative potential, ability to undergo somatic hypermutation also make these cells prone to lymphomagenesis [109]. Therefore, small dysregulations in GC B cell programming can lead to a premalignant state that subsequently transforms into B cell lymphoma upon accumulation of additional mutations. As discussed in Chapter 7, balance between apoptosis, proliferation and terminal differentiation of B cells is important for GC maintenance. GCs start to contract when the contribution of apoptosis and terminal differentiation to GC volume exceed the contribution by proliferation. Alterations in GC B cell proliferation, apoptosis and terminal differentiation are also associated with GC derived B cell lymphomas. Cell cycle progression in GC B cells is regulated by various factors and their dysregulation can lead to excess proliferation of GC B cells. Transcriptional factors such as cMyc, mTOR and FOXO are involved in the regulation of cell cycle progression in GC B cells [40, 42, 70]. Cyclin D3 has been shown to be an important mediator and dose dependent controller of GC B cell divisions and gain of function mutations in *ccnd3* gene increased the size of GCs by increasing proliferation [116]. Translocation of BCL-2 can disrupt the normal apoptotic program of GC B cells [137]. Failure in terminal differentiation and exit from GCs due to mutations in *Blimp1*

[94] and *TET2* [35] can also trigger lymphomagenesis. Studying the role of such mutations is the key to understand the development of B cell lymphomas.

8.3 Experimental background

Missense mutations in *BTG1* gene are associated with the development of GC-derived B cell lymphomas. Mlynarczyk et al., discovered that in the GCs, *BTG1* mutant B cells show a competitive advantage over the Wild type (WT) B cells leading to a progressive increase in the fraction of *BTG1* mutant cells using an adoptive transfer system (1:1 ratio of *BTG1* mutant and WT B cells, referred as competitive set-up). Higher fraction of cMyc expressing *BTG1* mutant GC B cells compared to WT was also observed suggesting an increased Tfh help received by *BTG1* mutant cells. Similarly, gene enrichment analysis indicated an increase in anabolic program and Light Zone (LZ) to Dark zone (DZ) recycling program in mutant GC B cells. However, in experimental set up with *BTG1* mutant and WT B cells in individual mice (referred as non-competitive setup), GC volume in the presence of *BTG1* mutation in B cells did not show any alterations compared to WT mice. Despite the progressive increase of *BTG1* mutant B cells in competitive setup, the DZ-LZ polarity of GC was unaltered both in the competitive and non-competitive setups. Detailed analysis suggested a mechanism of post-transcriptional control of cMyc by *BTG1* (unpublished data, Mlynarczyk et al.).

8.4 Methods

Recent version of hyphasma with detailed selection mechanisms (DisseD, MiXed and BCinTime) involving signaling molecules cMyc, mTOR and FOXO [103] incorporated as explained in Chapter 2 was used for the simulations. Two different set of simulations were performed to reproduce the experimental results *in silico*, that mimic the competitive and non-competitive set ups used in the experiments. For the competitive set-up, *in silico* GCs were seeded with 50% WT and 50 % *BTG1* mutant B cells. Further, to mimic the high affinities of B1-8hi cells, the seeder cell affinities were chosen at a distance of 2 mutations from the optimal position in shape space (detailed description in Chapter 2). In the non-competitive set-ups, separate simulations were performed each with 100% mutant *BTG1* or WT B cells and founder cell affinities were chosen randomly anywhere in the shape space.

In each set up two different models were considered based on experimental evidences.

1) Faster Tfh help: In this model, *BTG1* mutant B cells were assumed to upregulate signaling molecules mTOR and cMyc at a faster rate than the WT [1.12 times higher in DisseD and MiXed theories]. In the BCinTime theory, as mTOR and cMyc are not explicitly considered, acquisition of Tfh signals was increased 1.2 times in *BTG1* mutant compared to WT.

2) Faster Tfh help with shorter cell cycle: In addition to faster Tfh help, cell cycle duration of recycling mutant GC B cells were shortened by 0.75 h.

8.5 Simulation of GCs with *BTG1* mutation

In silico simulations were performed to test whether a faster acquisition of Tfh help was able to recapture the fitness advantage of mutant GC B cells, without changes in polarity and GC volume. Small increase in Tfh help in DisseD theory was sufficient to confer

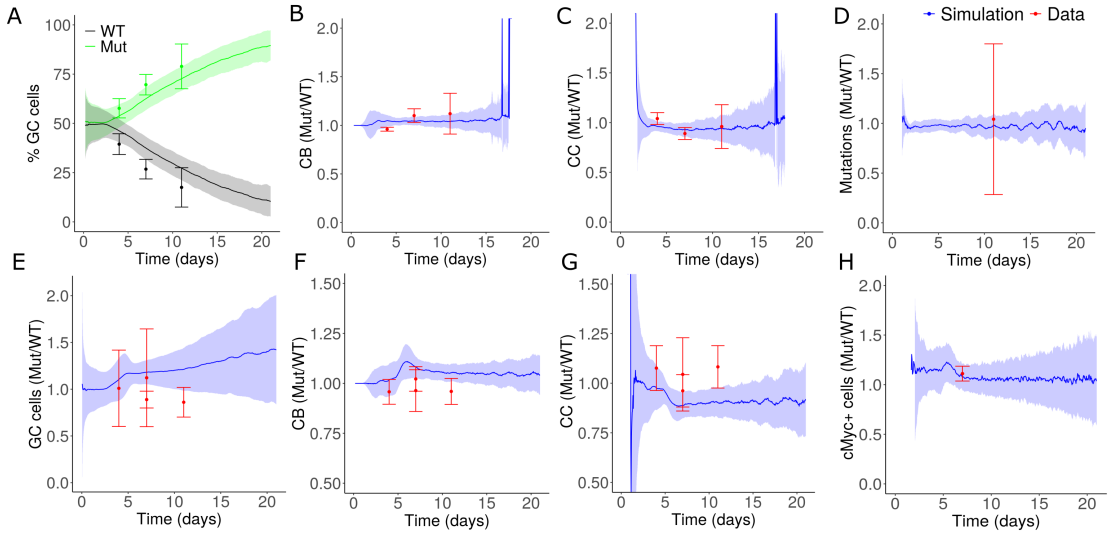

Figure 8.1: Simulations of faster Tfh help model using DisseD theory. A and E) % of *BTG1* mutant and WT GC B cells, B and F) Fraction of CB, C and G) Fraction of CC, D and H) Number of non-silent mutations. A-D) correspond to competitive set up and E-H) correspond to non-competitive set up. Experimental data and simulation readouts of *BTG1* mutant were normalized with WT control in panels B to H. Solid lines and shaded areas [in green, black and blue] are the average and standard deviation of 300 simulation repeats, respectively. CB: Centroblast; CC: Centrocyte; Mut: *BTG1* mutant; WT: Wild type; GC: Germinal centre. mTOR and cMyc upregulation was 1.12 times faster in mutant compared to WT. Experimental data was provided by Coraline Mlynarczyk and Ari Melnick.

competitive advantage [Figure 8.1 A]. However, small alterations were observed in the DZ-LZ polarity and GC volume changes (Figure 8.1 E, F and G).

Considering the previous finding that higher Tfh help can shorten the cell cycle duration of GC B cells [46] and the experimental indications of faster cell cycle progression in *BTG1* mutant B cells (unpublished data, Mlynarczyk et al)., cell cycle duration of *BTG1* mutant cells were shortened in addition to the increased upregulation of Tfh-induced signaling molecules. Shortening the cell cycle duration was able to overcome the changes in polarity and GC volume induced due to faster Tfh help as shown in Figure 8.2.

Model with shorter cell cycle duration and faster Tfh help for *BTG1* mutant was also consistent with the competitive fitness advantage [Figure 8.3A] and other experimental observations [Figure 8.3]. This model predicted that faster Tfh help would lead to increased number of cell divisions for the *BTG1* mutant B cells [Figure 8.4D] in DisseD theory due to an increased fraction of cMyc expressing *BTG1* mutant cells that explains the competitive advantage seen in the experiments. Comparison of interzonal transition of *BTG1* mutant and WT B cells predicted a faster cycling of *BTG1* mutant B cells between the GC zones [Figure 8.4C]. This was due to a decrease in the DZ and LZ residencd times of *BTG1* mutant B cells [Figure 8.4A-B]. Faster upregulation of mTOR and cMyc led to a faster selection of *BTG1* mutant cells and slightly decreased the LZ residence time per GC round [Figure 8.4B]. Shorter cell cycle durations of *BTG1* mutant cells led to decreased DZ residence time despite the increased number of divisions [Figure 8.4A].

As the selection theories proposed in [103] differ in characteristics such as the LZ passage time of GC B cells, these predictions were confirmed with the other two selection theories – BCinTime and MiXed. Predictions of BCinTime and MiXed theories [Figure 8.5] were

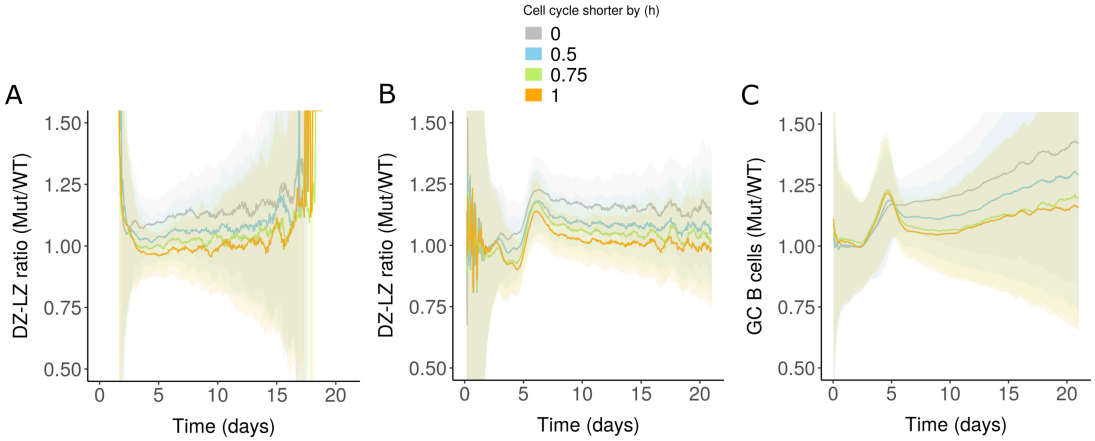

Figure 8.2: Effect of shortening cell cycle duration of *BTG1* mutant on GC volume and DZ-LZ polarity in DisseD theory. A and B) DZ-LZ ratio in competitive and non-competitive setups respectively. C) Number of GC B cells in non-competitive setup. Readouts of *BTG1* mutant were normalized with WT. Solid lines and shaded areas are the average and standard deviation of 300 simulations. Inset shows the shortening of cell cycle duration in hours for *BTG1* mutant with respect to WT. DZ: Dark zone; LZ: Light zone; Mut: *BTG1* mutant; WT: Wild type; GC: Germinal centre. mTOR and cMyc upregulation was 1.12 times faster in mutant compared to WT.

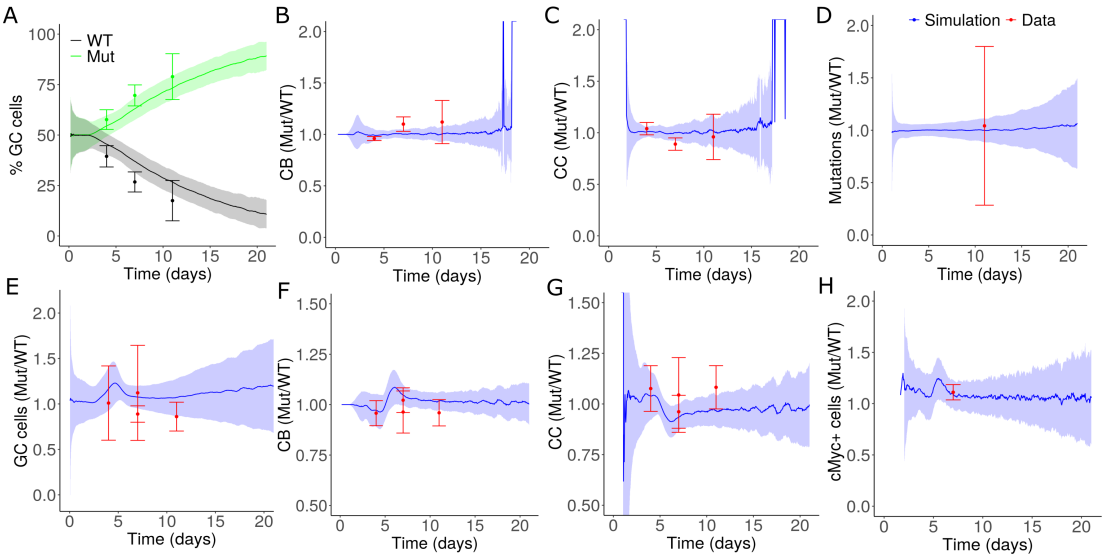

Figure 8.3: Simulations of faster Tfh help with shorter cell cycle in *BTG1* mutant using DisseD theory. A and E) % of *BTG1* mutant and WT GC B cells. B and F) Fraction of CB. C and G) Fraction of CC. D and H) Number of non-silent mutations. A-D) correspond to competitive set up and E-H) correspond to non-competitive set up. Experimental data and simulation readouts of *BTG1* mutant were normalized with WT control in panels B to H. Solid lines and shaded areas [in green, black and blue] are the average and standard deviation of 300 simulation repeats, respectively. CB: Centroblast; CC: Centrocyte; Mut: *BTG1* mutant; WT: Wild type; GC: Germinal centre. mTOR and cMyc upregulation was 1.12 times faster and cell cycle duration was shortened by 0.75 h in mutant compared to WT. Experimental data was provided by Coraline Mlynarczyk and Ari Melnick.

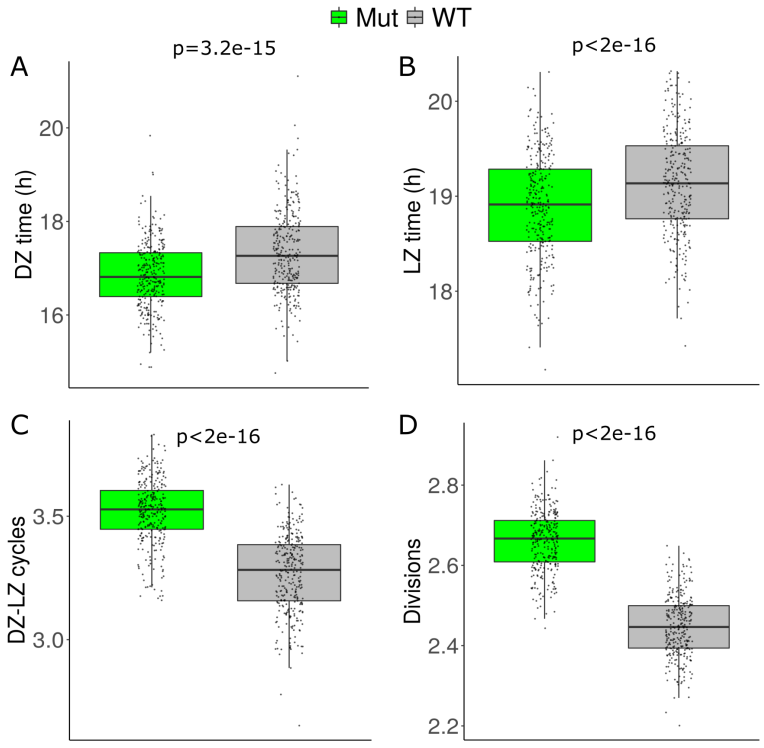

Figure 8.4: Predictions of the faster Tfh help with shorter cell cycle model for mutant *BTG1* B cells in DisseD theory. A) Residence time of GC B cells in DZ per GC round in hours, B) Residence time of GC B cells in the LZ per GC round in hours, C) Number of DZ-LZ cycles underwent by GC B cells until day 7 of the GC simulation, D) Number of divisions of GC B cells. Readouts are from day 7 of the GC simulation (approximately day 10 after immunization). Simulation data points are shown as dots. Statistical significance was tested by Wilcoxon test. *BTG1* mutant and WT samples from the same simulation were considered as paired samples. Each simulation was repeated 300 times. mTOR and cMyc upregulation was 1.12 times faster and cell cycle duration was shortened by 0.75 h in mutant compared to WT. DZ: Dark zone, LZ: Light zone, GC: Germinal centre.

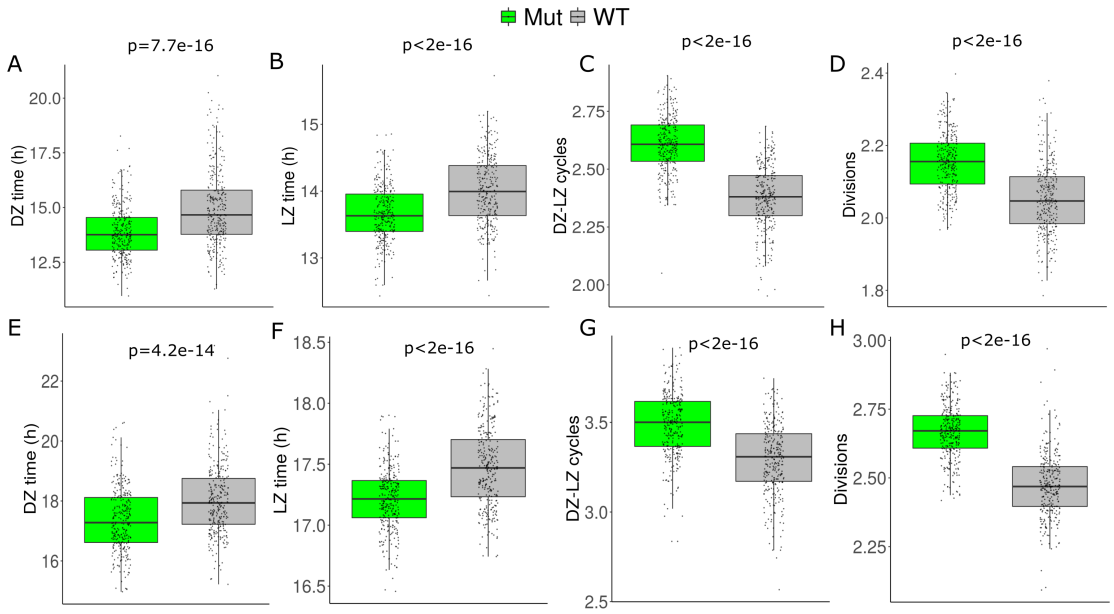

Figure 8.5: Predictions of the faster Tfh help with shorter cell cycle model for mutant *BTG1* B cells in BCinTime (A-D) and MiXed theories (E-H). A and E) Residence time of GC B cells in DZ per GC round in hours, B and F) Residence time of GC B cells in the LZ per GC round in hours, C and G) Number of DZ-LZ cycles underwent by GC B cells until day 7 of the GC simulation, D and H) Number of divisions of GC B cells. Readouts are from day 7 of the GC simulation (approximately day 10 after immunization). Simulation data points are shown as dots. Statistical significance was tested by Wilcoxon test. *BTG1* mutant and WT samples from the same simulation were considered as paired samples. Each simulation was repeated 300 times. In the BCinTime model, Tfh signal acquisition was 1.2 times faster and cell cycle duration was shortened by 0.75 h in mutant compared to WT. In the MiXed model, mTOR and cMyc upregulation was 1.12 times faster and cell cycle duration was shortened by 0.75 h in mutant compared to WT. DZ: Dark zone, LZ: Light zone, GC: Germinal centre.

consistent with the DisseD theory where the *BTG1* mutant GC B cells showed increased number of cell divisions and faster transition between the GC zones, suggesting that these predictions are not a bias of the selection theory considered.

8.6 Conclusions

Providing *BTG1* mutant GC B cells with faster Tfh help was able to recapture the competitive advantage suggesting that such small alterations are sufficient to confer dramatic competitive advantage as observed *in vivo*. While faster Tfh signal acquisition induced small alterations in DZ-LZ polarity and GC volume *in silico*, shortening the cell cycle duration of *BTG1* mutant GC B cells was able to overcome these alterations. Therefore, *in silico* simulations suggest that small advantage in cMyc induction is indeed consistent with the changes observed *in vivo*.

Simulations predicted that the fitness advantage is due to increased number of *BTG1* mutant cell divisions. These results suggested that small changes in GC B cell proliferative potential can dysregulate the GC reactions and can trigger premalignant transformation. Faster transition between GC zones also suggests that *BTG1* mutant B cells might be more prone to malignant transformation in the presence of additional mutations. More-

over, observed increase in competitive advantage of mutant B cells without observable alterations in kinetics, highlights the robust nature of GC kinetics which might be a consequence of the presence of multiple co-existing mechanisms regulating GC kinetics and shutdown as discussed in Chapter 7.

Chapter 9

Discussion and future perspectives

Despite the progress in GC research, GC shutdown remains a poorly understood phenomenon. Identifying strategies to modulate the GC lifetime by targeting GC shutdown would be invaluable for enhancing vaccine efficacy and blocking the progression of pathologic GCs. In view of these implications, an *in-silico* approach was used to investigate the regulation of GC shutdown by various processes and to identify potential causes of GC shutdown, considering the present experimental evidences.

One of the earliest hypotheses proposed in the literature was that the GC shutdown is due to antigen limitation [80, 77]. Although, there is no direct evidence for antigen limitation as a mechanism of shutdown, simulations in Chapter 7 supported this hypothesis as mechanisms leading to antigen limitation were capable of terminating GCs independently. Decrease in antigen access of GC B cells can occur by antibody feedback, due to masking of FDC antigen by soluble antibodies. Results discussed in Chapter 3 suggested that antibody feedback can accelerate the termination of GCs and stop the affinity maturation of B cells at an early time point. Consequently, a small decrease in average plasma cell affinities together with reduced plasma cell production decreases the efficiency of the GC reaction. When the GC onset is asynchronous, soluble antibodies from early formed GCs terminated the late formed GCs at a very early stage and considerably reduced the plasma cell production. There was a small increase in the mean affinity of plasma cells produced at early stages that did not persist at later time points due to earlier termination in affinity maturation. Despite the small increase in mean affinity, efficiency of late GC was reduced irrespective of the time point considered. Importantly, the increased selection pressure due to antigen limitation did not enhance the affinity maturation in a long term or GC efficiency, but was detrimental for the functioning of GCs.

As the impact of late GC on early GCs was ignored in Chapter 3, more realistic model of a network of interacting asynchronous GCs was developed in Chapter 6. To investigate the impact of GC-GC interactions on the entire system of GCs and individual GCs, strength of interaction between GCs was varied in the simulations. Simulation results predicted that high antibody feedback limits the overall magnitude of GC response, decreases mean affinity and number of plasma cells produced. Similarly, individual GCs composing the overall GC response were terminated earlier and were inhibited. However, the extent of inhibition varied among the GCs and the late formed GCs were more sensitive to antibody mediated inhibition compared to early initialized GCs. On the other hand, if all GCs were synchronously initiated, individual GCs were similarly impacted by antibody feedback. This suggested that the impact of GC-GC interactions on individual GCs and overall GC response might vary depending on the initiation time of individual GCs. Late GCs were able to overcome antibody mediated inhibition partially when founder cells had high

affinities. As the nature of seeder cells in GCs initialized at different time points is not known, this suggests a need to test whether the memory B cells act as seeders in the late formed GCs in a primary immune response.

In the presence of GC-GC interactions, plasma cells from late formed GCs showed a bias in affinity maturation towards one of the epitopes, when two epitopes were considered in equal proportions. This is likely due to the earlier termination of late GCs, that allowed it to focus only on a single epitope. In the presence of two antigen epitopes in unequal proportions, late GCs showed better affinity maturation towards rare epitope. These results predict that GC-GC interactions can induce differences in the behavior of GCs when the onset of GCs is asynchronous, and might partly explain the differences observed between single GCs in experimental studies. Therefore, it might be expected that the late formed GCs have reduced plasma cell production, focus on few epitopes and show higher affinity maturation to rare epitopes compared to the early formed GCs. Apart from the differences in the behavior of GCs arising due to antibody feedback discussed in Chapter 6, analysis of GC kinetics data in Chapter 5, suggested that lifetime of GCs might be variable even among the GCs present within the same lymphoid organ. Simulation results were consistent with the data when the GCs were assumed to have different antigen concentrations or founder cell compositions. However, the variability arising due to intercommunication of GCs was solely insufficient to fit the data. Considering different founder cell compositions among individual GCs in the simulations of GC-GC interactions suggested that founder cell composition is a critical factor that influences the extent and impact of intercommunication. As the role of antibody feedback is hard to investigate experimentally, characteristic differences among individual GCs predicted by the simulations in Chapter 6, might be considered as a first step to investigate the existence of GC-GC intercommunication by soluble antibodies. GCs might also intercommunicate by the exchange of Tfh cells [144] and the implication of Tfh exchange on GC shutdown is unclear and needs future investigation.

Similar to the regulation of antigen accessibility by antibody feedback, ICs in FDCs undergo cycling suggesting a potential role of antigen presentation dynamics in regulating GC shutdown as discussed in Chapter 4. Time scale of PE-IC cycling was predicted to be of the order of 1 hour. Changes in IC cycling kinetics impacted GC dynamics by affecting antigen protection from degradation and antigen uptake of GC B cells. With limiting antigen concentration, there was a trade-off between IC protection in the FDC interior and IC uptake by B cells from FDC surface depending on the IC cycling kinetics. Blocking IC cycling was also able to terminate GCs suggesting the importance of dynamic antigen presentation in the maintenance of GC reaction. This also suggested that IC cycling might be a potential target to block the development of pathologic GCs. While the mechanism and regulation of IC cycling in FDCs have not been investigated so far, it can be speculated that IC cycling dynamics might vary during the GC reaction. Analysis in Chapter 7 suggested that changes in antigen presentation kinetics of FDCs during the course of GC reaction, might lead to accumulation of antigen in the interior of FDCs and was independently capable of terminating GCs, suggesting the need to examine changes in FDC antigen presentation as the GC evolves.

Apart from antibody feedback and changes in IC cycling kinetics, other mechanisms were also able to lead to antigen limitation. This includes antigen consumption by B cells and morphological changes in FDCs. While, antigen consumption by B cells leads to mild decrease in total antigen amount, morphological changes such as FDC contraction can decrease the antigen accessibility in the GCs. In the presence of antigen limitation due to any of the above described mechanisms, it might be expected that the average density of pMHC presentation of GC B cells would decrease when the GC is contracting. While

morphological changes in FDCs and dynamic changes in antigen presentation could also terminate GCs, it is not clear whether these mechanisms exist and need experimental verification. Given that antigen collection is the first step of GC B cell selection process and several mechanisms can lead to changes in antigen availability or accessibility, it might be expected that antigen limitation is the primary cause of GC shutdown and alterations seen in Tfh dynamics or other cell types during GC reaction are consequences of antigen limitation. In any case, antigen limitation might be a major factor contributing to GC shutdown atleast under conditions where the antigen concentration is limiting.

In the absence of antigen limitation, changes in Tfh cells and GC B cell division capacity were also able to terminate GCs *in silico*. In the former model, Tfh signaling capacity was assumed to decrease during the GC reaction. This can be justified by the action of Tfr cells [130, 136, 173] as the Tfh/Tfr ratio decreases [166, 174] when the GC is contracting. In the mechanisms proposed, shutdown of GCs is ultimately due to decreased proliferation of GC B cells either due to reduced number of recycling GC B cells or due to reduced number of divisions per recycling GC B cell.

Taken together, results presented in this thesis suggest that potentially numerous mechanisms might coexist and contribution of these mechanisms to GC shutdown might vary under different immunization conditions. Predicted variability in the lifetime of GCs within the same organ in Chapter 5 also suggests that individual GCs might be highly complex and differ in numerous characteristics, and therefore it is important to analyze whether the individual GCs undergo shutdown by the same mechanism. Numerous changes are observed in the GC microenvironment and cell types as the GC evolves [18, 170, 172, 171, 99]. Understanding the basis of such remodeling such as the characteristic changes in Tfh, Tfr, FDCs and GC B cells and their interdependence is the key for a mechanistic understanding of GC shutdown. Longitudinal analysis of GCs is a challenging task, however future technical advances might enable us to image GCs for sufficiently long periods of time and might unravel the basis of these unexplained observations. Moreover, most studies focus on the early stages of GC reaction, however, numerous changes occur at late stages and are under appreciated. Thus, studies focusing on late stages of GC reaction are needed to promote a better understanding of GC shutdown.

Apart from the role of GC B cell divisions in maintaining GC reaction, dysregulated GC B cell divisions are also associated with B cell lymphomas. In Chapter 8, Experimental data of GC dynamics in the presence of *BTG1* mutant GC B cells was analyzed *in silico*. This suggested that small enhancement in T cell help to a sub-population of GC B cells can induce higher number of divisions and can confer dramatic competitive advantage, even without observable changes in the GC reaction kinetics. Similarly, changes in GC B cell diversity has been noticed without observable changes in GC magnitude [160]. Therefore, GC kinetics is relatively robust likely due to multiple co-existing mechanisms of regulation.

Bibliography

[1] Yu Adachi, Taishi Onodera, Yuki Yamada, Rina Daio, Makoto Tsuiji, Takeshi Inoue, Kazuo Kobayashi, Tomohiro Kurosaki, Manabu Ato, and Yoshimasa Takahashi. Distinct germinal center selection at local sites shapes memory b cell response to viral escape. *Journal of Experimental Medicine*, 212(10):1709–1723, 2015.

[2] Ahmed Al-Qahtani, Zhenming Xu, Hong Zan, Craig M Walsh, and Paolo Casali. A role for drak2 in the germinal center reaction and the antibody response. *Autoimmunity*, 41(5):341–352, 2008.

[3] Christopher DC Allen, K Mark Ansel, Caroline Low, Robin Lesley, Hirokazu Tamamura, Nobutaka Fujii, and Jason G Cyster. Germinal center dark and light zone organization is mediated by cxcr4 and cxcr5. *Nature immunology*, 5(9):943–952, 2004.

[4] Christopher DC Allen, Takaharu Okada, and Jason G Cyster. Germinal-center organization and cellular dynamics. *Immunity*, 27(2):190–202, 2007.

[5] Christopher DC Allen, Takaharu Okada, H Lucy Tang, and Jason G Cyster. Imaging of germinal center selection events during affinity maturation. *Science*, 315(5811):528–531, 2007.

[6] Francesca Aloisi and Ricardo Pujol-Borrell. Lymphoid neogenesis in chronic inflammatory diseases. *Nature Reviews Immunology*, 6(3):205–217, 2006.

[7] Theinmozhi Arulraj, Sebastian C Binder, Philippe A Robert, and Michael Meyer-Hermann. Synchronous germinal center onset impacts the efficiency of antibody responses. *Frontiers in immunology*, 10:2116, 2019.

[8] Wendy Béguelin, Martín A Rivas, María T Calvo Fernández, Matt Teater, Alberto Purwada, David Redmond, Hao Shen, Matt F Challman, Olivier Elemento, Ankur Singh, et al. Ezh2 enables germinal centre formation through epigenetic silencing of cdkn1a and an rb-e2f1 feedback loop. *Nature communications*, 8(1):1–16, 2017.

[9] C Berek, A Berger, and M Apel. Maturation of the immune response in germinal centers. *Cell*, 67(6):1121–1129, 1991.

[10] M Jeff Bergen, Chien-Hsiung Pan, Catherine E Greer, Harold S Legg, John M Polo, and Diane E Griffin. Comparison of the immune responses induced by chimeric alphavirus-vectored and formalin-inactivated alum-precipitated measles vaccines in mice. *PLoS One*, 5(4):e10297, 2010.

[11] Joakim JE Bergström, Hui Xu, and Birgitta Heyman. Epitope-specific suppression of igg responses by passively administered specific igg: evidence of epitope masking. *Frontiers in immunology*, 8:238, 2017.

[12] Amy Bergtold, Dharmesh D Desai, Anamika Gavhane, and Raphael Clynes. Cell surface recycling of internalized antigen permits dendritic cell priming of b cells. *Immunity*, 23(5):503–514, 2005.

[13] Tilo Beyer and Michael Meyer-Hermann. Cell transmembrane receptors determine tissue pattern stability. *Physical review letters*, 101(14):148102, 2008.

[14] Tilo Beyer and Michael Meyer-Hermann. Mechanisms of organogenesis of primary lymphoid follicles. *International Immunology*, 20(4):615–623, 03 2008.

[15] Sebastian C Binder and Michael Meyer-Hermann. Implications of intravital imaging of murine germinal centers on the control of b cell selection and division. *Frontiers in immunology*, 7:593, 2016.

[16] Lisa Buchauer and Hedda Wardemann. Calculating germinal centre reactions. *Current Opinion in Systems Biology*, 18:1–8, 2019.

[17] Kurt Buchmann. Evolution of innate immunity: clues from invertebrates via fish to mammals. *Frontiers in immunology*, 5:459, 2014.

[18] Stephanie A Camacho, Marie H Kosco-Vilbois, and Claudia Berek. The dynamic structure of the germinal center. *Immunology today*, 19(11):511–514, 1998.

[19] Pablo F Cañete, Rebecca A Sweet, Paula Gonzalez-Figueroa, Ilenia Papa, Naganari Ohkura, Holly Bolton, Jonathan A Roco, Marta Cuenca, Katharine J Bassett, Ismail Sayin, et al. Regulatory roles of il-10–producing human follicular t cells. *Journal of Experimental Medicine*, 216(8):1843–1856, 2019.

[20] Tyani D Chan, Dominique Gatto, Katherine Wood, Tahra Camidge, Antony Basten, and Robert Brink. Antigen affinity controls rapid t-dependent antibody production by driving the expansion rather than the differentiation or extrafollicular migration of early plasmablasts. *The Journal of Immunology*, 183(5):3139–3149, 2009.

[21] Lei L Chen, Judy C Adams, and Ralph M Steinman. Anatomy of germinal centers in mouse spleen, with special reference to follicular dendritic cells. *Journal of Cell Biology*, 77(1):148–164, 1978.

[22] Kimberly M Cirelli, Diane G Carnathan, Bartek Nogal, Jacob T Martin, Oscar L Rodriguez, Amit A Upadhyay, Chiamaka A Enemuo, Etse H Gebru, Yury Choe, Federico Viviano, et al. Slow delivery immunization enhances hiv neutralizing antibody and germinal center responses via modulation of immunodominance. *Cell*, 177(5):1153–1171, 2019.

[23] Kimberly M Cirelli and Shane Crotty. Germinal center enhancement by extended antigen availability. *Current opinion in immunology*, 47:64–69, 2017.

[24] Cyril A Clarke, WTA Donohoe, RB McConnell, JC Woodrow, R Finn, JR Krevans, W Kulke, D Lehane, and PM Sheppard. Further experimental studies on the prevention of rh haemolytic disease. In *Rhesus haemolytic disease*, pages 191–197. Springer, 1963.

[25] Max D Cooper and Matthew N Alder. The evolution of adaptive immune systems. *Cell*, 124(4):815–822, 2006.

[26] Elisa Corsiero, Alessandra Nerviani, Michele Bombardieri, and Costantino Pitzalis. Ectopic lymphoid structures: powerhouse of autoimmunity. *Frontiers in immunology*, 7:430, 2016.

[27] A. Corthay. How do regulatory t cells work? *Scandinavian Journal of Immunology*, 70(4):326–336, 2009.

[28] Blessing Crimeen-Irwin, K Scalzo, S Gloster, PL Mottram, and M Plebanski. Failure of immune homeostasis-the consequences of under and over reactivity. *CURRENT DRUG TARGETS-IMMUNE ENDOCRINE AND METABOLIC DISORDERS-*, 5(4):413, 2005.

[29] Shane Crotty. T follicular helper cell differentiation, function, and roles in disease. *Immunity*, 41(4):529–542, 2014.

[30] Jason G Cyster, K Mark Ansel, Karin Reif, Eric H Ekland, Paul L Hyman, H Lucy Tang, Sanjiv A Luther, and Vu N Ngo. Follicular stromal cells and lymphocyte homing to follicles. *Immunological reviews*, 176:181–193, 2000.

[31] Carola García de Vinuesa, Matthew C. Cook, Jennifer Ball, Marion Drew, Yvonne Sunners, Marilia Cascalho, Matthias Wabl, Gerry G.B. Klaus, and Ian C.M. MacLennan. Germinal Centers without T Cells. *Journal of Experimental Medicine*, 191(3):485–494, 02 2000.

[32] Søren E Degn, Cees E van der Poel, Daniel J Firl, Burcu Ayoglu, Fahd A Al Qureshah, Goran Bajic, Luka Mesin, Claude-Agnès Reynaud, Jean-Claude Weill, Paul J Utz, et al. Clonal evolution of autoreactive germinal centers. *Cell*, 170(5):913–926, 2017.

[33] Christine D Dijkstra, NJ Van Tilburg, and EA Döpp. Ontogenetic aspects of immune-complex trapping in the spleen and popliteal lymph nodes of the rat. *Cell and tissue research*, 223(3):545–552, 1982.

[34] Ismail Dogan, Barbara Bertocci, Valérie Vilmont, Frédéric Delbos, Jérome Mégret, Sébastien Storck, Claude-Agnès Reynaud, and Jean-Claude Weill. Multiple layers of b cell memory with different effector functions. *Nature immunology*, 10(12):1292–1299, 2009.

[35] Pilar M Dominguez, Hussein Ghamlouch, Wojciech Rosikiewicz, Parveen Kumar, Wendy Béguelin, Lorena Fontan, Martín A Rivas, Patrycja Pawlikowska, Marine Armand, Enguerran Mouly, et al. Tet2 deficiency causes germinal center hyperplasia, impairs plasma cell differentiation, and promotes b-cell lymphomagenesis. *Cancer discovery*, 8(12):1632–1653, 2018.

[36] David Dominguez-Sola, Gabriel D Victora, Carol Y Ying, Ryan T Phan, Masumichi Saito, Michel C Nussenzweig, and Riccardo Dalla-Favera. The proto-oncogene myc is required for selection in the germinal center and cyclic reentry. *Nature immunology*, 13(11):1083–1091, 2012.

[37] Herman N Eisen and Gregory W Siskind. Variations in affinities of antibodies during the immune response. *Biochemistry*, 3(7):996–1008, 1964.

[38] Mohey Eldin El Shikh, Rania El Sayed, Andras K Szakal, and John G Tew. Follicular dendritic cell (fdc)-fcγriib engagement via immune complexes induces the activated fdc phenotype associated with secondary follicle development. *European journal of immunology*, 36(10):2715–2724, 2006.

[39] Robert Endres, Marat B Alimzhanov, Thomas Plitz, Agnes Fütterer, Marie H Kosco-Vilbois, Sergei A Nedospasov, Klaus Rajewsky, and Klaus Pfeffer. Mature follicular dendritic cell networks depend on expression of lymphotoxin β receptor by radiore-

sistant stromal cells and of lymphotoxin β and tumor necrosis factor by b cells. *The Journal of experimental medicine*, 189(1):159–168, 1999.

[40] Jonatan Ersching, Alejo Efeyan, Luka Mesin, Johanne T. Jacobsen, Giulia Pasqual, Brian C. Grabiner, David Dominguez-Sola, David M. Sabatini, and Gabriel D. Victora. Germinal center selection and affinity maturation require dynamic regulation of mtorc1 kinase. *Immunity*, 46(6):1045–1058.e6, 2017.

[41] Marc Thilo Figge, Alexandre Garin, Matthias Gunzer, Marie Kosco-Vilbois, Kai-Michael Toellner, and Michael Meyer-Hermann. Deriving a germinal center lymphocyte migration model from two-photon data . *Journal of Experimental Medicine*, 205(13):3019–3029, 12 2008.

[42] Shlomo Finkin, Harald Hartweger, Thiago Y. Oliveira, Ervin E. Kara, and Michel C. Nussenzweig. Protein amounts of the myc transcription factor determine germinal center b cell division capacity. *Immunity*, 51(2):324–336.e5, 2019.

[43] Daniel J Firl, Soren E Degn, Timothy Padera, and Michael C Carroll. Capturing change in clonal composition amongst single mouse germinal centers. *Elife*, 7:e33051, 2018.

[44] Walther Flemming. Studien über regeneration der gewebe. *Archiv für mikroskopische Anatomie*, 24(1):50–91, 1884.

[45] Alexandre Garin, Michael Meyer-Hermann, Mathias Contie, Marc Thilo Figge, Vanessa Buatois, Matthias Gunzer, Kai-Michael Toellner, Greg Elson, and Marie H. Kosco-Vilbois. Toll-like receptor 4 signaling by follicular dendritic cells is pivotal for germinal center onset and affinity maturation. *Immunity*, 33(1):84–95, 2010.

[46] Alexander D Gitlin, Christian T Mayer, Thiago Y Oliveira, Ziv Shulman, Mathew JK Jones, Amnon Koren, and Michel C Nussenzweig. T cell help controls the speed of the cell cycle in germinal center b cells. *Science*, 349(6248):643–646, 2015.

[47] Alexander D Gitlin, Ziv Shulman, and Michel C Nussenzweig. Clonal selection in the germinal centre by regulated proliferation and hypermutation. *Nature*, 509(7502):637–640, 2014.

[48] Mercedes Gonzalez, Fabienne Mackay, Jeffrey L. Browning, Marie H. Kosco-Vilbois, and Randolph J. Noelle. The Sequential Role of Lymphotoxin and B Cells in the Development of Splenic Follicles . *Journal of Experimental Medicine*, 187(7):997–1007, 04 1998.

[49] Santiago F. Gonzalez, Søren E. Degn, Lisa A. Pitcher, Matthew Woodruff, Balthasar A. Heesters, and Michael C. Carroll. Trafficking of b cell antigen in lymph nodes. *Annual Review of Immunology*, 29(1):215–233, 2011. PMID: 21219172.

[50] Santiago F. Gonzalez, Veronika Lukacs-Kornek, Michael P. Kuligowski, Lisa A. Pitcher, Søren E. Degn, Shannon J. Turley, and Michael C. Carroll. Complement-dependent transport of antigen into b cell follicles. *The Journal of Immunology*, 185(5):2659–2664, 2010.

[51] Kim L Good-Jacobson, Courtney G Szumilas, Lieping Chen, Arlene H Sharpe, Mary M Tomayko, and Mark J Shlomchik. Pd-1 regulates germinal center b cell survival and the formation and affinity of long-lived plasma cells. *Nature immunology*, 11(6):535–542, 2010.

[52] Leonid Gorelik, Kevin Gilbride, Max Dobles, Susan L. Kalled, Daniel Zandman, and Martin L. Scott. Normal B Cell Homeostasis Requires B Cell Activation Factor Production by Radiation-resistant Cells . *Journal of Experimental Medicine*, 198(6):937–945, 09 2003.

[53] Spencer M. Grant, Meng Lou, Li Yao, Ronald N. Germain, Andrea J. Radtke, and Ana-Maria Lennon-Duménil. The lymph node at a glance – how spatial organization optimizes the immune response. *Journal of Cell Science*, 133(5), 03 2020. jcs241828.

[54] David R. Gruber, Amanda L. Richards, Heather L. Howie, Ariel M. Hay, Jenna N. Lebedev, Xiaohong Wang, James C. Zimring, and Krystalyn E. Hudson. Passively transferred IgG enhances humoral immunity to a red blood cell alloantigen in mice. *Blood Advances*, 4(7):1526–1537, 04 2020.

[55] MG Hanna Jr, Mary W Francis, and Leona C Peters. Localization of 125i-labelled antigen in germinal centres of mouse spleen: effects of competitive injection of specific or non-cross-reacting antigen. *Immunology*, 15(1):75, 1968.

[56] Lynn G. Hannum, Ann M. Haberman, Shannon M. Anderson, and Mark J. Shlomchik. Germinal Center Initiation, Variable Gene Region Hypermutation, and Mutant B Cell Selection without Detectable Immune Complexes on Follicular Dendritic Cells. *Journal of Experimental Medicine*, 192(7):931–942, 09 2000.

[57] Hidenori Hase, Yumiko Kanno, Masaru Kojima, Kaoru Hasegawa, Daisuke Sakurai, Hidefumi Kojima, Naoyuki Tsuchiya, Katsushi Tokunaga, Nobuhide Masawa, Miyuki Azuma, Ko Okumura, and Tetsuji Kobata. BAFF/BLyS can potentiate B-cell selection with the B-cell coreceptor complex. *Blood*, 103(6):2257–2265, 03 2004.

[58] Anja E. Hauser, Tobias Junt, Thorsten R. Mempel, Michael W. Sneddon, Steven H. Kleinstein, Sarah E. Henrickson, Ulrich H. von Andrian, Mark J. Shlomchik, and Ann M. Haberman. Definition of germinal-center b cell migration in vivo reveals predominant intrazonal circulation patterns. *Immunity*, 26(5):655–667, 2007.

[59] Colin Havenar-Daughton, Diane G. Carnathan, Archana V. Boopathy, Amit A. Upadhyay, Ben Murrell, Samantha M. Reiss, Chiamaka A. Enemuo, Etse H. Gebru, Yury Choe, Pallavi Dhadvai, Federico Viviano, Kirti Kaushik, Jinal N. Bhiman, Bryan Briney, Dennis R. Burton, Steven E. Bosinger, William R. Schief, Darrell J. Irvine, Guido Silvestri, and Shane Crotty. Rapid germinal center and antibody responses in non-human primates after a single nanoparticle vaccine immunization. *Cell Reports*, 29(7):1756–1766.e8, 2019.

[60] Barton F. Haynes, Dennis R. Burton, and John R. Mascola. Multiple roles for hiv broadly neutralizing antibodies. *Science Translational Medicine*, 11(516), 2019.

[61] Balthasar A Heesters, Madelene Lindqvist, Parsia A Vagefi, Eileen P Scully, Frank A Schildberg, Marcus Altfeld, Bruce D Walker, Daniel E Kaufmann, and Michael C Carroll. Follicular dendritic cells retain infectious hiv in cycling endosomes. *PLoS pathogens*, 11(12):e1005285, 2015.

[62] Balthasar A. Heesters, Priyadarshini Chatterjee, Young-A. Kim, Santiago F. Gonzalez, Michael P. Kuligowski, Tomas Kirchhausen, and Michael C. Carroll. Endocytosis and recycling of immune complexes by follicular dendritic cells enhances b cell antigen binding and activation. *Immunity*, 38(6):1164–1175, 2013.

[63] B Heyman, L Pilström, and M J Shulman. Complement activation is required for IgM-mediated enhancement of the antibody response. *Journal of Experimental Medicine*, 167(6):1999–2004, 06 1988.

[64] Birgitta Heyman. Regulation of antibody responses via antibodies, complement, and fc receptors. *Annual Review of Immunology*, 18(1):709–737, 2000. PMID: 10837073.

[65] F. Hjelm, F. Carlsson, A. Getahun, and B. Heyman. Antibody-mediated regulation of the immune response. *Scandinavian Journal of Immunology*, 64(3):177–184, 2006.

[66] Kevin Hollowood and John R. Goodlad. Germinal centre cell kinetics. *The Journal of Pathology*, 185(3):229–233, 1998.

[67] Kevin Hollowood and James Macartney. Cell kinetics of the germinal center reaction - a stathmokinetic study. *European Journal of Immunology*, 22(1):261–266, 1992.

[68] Rikard Holmdahl, Vivianne Malmström, and Harald Burkhardt. Autoimmune priming, tissue attack and chronic inflammation — the three stages of rheumatoid arthritis. *European Journal of Immunology*, 44(6):1593–1599, 2014.

[69] Hajime Hoshi, K Horie, and D Chen. Development of immune complex trapping: experimental study of lymphoid follicles and germinal centers newly induced by exogenous stimulants in mouse popliteal lymph nodes. *Histology and histopathology*, 14(1):11–21, 1999.

[70] Takeshi Inoue, Ryo Shinnakasu, Wataru Ise, Chie Kawai, Takeshi Egawa, and Tomohiro Kurosaki. The transcription factor Foxo1 controls germinal center B cell proliferation in response to T cell help. *Journal of Experimental Medicine*, 214(4):1181–1198, 03 2017.

[71] Wataru Ise, Kentaro Fujii, Katsuyuki Shiroguchi, Ayako Ito, Kohei Kometani, Kiyoshi Takeda, Eiryo Kawakami, Kazuo Yamashita, Kazuhiro Suzuki, Takaharu Okada, et al. T follicular helper cell-germinal center b cell interaction strength regulates entry into plasma cell or recycling germinal center cell fate. *Immunity*, 48(4):702–715, 2018.

[72] J Jacob, R Kassir, and G Kelsoe. In situ studies of the primary immune response to (4-hydroxy-3-nitrophenyl)acetyl. I. The architecture and dynamics of responding cell populations. *Journal of Experimental Medicine*, 173(5):1165–1175, 05 1991.

[73] Charles A Janeway Jr, Paul Travers, Mark Walport, and Mark J Shlomchik. Principles of innate and adaptive immunity. In *Immunobiology: The Immune System in Health and Disease. 5th edition*. Garland Science, 2001.

[74] Meryem Jarjour, Audrey Jorquera, Isabelle Mondor, Stephan Wienert, Priyanka Narang, Mark C. Coles, Frederick Klauschen, and Marc Bajénoff. Fate mapping reveals origin and dynamics of lymph node follicular dendritic cells. *Journal of Experimental Medicine*, 211(6):1109–1122, 05 2014.

[75] Sudhir Pai Kasturi, Ioanna Skountzou, Randy A Albrecht, Dimitrios Koutsonanos, Tang Hua, Helder I Nakaya, Rajesh Ravindran, Shelley Stewart, Munir Alam, Marcin Kwissa, et al. Programming the magnitude and persistence of antibody responses with innate immunity. *Nature*, 470(7335):543–547, 2011.

[76] Thomas B Kepler and Alan S Perelson. Cyclic re-entry of germinal center b cells and the efficiency of affinity maturation. *Immunology today*, 14(8):412–415, 1993.

[77] Can Keşmir and Rob J. De Boer. A mathematical model on germinal center kinetics and termination. *The Journal of Immunology*, 163(5):2463–2469, 1999.

[78] Marie H. Kosco and David Gray. Signals involved in germinal center reactions. *Immunological Reviews*, 126(1):63–76, 1992.

[79] Marie H Kosco-Vilbois. Are follicular dendritic cells really good for nothing? *Nature Reviews Immunology*, 3(9):764–769, 2003.

[80] Marie H Kosco-Vilbois, Hanswalter Zentgraf, Johannes Gerdes, and Jean-Yves Bonnefoy. To 'b'or not to 'b'a germinal center? *Immunology today*, 18(5):225–230, 1997.

[81] Nike Julia Krautler, Veronika Kana, Jan Kranich, Yinghua Tian, Dushan Perera, Doreen Lemm, Petra Schwarz, Annika Armulik, Jeffrey L Browning, Michelle Tallquist, et al. Follicular dendritic cells emerge from ubiquitous perivascular precursors. *Cell*, 150(1):194–206, 2012.

[82] Nike Julia Kräutler, Alexander Yermanos, Alessandro Pedrioli, Suzanne PM Welten, Dominique Lorgé, Ute Greczmiel, Ilka Bartsch, Jörg Scheuermann, Jonathan D Kiefer, Klaus Eyer, et al. Quantitative and qualitative analysis of humoral immunity reveals continued and personalized evolution in chronic viral infection. *Cell reports*, 30(4):997–1012, 2020.

[83] Brian J. Laidlaw, Yisi Lu, Robert A. Amezquita, Jason S. Weinstein, Jason A. Vander Heiden, Namita T. Gupta, Steven H. Kleinstein, Susan M. Kaech, and Joe Craft. Interleukin-10 from cd4+ follicular regulatory t cells promotes the germinal center response. *Science Immunology*, 2(16), 2017.

[84] Ernst Lindhout, Cornelis de Groot, Gerrit Koopman, and Steven T Pals. Triple check for antigen specificity of b cells during germinal centre reactions. *Immunology today*, 18(12):573–577, 1997.

[85] Alexander Link, Franziska Zabel, Yvonne Schnetzler, Alexander Titz, Frank Brombacher, and Martin F. Bachmann. Innate immunity mediates follicular transport of particulate but not soluble protein antigen. *The Journal of Immunology*, 188(8):3724–3733, 2012.

[86] Dan Liu, Heping Xu, Changming Shih, Zurong Wan, Xiaopeng Ma, Weiwei Ma, Dan Luo, and Hai Qi. T–b-cell entanglement and icosl-driven feed-forward regulation of germinal centre reaction. *Nature*, 517(7533):214–218, 2015.

[87] Yong-Jun Liu, Jun Zhang, Peter J. L. Lane, Eric Y.-T. Chan, and Ian C. M. Maclennan. Sites of specific b cell activation in primary and secondary responses to t cell-dependent and t cell-independent antigens. *European Journal of Immunology*, 21(12):2951–2962, 1991.

[88] Jean Livet, Tamily A Weissman, Hyuno Kang, Ryan W Draft, Ju Lu, Robyn A Bennis, Joshua R Sanes, and Jeff W Lichtman. Transgenic strategies for combinatorial expression of fluorescent proteins in the nervous system. *Nature*, 450(7166):56–62, 2007.

[89] Erick Lu, Finn D Wolfreys, Jagan R Muppidi, Ying Xu, and Jason G Cyster. S-geranylgeranyl-l-glutathione is a ligand for human b cell-confinement receptor p2ry8. *Nature*, 567(7747):244–248, 2019.

[90] Wei Luo, Florian Weisel, and Mark J Shlomchik. B cell receptor and cd40 signaling are rewired for synergistic induction of the c-myc transcription factor in germinal center b cells. *Immunity*, 48(2):313–326, 2018.

[91] Ian C. M. MacLennan. Germinal centers. *Annual Review of Immunology*, 12(1):117–139, 1994. PMID: 8011279.

[92] Christoph Mancao, Markus Altmann, Berit Jungnickel, and Wolfgang Hammerschmidt. Rescue of "crippled" germinal center B cells from apoptosis by Epstein-Barr virus. *Blood*, 106(13):4339–4344, 12 2005.

[93] TE Mandel, RP Phipps, AP Abbot, and JG Tew. Long-term antigen retention by dendritic cells in the popliteal lymph node of immunized mice. *Immunology*, 43(2):353, 1981.

[94] Jonathan Mandelbaum, Govind Bhagat, Hongyan Tang, Tongwei Mo, Manisha Brahmachary, Qiong Shen, Amy Chadburn, Klaus Rajewsky, Alexander Tarakhovsky, Laura Pasqualucci, et al. Blimp1 is a tumor suppressor gene frequently disrupted in activated b cell-like diffuse large b cell lymphoma. *Cancer cell*, 18(6):568–579, 2010.

[95] Tim Manser. Textbook germinal centers? *The Journal of Immunology*, 172(6):3369–3375, 2004.

[96] María Rodríguez Martínez, Alberto Corradin, Ulf Klein, Mariano Javier Álvarez, Gianna M. Toffolo, Barbara di Camillo, Andrea Califano, and Gustavo A. Stolovitzky. Quantitative modeling of the terminal differentiation of b cells and mechanisms of lymphomagenesis. *Proceedings of the National Academy of Sciences*, 109(7):2672–2677, 2012.

[97] Christian T. Mayer, Anna Gazumyan, Ervin E. Kara, Alexander D. Gitlin, Jovana Golijanin, Charlotte Viant, Joy Pai, Thiago Y. Oliveira, Qiao Wang, Amelia Escolano, Max Medina-Ramirez, Rogier W. Sanders, and Michel C. Nussenzweig. The microanatomic segregation of selection by apoptosis in the germinal center. *Science*, 358(6360), 2017.

[98] Elena Merino Tejero, Danial Lashgari, Rodrigo García-Valiente, Xuefeng Gao, Fabien Crauste, Philippe A. Robert, Michael Meyer-Hermann, María Rodríguez Martínez, S. Marieke van Ham, Jeroen E. J. Guikema, Huub Hoefsloot, and Antoine H. C. van Kampen. Multiscale modeling of germinal center recapitulates the temporal transition from memory b cells to plasma cells differentiation as regulated by antigen affinity-based tfh cell help. *Frontiers in Immunology*, 11:3805, 2021.

[99] Julia Merkenschlager, Shlomo Finkin, Victor Ramos, Julian Kraft, Melissa Cipolla, Carla R Nowosad, Harald Hartweger, Wenzhu Zhang, Paul Dominic B Olinares, Anna Gazumyan, et al. Dynamic regulation of t fh selection during the germinal centre reaction. *Nature*, 591(7850):458–463, 2021.

[100] Luka Mesin, Ariën Schiepers, Jonatan Ersching, Alexandru Barbulescu, Cecília B Cavazzoni, Alessandro Angelini, Takaharu Okada, Tomohiro Kurosaki, and Gabriel D Victora. Restricted clonality and limited germinal center reentry characterize memory b cell reactivation by boosting. *Cell*, 180(1):92–106, 2020.

[101] Michael Meyer-Hermann. Overcoming the dichotomy of quantity and quality in antibody responses. *The Journal of Immunology*, 193(11):5414–5419, 2014.

[102] Michael Meyer-Hermann. Injection of antibodies against immunodominant epitopes tunes germinal centers to generate broadly neutralizing antibodies. *Cell reports*, 29(5):1066–1073, 2019.

[103] Michael Meyer-Hermann. Germinal center b cells separate signals for selection and division like compact discs. *bioRxiv*, 2020.

[104] Michael Meyer-Hermann, Sebastian C. Binder, Luka Mesin, and Gabriel D. Victora. Computer simulation of multi-color brainbow staining and clonal evolution of b cells in germinal centers. *Frontiers in Immunology*, 9:2020, 2018.

[105] Michael Meyer-Hermann, Andreas Deutsch, and Michal Or-Guil. Recycling probability and dynamical properties of germinal center reactions. *Journal of Theoretical Biology*, 210(3):265–285, 2001.

[106] Michael Meyer-Hermann, Marc Thilo Figge, and Kai-Michael Toellner. Germinal centres seen through the mathematical eye: B-cell models on the catwalk. *Trends in immunology*, 30(4):157–164, 2009.

[107] Michael Meyer-Hermann, Elodie Mohr, Nadége Pelletier, Yang Zhang, Gabriel D Victora, and Kai-Michael Toellner. A theory of germinal center b cell selection, division, and exit. *Cell reports*, 2(1):162–174, 2012.

[108] Michael E. Meyer-Hermann and Philip K. Maini. Interpreting two-photon imaging data of lymphocyte motility. *Phys. Rev. E*, 71:061912, Jun 2005.

[109] Coraline Mlynarczyk, Lorena Fontán, and Ari Melnick. Germinal center-derived lymphomas: The darkest side of humoral immunity. *Immunological Reviews*, 288(1):214–239, 2019.

[110] Elisa Monzón-Casanova, Michael Screen, Manuel D Díaz-Muñoz, Richard MR Coulson, Sarah E Bell, Greta Lamers, Michele Solimena, Christopher WJ Smith, and Martin Turner. The rna-binding protein ptbp1 is necessary for b cell selection in germinal centers. *Nature immunology*, 19(3):267–278, 2018.

[111] Joana S. Moreira and Jose Faro. Modelling two possible mechanisms for the regulation of the germinal center dynamics. *The Journal of Immunology*, 177(6):3705–3710, 2006.

[112] Raquel Muñoz-Fernández, Alejandro Prados, Irene Tirado-González, Francisco Martín, Ana C Abadía, and Enrique G Olivares. Contractile activity of human follicular dendritic cells. *Immunology & Cell Biology*, 92(10):851–859, 2014.

[113] Kim Newton and Vishva M Dixit. Signaling in innate immunity and inflammation. *Cold Spring Harbor perspectives in biology*, 4(3):a006049, 2012.

[114] Falk Nimmerjahn and Jeffrey V Ravetch. Fcγ receptors as regulators of immune responses. *Nature Reviews Immunology*, 8(1):34–47, 2008.

[115] Takaharu Okada, Mark J Miller, Ian Parker, Matthew F Krummel, Margaret Neighbors, Suzanne B Hartley, Anne O'Garra, Michael D Cahalan, and Jason G Cyster. Antigen-engaged b cells undergo chemotaxis toward the t zone and form motile conjugates with helper t cells. *PLoS Biol*, 3(6):e150, 2005.

[116] Juhee Pae, Jonatan Ersching, Tiago BR Castro, Marta Schips, Luka Mesin, Samuel J Allon, Jose Ordovas-Montanes, Coraline Mlynarczyk, Ari Melnick, Alejo Efeyan, et al. Cyclin d3 drives inertial cell cycling in dark zone germinal center b cells. *Journal of Experimental Medicine*, 218(4), 2020.

[117] Ilenia Papa, David Saliba, Maurilio Ponzoni, Sonia Bustamante, Pablo F Canete, Paula Gonzalez-Figueroa, Hayley A McNamara, Salvatore Valvo, Michele Grimbaldeston, Rebecca A Sweet, et al. T fh-derived dopamine accelerates productive synapses in germinal centres. *Nature*, 547(7663):318–323, 2017.

[118] Norbert Pardi, Michael J Hogan, Frederick W Porter, and Drew Weissman. mrna vaccines—a new era in vaccinology. *Nature reviews Drug discovery*, 17(4):261, 2018.

[119] Gabriel Kristian Pedersen, Katharina Wørzner, Peter Andersen, and Dennis Christensen. Vaccine adjuvants differentially affect kinetics of antibody and germinal center responses. *Frontiers in Immunology*, 11:2302, 2020.

[120] Aurélien Pélissier, Youcef Akrout, Katharina Jahn, Jack Kuipers, Ulf Klein, Niko Beerenwinkel, and María Rodríguez Martínez. Computational model reveals a stochastic mechanism behind germinal center clonal bursts. *Cells*, 9(6):1448, 2020.

[121] Alan S Perelson and George F Oster. Theoretical studies of clonal selection: minimal antibody repertoire size and reliability of self-non-self discrimination. *Journal of theoretical biology*, 81(4):645–670, 1979.

[122] Tri Giang Phan, Irina Grigorova, Takaharu Okada, and Jason G Cyster. Subcapsular encounter and complement-dependent transport of immune complexes by lymph node b cells. *Nature immunology*, 8(9):992–1000, 2007.

[123] Pablo Pérez-Durán, Virginia G. de Yebenes, and Almudena R. Ramiro. Oncogenic events triggered by AID, the adverse effect of antibody diversification. *Carcinogenesis*, 28(12):2427–2433, 09 2007.

[124] Ziaur SM. Rahman, Sambasiva P. Rao, Susan L. Kalled, and Tim Manser. Normal Induction but Attenuated Progression of Germinal Center Responses in BAFF and BAFF-R Signaling–Deficient Mice . *Journal of Experimental Medicine*, 198(8):1157–1169, 10 2003.

[125] I. RANDEN, O. J. MELLBYE, Ø. FØRRE, and J. B. NATVIG. The identification of germinal centres and follicular dendritic cell networks in rheumatoid synovial tissue. *Scandinavian Journal of Immunology*, 41(5):481–486, 1995.

[126] Sambasiva P Rao, Kalpit A Vora, and Tim Manser. Differential expression of the inhibitory igg fc receptor fcγriib on germinal center cells: implications for selection of high-affinity b cells. *The Journal of Immunology*, 169(4):1859–1868, 2002.

[127] S K Ray, C Putterman, and B Diamond. Pathogenic autoantibodies are routinely generated during the response to foreign antigen: a paradigm for autoimmune disease. *Proceedings of the National Academy of Sciences*, 93(5):2019–2024, 1996.

[128] Dorothea Reimer, Michael Meyer-Hermann, Asylkhan Rakhymzhan, Tobit Steinmetz, Philipp Tripal, Jana Thomas, Martin Boettcher, Dimitrios Mougiakakos, Sebastian R Schulz, Sophia Urbanczyk, et al. B cell speed and b-fdc contacts in germinal centers determine plasma cell output via swiprosin-1/efhd2. *Cell Reports*, 32(6):108030, 2020.

[129] Polina Reshetova, Barbera D. C. van Schaik, Paul L. Klarenbeek, Marieke E. Doorenspleet, Rebecca E. E. Esveldt, Paul-Peter Tak, Jeroen E. J. Guikema, Niek de Vries, and Antoine H. C. van Kampen. Computational model reveals limited correlation between germinal center b-cell subclone abundancy and affinity: Implications for repertoire sequencing. *Frontiers in Immunology*, 8:221, 2017.

[130] Paul-Gydeon G Ritvo, Guillame Churlaud, Valentin Quiniou, Laura Florez, Faustine Brimaud, Gwladys Fourcade, Encarnita Mariotti-Ferrandiz, and David Klatzmann. Tfr cells lack il-2rα but express decoy il-1r2 and il-1ra and suppress the il-1–dependent activation of tfh cells. *Science immunology*, 2(15), 2017.

[131] Philippe A Robert, Andrea LJ Marschall, and Michael Meyer-Hermann. Induction of broadly neutralizing antibodies in germinal centre simulations. *Current Opinion in Biotechnology*, 51:137–145, 2018. Systems biology • Nanobiotechnology.

[132] Philippe A Robert and Michael Meyer-Hermann. A 3d structural affinity model for multi-epitope in silico germinal center simulations. *bioRxiv*, page 766535, 2019.

[133] Philippe A Robert, Ananya Rastogi, Sebastian C Binder, and Michael Meyer-Hermann. How to simulate a germinal center. *Germinal Centers*, pages 303–334, 2017.

[134] Jonathan A Roco, Luka Mesin, Sebastian C Binder, Christian Nefzger, Paula Gonzalez-Figueroa, Pablo F Canete, Julia Ellyard, Qian Shen, Philippe A Robert, Jean Cappello, et al. Class-switch recombination occurs infrequently in germinal centers. *Immunity*, 51(2):337–350, 2019.

[135] Nancy H. Ruddle and Eitan M. Akirav. Secondary lymphoid organs: Responding to genetic and environmental cues in ontogeny and the immune response. *The Journal of Immunology*, 183(4):2205–2212, 2009.

[136] Peter T. Sage, Alison M. Paterson, Scott B. Lovitch, and Arlene H. Sharpe. The coinhibitory receptor ctla-4 controls b cell responses by modulating t follicular helper, t follicular regulatory, and t regulatory cells. *Immunity*, 41(6):1026–1039, 2014.

[137] Masumichi Saito, Urban Novak, Erich Piovan, Katia Basso, Pavel Sumazin, Christof Schneider, Marta Crespo, Qiong Shen, Govind Bhagat, Andrea Califano, et al. Bcl6 suppression of bcl2 via miz1 and its disruption in diffuse large b cell lymphoma. *Proceedings of the National Academy of Sciences*, 106(27):11294–11299, 2009.

[138] H Scheller, S Tobollik, A Kutzera, M Eder, J Unterlehberg, I Pfeil, and B Jungnickel. c-myc overexpression promotes a germinal center-like program in burkitt's lymphoma. *Oncogene*, 29(6):888–897, 2010.

[139] Harry W Schroeder Jr and Lisa Cavacini. Structure and function of immunoglobulins. *Journal of Allergy and Clinical Immunology*, 125(2):S41–S52, 2010.

[140] JM Schuetz, NA Johnson, RD Morin, DW Scott, K Tan, S Ben-Nierah, M Boyle, GW Slack, MA Marra, JM Connors, et al. Bcl2 mutations in diffuse large b-cell lymphoma. *Leukemia*, 26(6):1383–1390, 2012.

[141] Tanja A Schwickert, Randall L Lindquist, Guy Shakhar, Geulah Livshits, Dimitris Skokos, Marie H Kosco-Vilbois, Michael L Dustin, and Michel C Nussenzweig. In vivo imaging of germinal centres reveals a dynamic open structure. *Nature*, 446(7131):83–87, 2007.

[142] Barbara Serafini, Barbara Rosicarelli, Roberta Magliozzi, Egidio Stigliano, and Francesca Aloisi. Detection of ectopic b-cell follicles with germinal centers in the meninges of patients with secondary progressive multiple sclerosis. *Brain pathology*, 14(2):164–174, 2004.

[143] Sudhanshu Shekhar and Xi Yang. The darker side of follicular helper t cells: from autoimmunity to immunodeficiency. *Cellular & molecular immunology*, 9(5):380–385, 2012.

[144] Ziv Shulman, Alexander D Gitlin, Sasha Targ, Mila Jankovic, Giulia Pasqual, Michel C Nussenzweig, and Gabriel D Victora. T follicular helper cell dynamics in germinal centers. *Science*, 341(6146):673–677, 2013.

[145] Stitaya Sirisinha. Insight into the mechanisms regulating immune homeostasis in health and disease. *Asian Pacific Journal of Allergy and Immunology*, 29(1):1, 2011.

[146] John P Smith, Gregory F Burton, John G Tew, and Andras K Szakal. Tinigible body macrophages in regulation of germinal center reactions. *Developmental immunology*, 6(3-4):285–294, 1998.

[147] Marisa Stebegg, Saumya D. Kumar, Alyssa Silva-Cayetano, Valter R. Fonseca, Michelle A. Linterman, and Luis Graca. Regulation of the germinal center response. *Frontiers in Immunology*, 9:2469, 2018.

[148] Isabelle Stewart, Daniel Radtke, Bethan Phillips, Simon J McGowan, and Oliver Bannard. Germinal center b cells replace their antigen receptors in dark zones and fail light zone entry when immunoglobulin gene mutations are damaging. *Immunity*, 49(3):477–489, 2018.

[149] Liat Stoler-Barak, Adi Biram, Natalia Davidzohn, Yoseph Addadi, Ofra Golani, and Ziv Shulman. B cell dissemination patterns during the germinal center reaction revealed by whole-organ imaging. *Journal of Experimental Medicine*, 216(11):2515–2530, 09 2019.

[150] Keiichiro Suzuki, Mikako Maruya, Shimpei Kawamoto, Katarzyna Sitnik, Hiroshi Kitamura, William W Agace, and Sidonia Fagarasan. The sensing of environmental stimuli by follicular dendritic cells promotes immunoglobulin a generation in the gut. *Immunity*, 33(1):71–83, 2010.

[151] Andras K. Szakal, Janet Kurowski Taylor, John P. Smith, Marie H. Kosco, Greg F. Burton, and John J. Tew. Kinetics of germinal center development in lymph nodes of young and aging immune mice. *The Anatomical Record*, 227(4):475–485, 1990.

[152] Seisuke Takemura, Andrea Braun, Cynthia Crowson, Paul J. Kurtin, Robert H. Cofield, William M. O'Fallon, Jörg J. Goronzy, and Cornelia M. Weyand. Lymphoid neogenesis in rheumatoid synovitis. *The Journal of Immunology*, 167(2):1072–1080, 2001.

[153] Hok Hei Tam, Mariane B. Melo, Myungsun Kang, Jeisa M. Pelet, Vera M. Ruda, Maria H. Foley, Joyce K. Hu, Sudha Kumari, Jordan Crampton, Alexis D. Baldeon, Rogier W. Sanders, John P. Moore, Shane Crotty, Robert Langer, Daniel G. Anderson, Arup K. Chakraborty, and Darrell J. Irvine. Sustained antigen availability during germinal center initiation enhances antibody responses to vaccination. *Proceedings of the National Academy of Sciences*, 113(43):E6639–E6648, 2016.

[154] Jeroen M. J. Tas, Luka Mesin, Giulia Pasqual, Sasha Targ, Johanne T. Jacobsen, Yasuko M. Mano, Casie S. Chen, Jean-Claude Weill, Claude-Agnès Reynaud, Edward P. Browne, Michael Meyer-Hermann, and Gabriel D. Victora. Visualizing antibody affinity maturation in germinal centers. *Science*, 351(6277):1048–1054, 2016.

[155] JG Tew and TE Mandel. Prolonged antigen half-life in the lymphoid follicles of specifically immunized mice. *Immunology*, 37(1):69, 1979.

[156] JG Tew, TE Mandel, and PL Rice. Immune elimination and immune retention: the relationship between antigen retained in the foot and the elicitation of footpad swelling. *Immunology*, 40(3):425, 1980.

[157] Olivier Thaunat, Aitor G. Granja, Patricia Barral, Andrew Filby, Beatriz Montaner, Lucy Collinson, Nuria Martinez-Martin, Naomi E. Harwood, Andreas Bruckbauer, and Facundo D. Batista. Asymmetric segregation of polarized antigen on b cell division shapes presentation capacity. *Science*, 335(6067):475–479, 2012.

[158] Marcel Jan Thomas, Ulf Klein, John Lygeros, and María Rodríguez Martínez. A probabilistic model of the germinal center reaction. *Frontiers in Immunology*, 10:689, 2019.

[159] Aleksei Uvarovskii. *Mathematical modelling of lymphocyte-mediated immune responses*. PhD thesis, 2017.

[160] Cees E van der Poel, Goran Bajic, Charles W Macaulay, Theo van den Broek, Christian D Ellson, Gerben Bouma, Gabriel D Victora, Søren E Degn, and Michael C Carroll. Follicular dendritic cells modulate germinal center b cell diversity through fcγriib. *Cell reports*, 29(9):2745–2755, 2019.

[161] Marco van Eijk, Jan Paul Medema, and Cornelis de Groot. Cutting edge: Cellular fas-associated death domain-like il-1-converting enzyme-inhibitory protein protects germinal center b cells from apoptosis during germinal center reactions. *The Journal of Immunology*, 166(11):6473–6476, 2001.

[162] Charlotte Viant, Georg HJ Weymar, Amelia Escolano, Spencer Chen, Harald Hartweger, Melissa Cipolla, Anna Gazumyan, and Michel C Nussenzweig. Antibody affinity shapes the choice between memory and germinal center b cell fates. *Cell*, 183(5):1298–1311, 2020.

[163] Gabriel D Victora, Tanja A Schwickert, David R Fooksman, Alice O Kamphorst, Michael Meyer-Hermann, Michael L Dustin, and Michel C Nussenzweig. Germinal center dynamics revealed by multiphoton microscopy with a photoactivatable fluorescent reporter. *Cell*, 143(4):592–605, 2010.

[164] Carola G Vinuesa, Iñaki Sanz, and Matthew C Cook. Dysregulation of germinal centres in autoimmune disease. *Nature Reviews Immunology*, 9(12):845–857, 2009.

[165] Maria Vono, Christiane Sigrid Eberhardt, Floriane Auderset, Beatris Mastelic-Gavillet, Sylvain Lemeille, Dennis Christensen, Peter Andersen, Paul-Henri Lambert, and Claire-Anne Siegrist. Maternal antibodies inhibit neonatal and infant responses to vaccination by shaping the early-life b cell repertoire within germinal centers. *Cell reports*, 28(7):1773–1784, 2019.

[166] Elizabeth F Wallin. T follicular regulatory cells and antibody responses in transplantation. *Transplantation*, 102(10):1614, 2018.

[167] Xiaoming Wang, Bryan Cho, Kazuhiro Suzuki, Ying Xu, Jesse A. Green, Jinping An, and Jason G. Cyster. Follicular dendritic cells help establish follicle identity and promote B cell retention in germinal centers. *Journal of Experimental Medicine*, 208(12):2497–2510, 10 2011.

[168] Xuan-Yi Wang, Bin Wang, and Yu-Mei Wen. From therapeutic antibodies to immune complex vaccines. *npj Vaccines*, 4(1):1–8, 2019.

[169] Yue Wang and Robert H Carter. Cd19 regulates b cell maturation, proliferation, and positive selection in the fdc zone of murine splenic germinal centers. *Immunity*, 22(6):749–761, 2005.

[170] Jason S Weinstein, Edward I Herman, Begoña Lainez, Paula Licona-Limón, Enric Esplugues, Richard Flavell, and Joe Craft. T fh cells progressively differentiate to regulate the germinal center response. *Nature immunology*, 17(10):1197–1205, 2016.

[171] Florian J Weisel, Steven J Mullett, Rebecca A Elsner, Ashley V Menk, Nikita Trivedi, Wei Luo, Daniel Wikenheiser, William F Hawse, Maria Chikina, Shuchi Smita, et al. Germinal center b cells selectively oxidize fatty acids for energy while conducting minimal glycolysis. *Nature immunology*, 21(3):331–342, 2020.

[172] Florian J Weisel, Griselda V Zuccarino-Catania, Maria Chikina, and Mark J Shlomchik. A temporal switch in the germinal center determines differential output of memory b and plasma cells. *Immunity*, 44(1):116–130, 2016.

[173] James B. Wing, Murat Tekgüç, and Shimon Sakaguchi. Control of germinal center responses by t-follicular regulatory cells. *Frontiers in Immunology*, 9:1910, 2018.

[174] Ivonne Wollenberg, Ana Agua-Doce, Andrea Hernández, Catarina Almeida, Vanessa G. Oliveira, Jose Faro, and Luis Graca. Regulation of the germinal center reaction by foxp3+ follicular regulatory t cells. *The Journal of Immunology*, 187(9):4553–4560, 2011.

[175] Yongzhong Wu, Mohey Eldin M El Shikh, Rania M El Sayed, Al M Best, Andras K Szakal, and John G Tew. Il-6 produced by immune complex-activated follicular dendritic cells promotes germinal center reactions, igg responses and somatic hypermutation. *International immunology*, 21(6):745–756, 2009.

[176] Yi Xia, Zijun Y Xu-Monette, Alexandar Tzankov, Xin Li, Ganiraju C Manyam, Vundavalli Murty, Govind Bhagat, Shanxiang Zhang, Laura Pasqualucci, C Visco, et al. Loss of prdm1/blimp-1 function contributes to poor prognosis of activated b-cell-like diffuse large b-cell lymphoma. *Leukemia*, 31(3):625–636, 2017.

[177] Hui Xu, Lu Zhang, and Birgitta Heyman. Igg-mediated immune suppression in mice is epitope specific except during high epitope density conditions. *Scientific reports*, 8(1):1–10, 2018.

[178] Yang Zhang, Michael Meyer-Hermann, Laura A. George, Marc Thilo Figge, Mahmood Khan, Margaret Goodall, Stephen P. Young, Adam Reynolds, Francesco Falciani, Ari Waisman, Clare A. Notley, Michael R. Ehrenstein, Marie Kosco-Vilbois, and Kai-Michael Toellner. Germinal center B cells govern their own fate via antibody feedback. *Journal of Experimental Medicine*, 210(3):457–464, 02 2013.

[179] Yi-Nan Zhang, James Lazarovits, Wilson Poon, Ben Ouyang, Luan NM Nguyen, Benjamin R Kingston, and Warren CW Chan. Nanoparticle size influences antigen retention and presentation in lymph node follicles for humoral immunity. *Nano letters*, 19(10):7226–7235, 2019.

[180] Ángel F. Álvarez Prado, Pablo Pérez-Durán, Arantxa Pérez-García, Alberto Benguria, Carlos Torroja, Virginia G. de Yébenes, and Almudena R. Ramiro. A broad atlas of somatic hypermutation allows prediction of activation-induced deaminase targets. *Journal of Experimental Medicine*, 215(3):761–771, 01 2018.